RATIONAL DESIGN AND THERAPEUTIC POTENTIAL OF A NOVEL NOX1 INHIBITOR FOR THE TREATMENT OF PULMONARY HYPERTENSION: IN VITRO AND IN VIVO EFFECTS OF NOX1 INHIBITION

by

Daniel Jacob Ranayhossaini

Bachelor of Science, Penn State University, 2010

Submitted to the Graduate Faculty of

The University of Pittsburgh School of Medicine

in partial fulfillment of the requirements for the degree of

Doctor of Philosophy

University of Pittsburgh

UNIVERSITY OF PITTSBURGH

SCHOOL OF MEDICINE

This dissertation was presented

by

Daniel Jacob Ranayhossaini

It was defended on

August 18, 2014

and approved by

Committee Chair: Mark T. Gladwin, MD, Director, Vascular Medicine Institute

Aaron Barchowsky, PhD, Department of Environmental and Occupational Health

Donald B. DeFranco, PhD, Department of Pharmacology & Chemical Biology

Guillermo Romero, PhD, Department of Pharmacology & Chemical Biology

Dissertation Advisor:

Patrick J. Pagano, PhD, Department of Pharmacology & Chemical Biology

RATIONAL DESIGN AND THERAPEUTIC POTENTIAL OF A NOVEL NOX1 INHIBITOR FOR THE TREATMENT OF PULMONARY HYPERTENSION: IN VITRO AND IN VIVO EFFECTS OF NOX1 INHIBITION

Daniel Jacob Ranayhossaini, PhD

University of Pittsburgh, 2014

NADPH oxidases (Noxes) represent a family of enzymes who produce reactive oxygen species. Excessive Nox activity is associated with multiple pathological conditions, including hypertension. Despite Nox1's association with morbidity, there is a paucity of specific Nox1 inhibitors. The overarching hypothesis of this project was that Nox1 promotes endothelial phenotypes contributing to pulmonary hypertension and associated cardiac dysfunction. Pharmacological Nox1 inhibition testing this hypothesis was performed via designing the first specific peptidic Nox1 inhibitor (NoxA1ds). Our results show that Nox1 is key to endothelial $O_2\cdot^-$ and VEGF-stimulated migration and that Nox1 contributes to left ventricle cardiac dysfunction.

Functional Nox1 is activated in part by association of Nox1 with one of its essential cytosolic subunits NOXA1. NoxA1ds was designed to mimic a putative activation domain in NOXA1 with a single F199A amino acid mutation. NoxA1ds specifically inhibited Nox1 but not Nox2, Nox4, Nox5 in reconstituted cell-free systems. Mechanistically, we found that NoxA1ds binds to Nox1 and disrupts Nox1:NOXA1 association and thus enzyme assembly.

To identify the relative roles of Nox1 and Nox2 in human pulmonary artery endothelial cell (HPAEC) physiology, the relative specificity of Nox2ds for Nox2 vs Nox1 required validation. In part, this thesis established Nox2ds as specific for Nox2 over canonical, hybrid, or

inducible Nox1 and Nox4. NoxA1ds and Nox2ds were then used to establish that Nox1, but not Nox2, is responsible for hypoxia-induced $O_2^{\cdot -}$ in HPAEC and VEGF-stimulated HPAEC migration. Additional data revealed that VEGF stimulates Nox1:NOXA1 association and identified fibroblasts as a source for hypoxic VEGF production.

The role of Nox1 in HPAEC O_2^- and migration suggested that Nox1 may contribute to of the development of pulmonary arterial hypertension. Treatment of pulmonary hypertensive rats with aerosolized NoxA1ds improved left ventricular dilation but displayed minimal benefit in the right ventricle, indicating Nox1 may play a predominant role in the systemic vs pulmonary vasculature.

Major contributions of this study include the design and characterization a novel Nox1 inhibitor (NoxA1ds), the identification of pulmonary endothelial phenotypes mediated by Nox1 rather than Nox2, and that the contribution of Nox1 to left ventricular dilation in the context of severe PAH.

TABLE OF CONTENTS

LIST OF TABLES

LIST OF FIGURES

PREFACE

ACKNOWLEDGEMENTS

This dissertation represents the culmination of my career as a scientist thus far, and I am forever grateful to those who have contributed to my growth as such. My greatest thanks go to my parents, who fostered my inherent curiosity of the natural world from the earliest days of my childhood and have remained eager to hear the progress I make. Second only to my parents are my brothers, who have always made my life tremendously fun and exciting and provided much needed breaks from the daily stress in the preparation of my thesis. I expect that we still have many more adventures to come.

I also extend my thanks to the many scientific mentors I have had over the years. Patty Griest, Rebecca Finch, and Matthew Delp: your advice and education at the earliest stages of my career set the stage for my future independent investigations. Margaret Voss, Michael Campbell, Pamela Silver: when I engaged in my first truly independent study, you gave me the freedom to pursue whichever direction my curiosity turned and provided invaluable guidance as I stepped forward in my quest for knowledge. Natalie Fursov and Russell Lingham: you opened my eyes to entirely new words of research in antibody engineering and gave me an entirely new paradigm on the role of scientific research in industrial pharmaceutical development. Gabor Csanyi and Imad Al Ghouleh: you were my brothers in the lab. I don't think I'll ever have as much fun working in a lab and maintaining productivity as I did with you two.

Last, and most certainly not the least, I must thank my mentor for the past four years, Patrick Pagano. My success in the pursuit of my PhD is largely to your credit and would not have been possible without your exemplary mentoring. Your guidance as I navigated the world

of experimental design, data presentation, funding agencies, and manuscript publication all whilst maintaining lab productivity was invaluable and your patience with my occasionally naïve and rushed actions has taught me countless invaluable lessons. You have been an outstanding mentor, and your academic, personal, and intellectual support has set the stage for the rest of my scientific career.

Parts of this work appear as published manuscripts on which I am an author and would not have been possible without the contributions of the co-authors:

1. Ranayhossaini DJ, Rodriguez AI, Sahoo S, Chen BB, Mallampalli RK, Kelley EE, Csanyi G, Gladwin MT, Romero G, Pagano PJ. Selective Recapitulation of Conserved and Nonconserved Regions of Putative NOXA1 Protein Activation Domain Confers Isoform-specific Inhibition of Nox1 Oxidase and Attenuation of Endothelial Cell Migration. J Biol Chem. 2013 Dec 20;288(51):36437-50

2. Ranayhossaini D, Pagano PJ. TrACEing Angiotensin II Type 1 to Right Ventricular Hypertrophy: Are the "Sartans" a Viable Course to Treating Pulmonary Arterial Hypertension? AJRCCM 2012 Oct 15, 186(8):705-7

3. Csányi G, Cifuentes-Pagano E, Al Ghouleh I, Ranayhossaini DJ, Egaña L, Lopes LR, Jackson HM, Kelley EE, Pagano PJ. Nox2 B-loop Peptide, Nox2ds, Specifically Inhibits Nox2 Oxidase. FRBM 2011 Sep 15;51(6):1116-25

LIST OF ABBREVIATIONS

ANOVA	analysis of variance
CFP	cyan fluorescent protein
COS-22	COS-7 cells transfected with $p22^{phox}$
COS-NOX1	COS-22 cells transfected with Nox1 NOXO1, and NOXA1
COS-NOX2	COS-22 cells transfected with Nox2, $p47^{phox}$, and $p67^{phox}$
COS-NOX4	COS-22 cells transfected with Nox4 and $p22^{phox}$
CPH	1-hydroxy-3-methoxycarbonyl-2,2,5,5-tetramethylpyrrolidine hydrochloride
DMSO	dimethyl sulfoxide
DPI	diphenyleneiodonium chloride
Duox	dual oxidase
EDPVR	end diastole pressure volume relationship
EDV	end diastolic volume
EGF	epidermal growth factor
EPR	electron paramagnetic resonance
eNOS	endothelial nitric oxide synthase
ESPVR	end systole pressure volume relationship
FAD	flavin adenine dinucleotide
FDA	United States Food and Drug Administration
FRAP	fluorescence recovery after photobleaching
FRET	fluorescence resonance energy transfer
H_2O_2	hydrogen peroxide

HFpEF	heart failure with preserved ejection fraction
HIF1α	hypoxia inducible factor 1α
HPAEC	human pulmonary artery endothelial cells
HPASMC	human pulmonary artery smooth muscle cells
HPAF	human pulmonary artery fibroblasts
HX	hypoxanthine
LV	left ventricle of the heart
mPAP	mean pulmonary artery pressure
MTT	Methylthiazolyldiphenyl-tetrazolium bromide
NADPH	nicotinamide adenine dinucleotide phosphate
NOS	nitric oxide synthase
Nox	NADPH oxidase
NOXA1	Nox activator subunit 1
NOXO1	Nox organizer subunit 1
$O_2 \cdot^-$	superoxide anion
OAB	oxidase assay buffer
PAH	pulmonary arterial hypertension
PBS	phosphate buffered saline
PMA	phorbol myristate acetate
RNS	reactive nitrogen species
ROS	reactive oxygen species
RV	right ventricle of the heart
SEM	standard error of the mean

SOD	superoxide dismutase
SUCH	SU5416 + chronic hypoxia model of PAH
VEGF	vascular endothelial growth factor
VEGFR	VEGF receptor
XO	xanthine oxidase
YFP	yellow fluorescent protein

1.0 INTRODUCTION

1.1 ROLES OF ROS/RNS IN CELLULAR BIOLOGY

1.1.1 Distinctions between individual ROS/RNS

The family of reactive oxygen species (ROS) and reactive nitrogen species (RNS) is an amalgamated collection of numerous distinct molecules that are differentiated by their atomic composition, charge state, and free vs. paired electron status. The majority of ROS and RNS share the primary atomic components of oxygen, nitrogen, and hydrogen and as such, the number and types of ROS/RNS family members is limited only by natural physical and chemical laws. Despite the great variety of potential ROS/RNS, selected species bear particular significance in biology. Particularly significant ROS/RNS in biological systems include hydrogen peroxide (H_2O_2), hydroxyl radical ($OH\cdot$), superoxide anion ($O_2\cdot^-$), nitric oxide ($NO\cdot$), and peroxynitrite ($ONOO^-$) (Table 1). These molecules are derived from enzymatic processes as well as redox reactions among ROS/RNS and other organic/inorganic molecules such as lipids, proteins and iron. The presence of charged moieties and free electrons on many of these species contribute greatly to their dynamic reactions, half-lives, and physiological signaling consequences.

1.1.2 Physiological ROS/RNS Dynamics

Cellular sources and inorganic catalysts of $O_2\cdot^-$ include NADPH oxidases (Noxes), uncoupled endothelial nitric oxide synthase (eNOS), free iron, and xanthine oxidoreductase (XO) [1-3]. To

mitigate the inherent reactivity of $O_2\cdot^-$, most mammalian cells abundantly express superoxide dismutase (SOD). The conversion of $O_2\cdot^-$ to H_2O_2 by copper/zinc superoxide dismutase (Cu,Zn-SOD) is an extremely fast reaction occurring with a rate constant of 6.4×10^9 $M^{-1}s^{-1}$ [4]. Less efficient Mn-SOD or Fe-SOD catalyze this reaction at approximately 6.4×10^8 $M^{-1}s^{-1}$ [4]. The speed of these reactions is necessary to protect the cell from the damaging reactions of $O_2\cdot^-$ with cellular enzymes, in particular, aconitase. Aconitase is a critical enzyme in the Krebs cycle for the conversion of citrate to isocitrate and its iron-sulfur core is rapidly oxidized and inactivated by $O_2\cdot^-$ at a reaction rate constant of 10^7 $M^{-1}s^{-1}$, only marginally slower than the reaction rate of SOD, further emphasizing the importance of antioxidant enzymes for cellular protection [5]. The reactive ability of $O_2\cdot^-$ extends to its potential to oxidize enzymatic cofactors, such as tetrahydrobiopterin, an essential cofactor of eNOS activation [6-8]. This reaction is also very rapid occurring at 3.9×10^5 $M^{-1}s^{-1}$ and is a significant cause of eNOS uncoupling leading to increased O_2^- production [8, 9]. Beyond its ability to inactivate enzymatic cofactors, $O_2\cdot^-$ is capable of reacting with thiols at reaction rate constants ranging from $1.0 - 5.0 \times 10^5$ $M^{-1}s^{-1}$, depending on thiol availability [10].

Species	**Name**	**Biological Sources**
H_2O_2	Hydrogen Peroxide	Nox, XO, SOD
$OH\cdot$	Hydroxyl Radical	$O_2\cdot^-$, Fenton Reaction
$O_2\cdot^-$	Superoxide	Nox, XO, eNOS, free iron
$NO\cdot$	Nitric Oxide	NOS, Nitrite reductases incl. myoglobin and neuroglobin
$ONOO^-$	Peroxynitrite	$O_2\cdot^-$ interaction with $NO\cdot$

Table 1-1: Selected Biological ROS/RNS.

$O_2\cdot^-$ very potently reacts with most cysteine containing enzymes and/or enzymatic cofactors. Through dismutation of $O_2\cdot^-$ to H_2O_2, the reactive properties and half-life of $O_2\cdot^-$ are significantly changed and provides an alternate route for H_2O_2-mediated protein modification and oxidation. H_2O_2 is arguably the most stable of the reactive oxygen species, with its half-life extending for days in solutions at room temperature [11]. Like $O_2\cdot^-$, H_2O_2 is capable of oxidizing cysteines and thus modifying protein function [12]. Kinetically, the oxidation reaction of H_2O_2 with cysteine occurs slowly at 720 $M^{-1}s^{-1}$, allowing H_2O_2 to diffuse away from its source and expanding its potential cellular targets [13]. The relatively low reaction rate constant of H_2O_2 with cysteine and its long half-life indicate that this molecule is capable of diffusing throughout and beyond the cell. This diffusion of H_2O_2 is limited, however, by the prevalence and distribution of catalase. Catalase is by far most significant negative contributor to the half-life of H_2O_2 by catalyzing the formation of oxygen and water from H_2O_2 at a rate constant of 6.62×10^7 $M^{-1}s^{-1}$. Catalase is ubiquitously expressed in most mammalian cells and is responsible for controlling diffusion of H_2O_2 beyond its intended target [14, 15]. In addition to catalase, a wide variety of cellular peroxidases participate in the metabolism of H_2O_2. Peroxidases utilize the oxidative capacity of H_2O_2 to perform a two-step reaction, first oxidizing themselves (reaction I), before transferring the oxidant to a target protein or porphyrin (reaction II) [16]. Physiologically relevant oxidation targets of peroxidases include pyridine nucleotides [16]. Peroxidase reaction I is often the rate limiting step of peroxidase activity, and depending on the class of peroxidase, target species, the kinetics of reaction I can be as slow as 5.4×10^5 $M^{-1}s^{-1}$ (lignin peroxidase) or as fast as 8.0×10^7 $M^{-1}s^{-1}$ (ascorbate peroxidase) [16, 17]. These kinetics are remarkably stable over wide pH ranges with horseradish peroxidase retaining its reaction rate constant of 1.8×10^7 $M^{-1}s^{-1}$ from pH 5-9 [17]. Together, SOD, catalase, and peroxidases perform the majority of

cellular ROS catabolism and in doing so, protect the cell from the damaging effects of dysregulated ROS and maintain targeted ROS activity for physiological signaling.

Perhaps the most widely studied RNS is nitric oxide (NO), which is a ubiquitous biological signaling molecule primarily produced by nitric oxide synthase (NOS) and nitrite reductases. While NO confers many physiological effects, it is best known for its vasodilatory properties [18-20]. A single unpaired electron on NO dictates which molecules it can favorably react with, these are typically either other free radicals or metals such as heme iron [21]. The stability of NO and its ability to freely diffuse across and also utilize aquaporin channels allows it to serve as a paracrine signaling factor between endothelial and smooth muscle cells, lending it extraordinary control of vasodilation by causing smooth muscle relaxation [18, 19, 22]. The half-life of physiological NO in aqueous solution is quite high with a half-life of about 5 min in solution [21]. In the cellular environment, this is greatly reduced to less than 1 minute, which can be doubled by the addition of SOD [18]. Indeed, the reaction between NO and $O_2\cdot^-$ to form $ONOO^-$ is diffusion-limited and thus very rapid. Hence, SOD leads to an increase in the half-life of NO by preventing this reaction [23]. The reaction of NO and $O_2\cdot^-$ to form $ONOO^-$ occurs at 6.7×10^9 $M^{-1}s^{-1}$[24]. This extremely fast reaction closely competes with SOD for $O_2\cdot^-$ radicals. In turn, $ONOO^-$ is stable for days in alkaline solutions [25]. In biological systems, only 20% of $ONOO^-$ will be protonated and subsequently degraded to nitrate with the remainder remaining capable of oxidizing cellular components, with a relatively short half-life of 1 second [25]. Biological protection from $ONOO^-$ appears to be achieved through the scavenging properties of uric acid [26].

The vasoprotective functions of NO are in stark contrast to the ability of $ONOO^-$ to damage the endothelium leading to cardiovascular disease [27]. $ONOO^-$mediated damage to

proteins is often observed as a consequence of the nitration of tyrosines, although $ONOO^-$ oxidation can occur on iron, sulfur, or zinc complexes as well as cysteine residues [21, 28]. $ONOO^-$ reaction rate constants differ widely based on the target and can proceed as slowly as 10^3 $M^{-1}s^{-1}$ or as rapidly as 10^7 $M^{-1}s^{-1}$ [3, 29, 30]. Beyond its direct effect on cellular components, protonation of $ONOO^-$ leads to formation of OH· radicals that are capable of reacting with most organic molecules, including nucleic and amino acids [27]. Reactions between OH· and most organic molecules are fairly rapid on the order of 10^8 to 10^9 $M^{-1}s^{-1}$ [31]. The speed of this reaction and the plethora of potential targets makes it extremely difficult to specifically scavenge OH·, and thus most efforts focus on preventing formation of its precursors.

To further appreciate the intricate relationship of interacting ROS/RNS species and thus protect cells from their detrimental effects, recent efforts have been focused on defining the exact mechanisms through which $ONOO^-$ and other ROS modify proteins. One mechanism that is potentially translatable across a wide range of proteins involves the targeting of heme coordination sites by ONOO-. Indeed, while all tyrosines are susceptible to nitration by ONOO-, tyrosines proximal to hexameric heme coordination sites are particularly important in protein function. When these tyrosines become nitrated, the integrity of heme coordination is greatly reduced and can cause deactivation of catalytic sites [32]. Through this mechanism and others yet to be delineated, tyrosine nitration by ONOO- can inactivate, activate, or engender new functions for proteins including SOD, cytochrome c, fibrinogen, and HSP90 [32-35].

While many unknowns remain in ROS/RNS signaling, consistent and sustained effort has helped to determine functional roles for biologically relevant ROS/RNS including OH·, $O_2\cdot^-$, NO·, $ONOO^-$, and H_2O_2. Each of these molecules is capable of modifying protein function through the modification of cysteines, tyrosines, or enzymatic cofactors among others, albeit at

significantly different rates. Negative regulators of ROS-mediated protein modification and protective cellular enzymes include SOD and catalase. SOD converts $O_2^{\cdot -}$ to less reactive H_2O_2 and in turn, catalase converts H_2O_2 to water. These reactions occur at very high rates of 6.4 x 10^9 $M^{-1}s^{-1}$ and 6.62 x 10^7 $M^{-1}s^{-1}$, respectively. Despite its very high reaction rate constant, SOD is incapable of completely preventing the formation of $ONOO^-$ from NO· and $O_2\cdot^-$ (rate = 6.7 x 10^9 $M^{-1}s^{-1}$). These reaction rate constants are so similar that a close competition for the fate of cellular O_2^-, H_2O_2, and NO· exists. The outcome of this competition largely depends on the concentrations and availability of each individual species, target availability, and antioxidant scavenging enzymes. The reactivity of these agents alone does not determine their influence *in vitro* or *in vivo* as different cell types and different stimuli can result in very different ROS profiles, in part as a result of different protein expression (e.g. SOD, catalase), subcellular localization, and available protein targets.

1.2 NADPH OXIDASE-DERIVED ROS IN THE VASCULATURE

1.2.1 NADPH Oxidase, Roles in Physiology

NADPH oxidases (Noxes) are a family of proteins taxonomically characterized by their ability to harvest electrons from NADPH and transfer these to O_2, producing ROS such as $O_2^{\cdot -}$ and H_2O_2. The Nox family includes the proteins Nox1, Nox2, Nox3, Nox4 Nox5 and the Dual Oxidases 1 and 2 (Duox1 and Duox2). Noxes 1, 2, 3 & 5 produce $O_2^{\cdot -}$, while Nox4 and the Duoxes reportedly produce H_2O_2 [36]. Somewhat of a misnomer, Nox2 was the first member of this family to be discovered and historically, has been referred to as the phagocyte oxidase for its role

in bactericidal activity of the neutrophil and other leukocytes [37-39]. Tissue expression of the Nox family is as diverse as their lineage, with predominant expression of Nox1 in colon epithelium, uterus, vascular smooth muscle and vascular endothelium; predominant expression of Nox2 in neutrophils, macrophages, endothelial cells, neurons, and fibroblasts [40-48]. Nox3 seems to be localized primarily to the inner ear, while Nox4 is ubiquitously expressed throughout the vasculature, with additional significant expression in in the kidney [48-52]. Nox5 is largely observed in vascular smooth muscle cells, but is also expressed in the endothelium, of higher mammals while the Duoxes are best known for their expression in the pulmonary epithelium [45, 53-56] (Table 2).

Beyond their differences in tissue expression, the Nox isoforms have distinct subcellular localization, with Nox expression being differentially expressed in an isoform-dependent manner in the plasma membrane, endosomes, phagosomes, and the endoplasmic reticulum (Table 2). These distinct subcellular locales are purported to be inextricably tied to the signal transduction consequences of the enzyme for two reasons: a) the reactive nature of the ROS produced and thus its radius of diffusion limits specific protein targeting and b) rapid scavenging by SOD and catalase prevents distal diffusion of ROS-mediated signal transduction, particularly in the case of $O_2^{\cdot -}$ and moderately less so for H_2O_2. While physiologically important for normal cardiovascular homeostasis and immune function, under pathological conditions excessive stimulation of Noxes often leads to hyperproliferative and migratory phenotypes as well as oxidative stress, often resulting in end-organ damage [57, 58]. Increasingly the role of individual Nox isoforms are being appreciated as playing highly-localized, specific, and temporal roles in disease progression. Broad and nonspecific antioxidant actions of ROS scavengers (i.e., vitamin antioxidants and antioxidant enzymes) cannot manipulate cellular signaling in the specific and

temporal manner necessary to elicit subtle changes in cell physiology and pathophysiology. Thus, while ROS scavengers/antioxidants are extremely valuable as controls and confirmatory tools, their utility is superseded by the need for highly-selective inhibitors of Nox-derived ROS production. Importantly, Noxes are increasingly being appreciated as key players in cardiovascular physiology through suppression of NO bioavailability, and induction of cell proliferation and vessel tone, for example, despite their long-emphasized major importance in the phagocytic oxidative burst.

1.2.2 Anatomy and Physiology of the Cardiovascular System

An essential component of vertebrate physiology is the cardiovascular system, which serves to provide oxygen and nutrients to tissue beds while removing waste for excretion by the kidneys. Mammalian hearts are divided into four chambers: the left atrium, left ventricle, right atrium, and right ventricle. Together, these chambers are the pump that drives the circulation of blood throughout the body. After tissue perfusion and oxygen depletion, blood returns to the right side of the heart via the superior vena cava where blood is sent via the pulmonary artery for oxygenation in the lungs. Via the left and right pulmonary veins, the left side of the heart receives oxygenated blood from the lungs and distributes it through the body (Figure 1-1) [59, 60]. Control of heart beats/contractions is achieved through sympathetic and parasympathetic innervation and it is through the sympathetic innervation which synchronous contraction of the left and right ventricles, or systole, is stimulated [60, 61]. Systolic contractions force ejection of the blood through the vasculature and is immediately followed by diastole, the relaxation of the heart muscle allowing its chambers to refill [60-62].

The progress of blood flow can be described by starting at the filling of the left atrium with blood draining from the pulmonary veins. In turn, contractions of the left atrium fill the

relaxed left ventricle (LV). The LV is the largest component of the heart and pumps oxygenated blood into the aorta, which branches distally to smaller conduit vessels and sequentially smaller and thinner arteries greater diffusion of oxygen from the vessels to organ systems occurs, with the greatest diffusion occurring between the smallest of vessels or capillaries. After oxygen diffusion, the blood returns to the heart via the vena cava as "venous return" and is drained by the right atrium which, during systole, fills the diastolic right ventricle (RV). Contraction of the RV sends blood through the pulmonary artery for oxygenation in the lungs before blood is and then transferred back to the left atrium and LV for subsequent distribution through the body [60, 63].

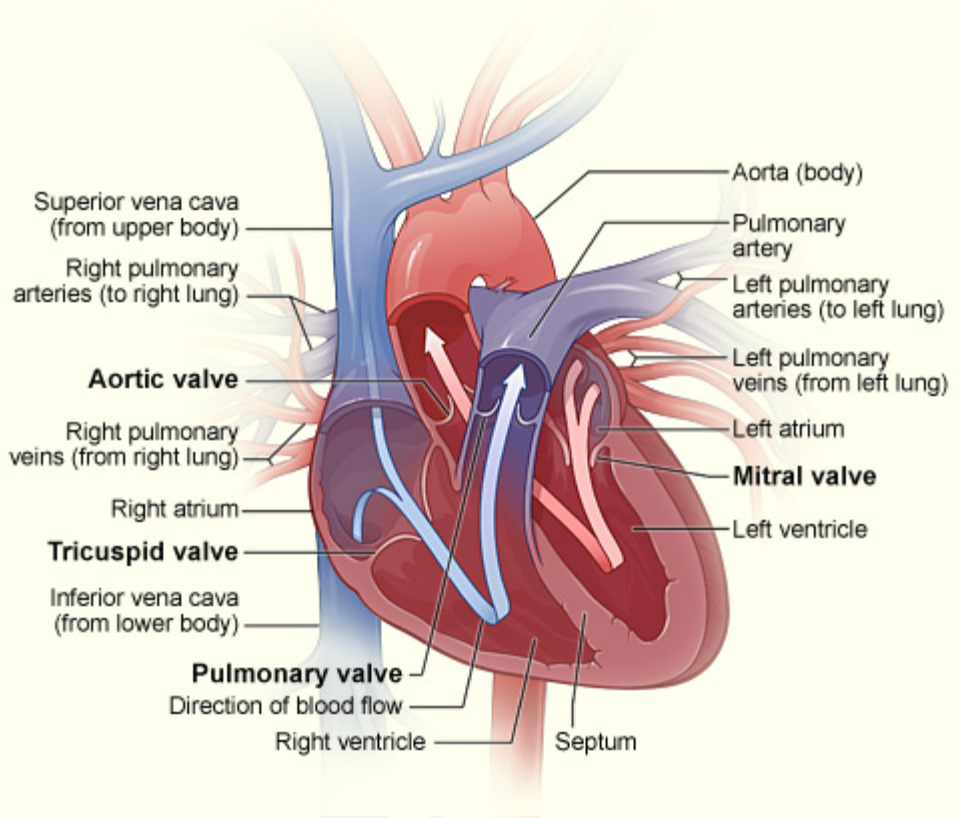

Figure 1-1: Blood flow and anatomy of the heart

Image from U.S. National Library of Medicine, no copyright restriction.

The cycle of blood flow through the heart through systolic contractions and diastolic relaxations causes substantial changes in pressures and volumes within the heart. Hemodynamic analysis of these pressures and volumes provides great detail concerning the function of each component of the heart and is best measured by pressure-volume conductance catheters and the resultant pressure-volume loops (PV loops) (Figure 1-1) [64]. Critical measures of ventricular function determined by PV loop analysis are the End Systole Pressure Volume Relationship (ESPVR) and the End Diastole Pressure Volume Relationship (EDPVR). ESPVR describes the maximal pressure that can be achieved at any given volume and is critical in determining ventricular contractility [65-67]. In turn, EDPVR describes the maximal volume that can be achieved at any given pressure and is a function of ventricular compliance [67-69] (Figure 1-2). Determining ESPVR/EDPVR by PV loop analysis offers the benefit of being a highly sensitive and load-independent technique for measuring cardiac states and is a key measure of cardiac function under any condition [70]. Deviation of either ESPVR or EDPVR from their initial slope values can indicate any one of a number of cardiomyopathies depending on the direction of the shift. For example, a decrease in the slope of EDPVR indicates a more compliant heart that fills more readily while an increase in ESPVR indicates a more contractile heart or one that is working against abnormally high pressures to move blood [68, 71].

Larger blood vessels that carry blood throughout the body are composed of three distinct layers and cell types: the innermost intima (endothelial cells), the central media (smooth muscle cells), and the outermost adventitia (fibroblasts, Figure 1-2) [72]. In the smallest of vessels including resistance vessels and capillaries, the smooth muscle cells and fibroblasts are replaced by pericytes [73]. The intima surrounds the interior of the vessel, the lumen, which contains the flowing blood, including plasma, erythrocytes, and leukocytes. Conduit arteries, which carry

blood away from the heart, maintain a significantly thicker media than veins returning blood to the heart with multiple layers of smooth muscle cells. As one progresses down the vascular tree, anywhere between 1 through 7 layer(s) of smooth muscle cells are found, with vessels of a larger diameter having more smooth muscle while the most distal arteries, veins, and capillaries have lesser to no virtually smooth muscle [60]. Functionally, the adventitia appears to preserve vascular tone, at least in part, through its production of $O_2^{\cdot-}$ and the subsequent destruction of NO while structurally supporting the vessel via production of matrix proteins including collagen [74-76]. The smooth muscle cells of the media provide the main contractile force that determines vessel diameter and consequent vascular resistance [77]. The innermost endothelial cells lining the vessel lumen counteract the contractile force of the media through primarily the production of NO and subsequent sGC activation in larger vessels as well as eicosanoids, H_2O_2, and adenosine in smaller vessels [18, 78-81].

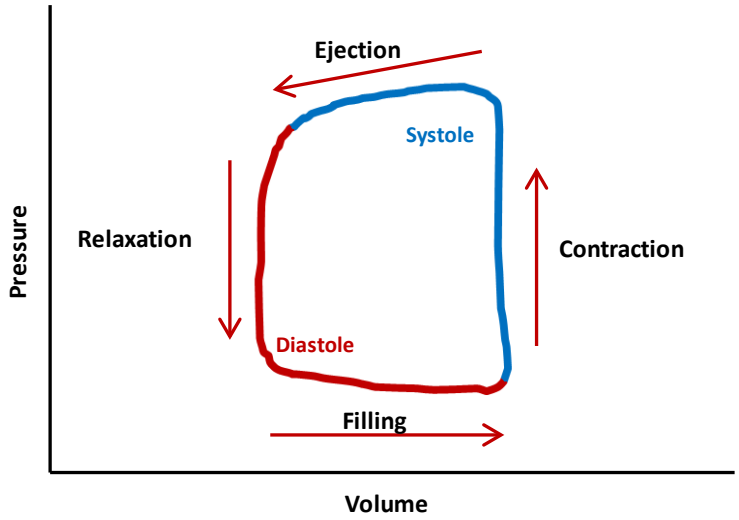

Figure 1-2: Schematic of an ideal PV loop.

The PV-loop is divided into two halves, systole and diastole with contraction and ejection occurring during systole and relaxation and filling occurring during diastole.

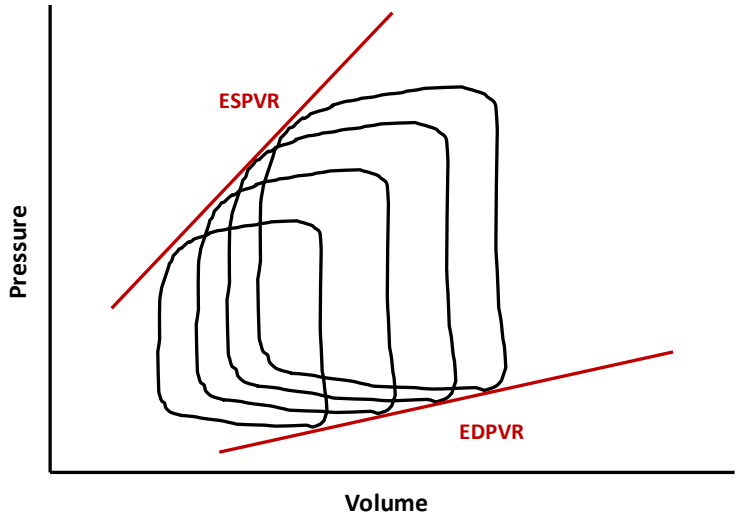

Figure 1-3: Relationship of ESPVR and EDPVR to an ideal series of PV loops.

End Systole Pressure Volume Relationship (ESPVR) indicates the maximum pressure that can be attained at any given volume while End Diastole Pressure Volume Relationship (EDPVR) indicates the maximum volume that can be attained at any given pressure. ESPVR and EDPVR are calculated though occlusion of the vena cava and reducing ventricular volume, leading to sequential PV loops shown. Calculation of ESPVR and EDPVR through this method contributes to the load independence of this cardiac measure.

Angiogenesis, the growth of new blood vessels, is a tightly-controlled vascular process that functions to extend the circulatory system to hypoxic growing and damaged tissue beds that are unable to survive on interstitial fluid alone [82]. Angiogenic signaling is driven primarily by oxygen gradients and is stimulated by multiple key proteins, including VEGF, HIF1α, and Noxes have emerged as important players in this process [82-85]. Originally described as a "vascular permeability factor" for its ability to rearrange endothelial cells and vascular superstructure in tumors, VEGF was later renamed as "vascular endothelial growth factor" when its mitogenic properties were being revealed [84, 86-89]. As an extremely potent stimulator of mitogenesis, endothelial migration, and angiogenic sprouting by vessels, VEGF is also a major contributor to

malignant tumor growth through its potentiation of angiogenesis [84, 88, 90]. Hypoxia inducible factor 1α (HIF1α) is the master regulator of oxygen sensitive angiogenic gene transcription, including the transcript for VEGF and potentially the transcripts for Noxes [85, 91]. HIF1α activity is tightly controlled by endogenous prolyl hydroxlases that target HIF1α for rapid proteolytic degradation through post-translational modification [92, 93]. However, under conditions of low oxygen, prolyl hydroxlases are inhibited, allowing HIF to remain active in the cell, leading to transcription of genes with HIF1α-responsive elements, including VEGF and Nox [85, 94]. Noxes are established contributors to angiogenic signaling, in part through oxidative activation of matrix metalloproteases that permit angiogenic remodeling through degradation of extracellular matrix proteins [95-97]. Nox1, Nox2, and Nox4 have each been identified as contributors to angiogenesis, with some evidence indicating that Nox1 may be more influential in angiogenic signaling [98, 99]. The important role of Nox1 in angiogenesis is likely not only due to potential ROS-mediated activation of metalloproteases, but also its potentiation of VEGF transcription [83, 95, 100]. This has generated some interest as to whether Nox inhibition may be a potential treatment for diseases mediated by angiogenic signaling and vessel remodeling, including cancer and pulmonary arterial hypertension.

1.2.3 Structure and Regulation of Vascular Nox Isoforms

Beyond their role in preventing bacterial pathogenesis, Nox1 and Nox2 are significant contributors to vascular cell proliferation and invasion [98, 100-106]. Tissue expression data and knockout mice have identified Nox1, Nox2, Nox4, and Nox5 as the most prominent Noxes in vascular physiology [46, 107-109]. These Noxes play key roles in vascular physiology in part through the destruction of NO via Nox-derived $O_2^{\cdot -}$ and subsequent generation of $ONOO^-$. While critical for normal vascular homeostasis, when this pathway is dysregulated, Nox1 and

Nox2 contribute to left heart failure, atherosclerosis and hypertension [101, 110-112]; and whereas the link between enhanced Nox1 & 2 activity and systemic vascular disease in experimental models is well established, less clear is the link between Nox4 and cardiovascular disease progression. Rather, significant controversy surrounds Nox4 as to whether this enzyme plays a protective or destructive role in cardiovascular disease [99, 113]. Nox5's role in the vasculature is less well defined, largely due to the lack of murine Nox5 expression and resulting lack of appropriate animal models and genetic tools to investigate cardiovascular disease. However, it is presumed that Nox5 potentiates similar signaling pathways as Nox1 through the production of $O_2^{\cdot -}$ [109, 114]. Additionally, the role of Nox1 and Nox2 in pulmonary vascular disorders is largely unknown.

As evidence has grown defining the role of Noxes in cardiovascular health and disease, Nox biochemistry has emerged as an area of great interest. Structurally, the cardiovascular Noxes1-5 bear significant differences in their amino acid sequence and assembly. Functional Nox1 and Nox2 oxidases are the most homologous vascular Noxes and, when structurally complete, are a multimeric protein complex consisting of a transmembrane catalytic core (either Nox1 or Nox2), a cytoplasmic GTPase (Rac1), a cytoplasmic organizing subunit (NOXO1 organizing Nox1; $p47^{phox}$ organizing Nox1 and 2), a cytoplasmic activating subunit (NOXA1 activating Nox1; $p67^{phox}$ activating Nox2) and the transmembrane stabilizing protein $p22^{phox}$ [115-123].

The cytoplasmic subunits NOXO1, $p47^{phox}$, NOXA1, and $p67^{phox}$ are critically important components of Nox activation *in vitro* and *in vivo*. Indeed, mutations in cytoplasmic Nox subunits can manifest as chronic granulomatous disease in humans, a condition of insufficient microbial clearance by the macrophage [124]. Through catalyzing enzyme assembly NOXO1

and p47^{phox} serve as the organizing subunits of Nox1 and Nox2, respectively. Although both proteins share significant homology, a major difference between the two is the presence of an auto-inhibitory domain in p47^{phox}. This domain prevents p47^{phox} interaction with either Nox1 or Nox2 until p47^{phox} is phosphorylated [125, 126]. NOXA1 and p67^{phox} serve as the key canonical activating proteins for Nox1 and Nox2, respectively. As testament to the key activating function of NOXA1/p67^{phox}, in reconstituted cell-free assays containing prenylated p67^{phox}, Nox2 can be activated independently of the organizing subunits p47^{phox}/NOXO1, at least in an experimental setting [119]. Within p67^{phox} exists a key activation domain extending through residues 190-210, that is critical for the successful transfer of electrons from NADPH to FAD in Nox2 [127, 128]. While the homologue of p67^{phox}'s activation domain in NOXA1 remains to be conclusively characterized as an activation domain, the significant homology between these two proteins, in particular residues 190-210, as well as their sensitivity to mutation, implies that residues 190-210 in NOXA1 may serve as a domain with a similar function for Nox1 [129].

Recent reports have suggested that NOXO1 and p47^{phox} are interchangeable organizers of either Nox1 or Nox2 while NOXA1 and p67^{phox} are interchangeable activators of either Nox1 or Nox2 in smooth muscle cells [46]. It would appear that cellular expression levels of the different organizing and activating subunits NOXO1, NOXA1, p47^{phox}, and p67^{phox} is the greatest determinant in whether a "hybrid" Nox system where Nox1 is associated with Nox2 subunits p47^{phox} and/or p67^{phox} exists. Hybrid Nox systems further complicate the expression profile and regulation of Noxes. That is, with respect to Nox1 or 2 systems utilizing p47^{phox}, these systems may be inducible through activation of protein kinase C-dependent p47^{phox} phosphorylation and subsequent repression of its auto-inhibitory domain [125, 130]. The presence of hybrid Nox1 and/or Nox2 systems complicates the use of pharmacological Nox inhibitors in that drugs

specifically targeting any Nox cytosolic organizing or activating component will potentially lack specificity against a single Nox oxidase complex, be they canonical or hybrid. As such, any drug targeting cytosolic Nox proteins must be carefully evaluated for its specificity against Nox hybrid systems.

In contrast to the multimeric protein organization of Nox1 and Nox2, Nox4 and Nox5 are simpler in nature. It is now generally accepted that the fully-functional Nox4 oxidase is the aggregate of two polypeptide chains, the first being $p22^{phox}$ and the second being the Nox4 catalytic core [52, 115, 131]. Even simpler yet is the single polypeptide transcript that constitutes the entire Nox5 oxidase [53]. However, the simplicity in constitution of Nox4 and Nox5 belies their more complex regulatory mechanisms, such as the stimulation of Nox4 by polymerase delta interaction protein 2, Poldip2 [132]. Separately, Nox5's transcript bears two calcium binding EF hands which serve to activate enzyme activity in response to increasing intracellular calcium concentrations [54]. As endothelin receptors are known potentiators of calcium release, it is possible that Nox5 is indirectly activated by endothelin receptor signaling [133]. The independent expression and regulation of these Noxes can lead to dramatically different vascular phenotypes in a context-dependent manner, in part due to the different cellular and intracellular localization of the enzyme.

1.2.4 Roles of Nox in Cardiovascular Physiology/Pathophysiology

A number of studies have provided evidence supporting a major role for Nox1 and Nox2 in vascular homeostasis and pathophysiological ischemic injury and systemic hypertension [2, 9, 75, 107, 134-136]. Multiple effectors of $O_2^{\cdot -}$ are responsible for the downstream signaling of Noxes in blood flow and vascular tone, with two major culprits being a) the destruction of NO and b) uncoupling of eNOS through BH_4 oxidation, with both resulting in a decreased soluble

guanylate cyclase activation and smooth muscle relaxation [8, 9, 23, 137]. Beyond prevention of smooth muscle relaxation and vasodilation, Nox1- and Nox2-derived $O_2^{\cdot-}$ are established contributors to neointimal and medial proliferation/cell migration and subsequent vessel occlusion [138, 139]. Intimal/medial structural abnormalities of the microvasculature, i.e. small arteries, and resistance vessels, have been correlated with hypertension and support the current paradigm that the majority of pathophysiological changes in arterial walls in hypertension occur in small resistance vessels [140, 141].

The role of Nox5 in the vasculature is presumed to be similar to that of Nox1 and Nox2, although substantially less is known about its function due to the Nox5 gene being absent in murine models. The ensuing lack of appropriate animal models of Nox5 in cardiovascular disease and its relatively recent discovery in the human vasculature limit clear phenotypic connections between Nox5 and cardiovascular physiology, with the most detailed studies suggesting a correlation between Nox5 expression and myocardial infarction and more recent interest in its role in kidney glomerular filtration barrier damage as well as spermatozoa maturation and capacitation [109, 142-144]. Furthermore, evidence exists for Nox5's role in carcinogenesis and its direct role in cell transformation and indirect potentiation of angiogenesis by increased ROS [109, 145, 146]. Pathophysiological effects of Nox-derived $O_2^{\cdot-}$ effects on hypertension inherently extend from resistance vessels to the heart where increased resistance vessel afterload forces cardiac adaptation to maintain adequate tissue perfusion. While multiple pathways contribute to cardiac compensation in response to afterload, one controversial pathways is a potentially protective role for Nox4 in myocardial damage by promoting compensatory cardiac hypertrophy, angiogenesis, and fibroblast→myofibroblast transformation [99, 113, 147]. In contrast, Nox2 appears to have a less controversial, deleterious role in cardiac

dysfunction, causing pathologic remodeling in response to myocardial infarction and chemotherapeutic agents [148, 149]. To date, most cardiac Nox research has been narrowly focused on the most highly-expressed cardiac Nox isoforms Nox2 and Nox4 and, as such, very little is known about Nox1 in cardiac tissue.

Beyond their role in systemic hypertension and left heart failure largely established through genetic knockouts and knockdowns, Noxes have been also been identified as contributors to other systemic CVD, including atherosclerosis, ischemia reperfusion injury, aberrant vessel growth and diabetic vasculopathy [150-154]. Most simply put, Nox1 directly augments vascular tone *via* its downstream effects on actin-myosin coupling, thus contributing to hypertension [136]. Additionally, Nox1 also contributes to intimal occlusion, vessel remodeling, and neointimal hyperplasia throughout the systemic vasculature [2, 138, 155]. Mechanistically-speaking, Nox1 contributes to neoplastic growth by uncoupling eNOS, increasing production of VEGF and the ROS produced by Nox1 are capable of activating matrix metalloproteases (MMP) [9, 83, 95, 100, 156]. By extension of these biochemical data, *in vitro* and *in vivo* data have shown Nox1 is an angiogenic factor [83, 98]. The contribution of Nox1 to neoplasia, angiogenesis, and eNOS uncoupling is strongly suggestive of a role for Nox1 in the development and progression of diseases linked to angiogenesis and vessel remodeling including cancer and pulmonary arterial hypertension. Specific pharmacological inhibitors of individual Nox isoforms remain highly sought after for their potential utility in scientific investigation and therapeutic intervention in a variety of pathologies. Furthermore, despite the well-established role of Noxes in systemic hypertension, little is known about Noxes in pulmonary hypertension.

Nox isoform	Cellular distribution	Subcellular localization	Primary ROS Product
Nox1	Colon epithelium, vascular smooth muscle cells, endothelial cells, osteoclasts, reproductive organs	Intracellular membranes close to ER, endosomes, signalosomes, caveolae	Superoxide anion
Nox2	Neutrophils, macrophages, endothelial cells, vascular smooth muscle cells, fibroblasts, skeletal muscle cells, cardiomyocytes	Plasma membrane, phagosomes, perinuclear	Superoxide anion
Nox3	Inner ear (vestibular system, cochlea), skull, brain, fetal tissues	Plasma membrane	Superoxide anion
Nox4	Kidney, vascular smooth muscle cells, fibroblasts, hematopoietic stem cells, osteoclasts, neurons, endothelial cells	Focal adhesions, ER, nucleus, mitochondria	Hydrogen Peroxide
Nox5	Vascular smooth muscle cells, endothelial cells, bone marrow, lymph nodes, spleen, reproductive tissues, stomach, pancreas	Plasma membrane, ER	Superoxide anion
Duox1/2	Thyroid, airway epithelia, prostate, digestive system (Duox2)	Apical membrane	Hydrogen Peroxide

Table 1-2: Cellular distribution of Nox expression.

Reprinted from FRBM, Vol. 51/7, Al Ghouleh et. al. "Oxidases and peroxidases in cardiovascular and lung disease: New concepts in reactive oxygen species signaling" pgs 1271-1288. ©2011. With permission from Elsevier, ref. [36].

1.2.5 Existing Nox Inhibitors

Current widely-used Nox inhibitors include a number of small molecules and peptides that exhibit either unknown or limited specificity for any particular Nox isoform. The most widely used Nox inhibitors today include diphenyleneiodonium (DPI), GKT137831, apocynin, and Nox2ds-tat [2, 112, 130, 157-162]. Historically, DPI and apocynin have played major roles in implicating the contribution of Nox-derived ROS to cellular processes, yet they are both burdened by a complete lack of specificity for any Nox isoforms. More specifically, while DPI is a highly efficacious Nox inhibitor, it also broadly inhibits all flavoproteins utilizing FAD as a cofactor including nitric oxide synthase and NADH dehydrogenase [157, 158, 163, 164]. In turn, apocynin is a pro-drug that inhibits Nox exclusively in cells expressing myeloperoxidase, those primarily being leukocytes [165]. When permeating cells other than leukocytes, apocynin is not converted into Nox-inhibiting apocynin dimers and could serve as a nonspecific antioxidant that scavenges H_2O_2 and $HO\cdot$ [165]. One of the very few compounds reported to be specific for Nox1 over Nox2 is ML171 [159]. While ML171 is reportedly an effective and specific Nox1 inhibitor, there is a complete lack of information concerning its mechanism of action and its binding target, thereby hindering its extension into pre-clinical trials. It is also untested whether ML171 acts on Nox4, Nox5, or XO-derived ROS production. The only Nox inhibitor to have reached clinical trials is GKT137831, a small molecule effective for Nox1/4 inhibition [160]. GKT137831 has shown good oral bioavailability and is being investigated in diabetic nephropathy, although its inability to distinguish between Nox1 and Nox4 may potentially cause undesired side effects [166]. Nox2ds is a peptide derived from the intracellular B-loop of Nox2 (residues 86-103) that has demonstrated utility in ischemic retinopathy, cerebral microcirculation, and angiotensin II-stimulated ROS when conjugated to the cell penetrating

sequence [H]-R-K-K-R-R-Q-R-R-R-[NH2], also known as “tat” for its derivation from the human immunodeficiency virus 1 protein of the same name [151, 167-169]. Despite the wide utility of Nox2ds, its specificity among Nox isoforms had not been tested prior to a comprehensive study by Csanyi et al. [130] which includes studies performed by this candidate as part of his training in the Pagano laboratory. This body of work, for which the candidate was a contributor, proved the specificity of Nox2ds for Nox2. Most importantly, this thesis describes the design and mechanistic characterization of a specific Nox1 inhibitor with a validated target (NoxA1ds). Further investigation revealed that Nox1 is the primary Nox responsible for pulmonary endothelial $O_2^{\cdot-}$ production and VEGF-stimulated migration followed by *in vivo* investigation of the therapeutic benefit of Nox1 inhibition in PAH.

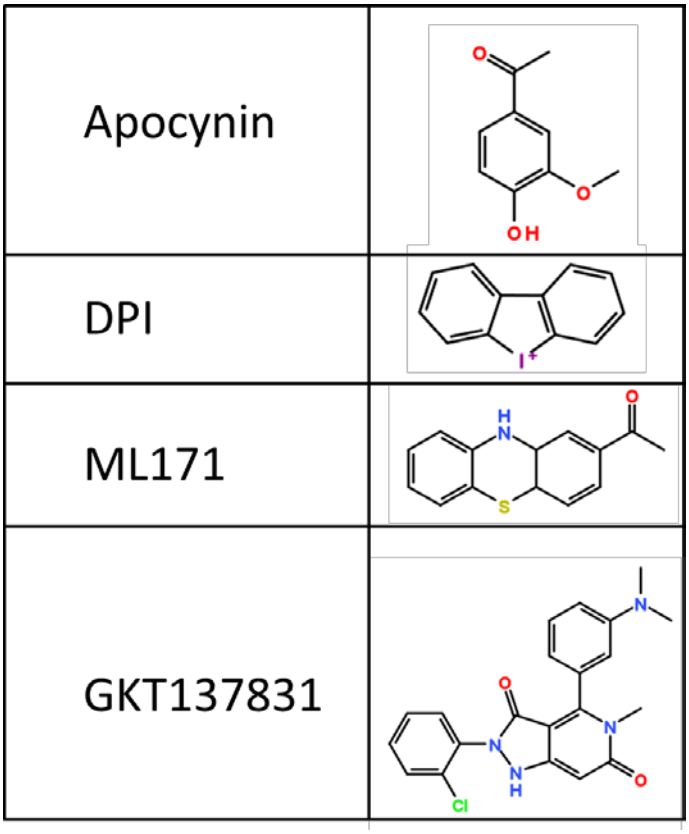

Figure 1-4 Structures of Existing Nox1 Inhibitors

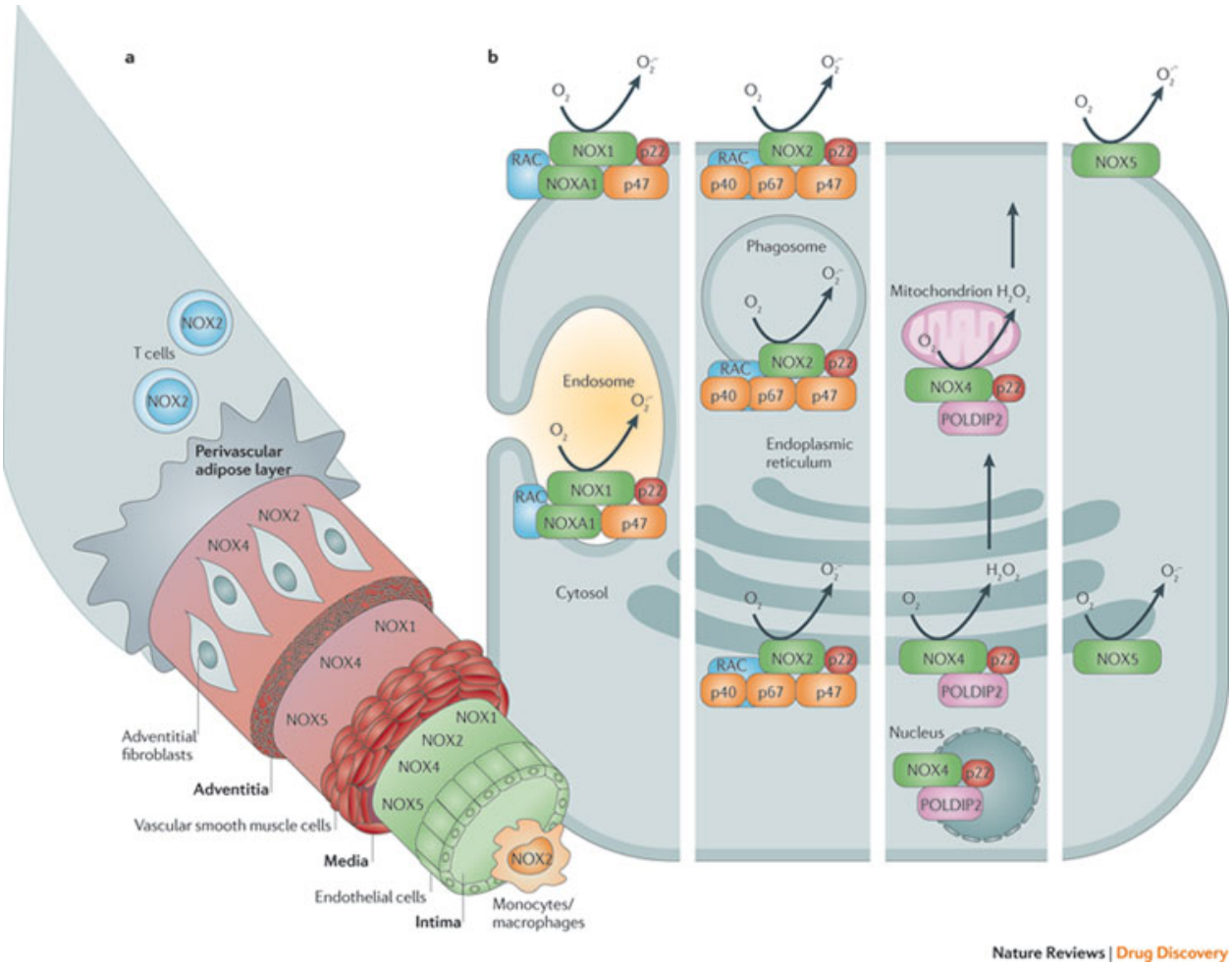

Figure 1-5: Tissue, cellular, and intracellular distribution of vascular Nox isoforms.

A) Schematic diagram showing cellular localization (endothelial cells, vascular smooth muscle cells, fibroblasts, macrophages and T cells) of NADPH oxidase isoforms (NOX1 oxidase, NOX2 oxidase, NOX4 oxidase and NOX5 oxidase) through a cross-section of an artery. **B)** Schematic diagram of a hypothetical cell in which all of the vascular NADPH oxidase isoforms (starting with NOX1 oxidase in the left hand column and finishing with NOX5 oxidase in the right hand column) are expressed in each of their possible subcellular locations. H_2O_2, hydrogen peroxide; NOXA1, NADPH oxidase activator 1; $O_2^{\bullet-}$, superoxide; p22, $p22^{phox}$; p40, $p40^{phox}$; p47, $p47^{phox}$; p67, $p67^{phox}$; POLDIP2, polymerase δ-interacting protein 2.

Reprinted by permission from Macmillan Publishers Ltd: [Nature Reviews Drug Discovery] Ref [72].

1.3 PULMONARY ARTERIAL HYPERTENSION

1.3.1 Pathophysiology of Pulmonary Arterial Hypertension

Pulmonary arterial hypertension (PAH) is a debilitating disease with high mortality characterized by a mean pulmonary artery pressure (mPAP) greater than 25 mmHg. Diagnosis of PAH through right heart catheterization is often performed after by exclusion of other diseases with similar symptoms, these symptoms including chest pain and a shortness of breath. Idiopathic PAH comprises nearly half of all cases of PAH, yet its cause is completely unknown and this progressive disease has no cure [170]. More common is the reversible, altitude-associated PAH. At high altitudes (>3500 meters), lung vasculature of healthy individuals compensates for reduced atmospheric oxygen through pulmonary vasoconstriction. This, in turn causes elevation of pulmonary artery pressures leading to clinical pulmonary hypertension which is ameliorated upon return to lower altitudes [171]. Epidemiological data from individuals with altitude-associated PAH and data indicating severe hypoxia in patients with idiopathic PAH are highly supportive of the paradigm that hypoxia plays a critical role in the pathogenesis of PAH [170, 171].

While hypoxia is a critical factor in the development of PAH, other factors including reduced NO bioavailability and vascular remodeling/occlusion contribute to the pathogenesis of PAH. Through abnormal proliferation of the intima, media and adventitia within the pulmonary vasculature; pathophysiological vessel remodeling occurs and plexiform lesions (PXLs) arise [170, 172]. The presence of angiogenic markers in PXLs indicates that these lesions may be the result of angiogenic signaling processes stimulated by hypoxia. Similarly, observational studies of clinical patients with PAH reveal that remodeling in pulmonary vessels is largely initiated by

endothelial cells and that proximal to the PXL, vessels exhibit an increase in intimal thickness [172-174]. Circumstantial evidence supporting the hypothesis that hypoxic angiogenic signaling contributes to PXL formation in PAH also is observed in the similarities between PXL histology and glomeruloid lesions in glioblastoma multiforme, a malignant cancer with particularly strong angiogenic signaling [172, 175]. The combination of proximal intimal remodeling and the redirection of blood flow around the PXLs are major contributors to a steady increase in pulmonary vascular resistance (PVR), RV ESPVR, and attendant pressure overload in the right ventricle.

1.3.2 Cellular Signaling Pathways Contributing to Pulmonary Arterial Hypertension

As evidenced by multiple *in vitro* and *in vivo* studies, hypoxia contributes to pulmonary vascular ROS production (via Nox and mitochondria), cell proliferation (through HIF1α), and pulmonary vessel remodeling [82, 94, 176, 177]. Each of these phenomena plays a role in attenuating pulmonary artery relaxation during hypoxia, either through $O_2^{\cdot-}$ scavenging of NO, pulmonary microvessel remodeling and occlusion, or reduced vascular compliance [178-181]. Through investigating cellular potentiators of PAH, caveolin-1 dysfunction has emerged as a consistent theme in the disease, despite continuing disagreement as to the exact mechanism [182, 183]. Though investigating the role of caveolin-1 in PAH, a clear relationship between it and ROS, eNOS and PAH has been established, as both caveolar dysfunction and ROS production attenuate NO bioavailability in pulmonary vessels through eNOS uncoupling [3, 183-186]. Beyond reduced activity of sGC and concomitant constriction of vascular smooth muscle cells, decreased NO bioavailability is also permissive of endothelial proliferation [187, 188]. ROS directly reduce NO availability by conversion of NO to $ONOO^-$ and by inhibiting NO production through inactivation of BH_4, resulting in uncoupled eNOS and in turn propagating systemic and

pulmonary endothelial proliferation [6, 7, 186]. Thus, an imbalance in favor of increased ROS vs. NO presumably would lead to increased endothelial proliferation and PAH. The two opposing functions suggest that regulation of eNOS and NO availability by Nox-derived $O_2^{\cdot-}$ may be a primary regulator of endothelial physiology and that the coupling or uncoupling of eNOS results in either endothelial maintenance or growth, respectively.

Beyond regulation of endothelial physiology by Nox-mediated eNOS uncoupling, soluble growth factors leading (i.e. VEGF, EGF) to proliferation of pulmonary endothelial cells are also implicated in the development of PAH [174, 189]. Endothelial growth and migration is a major component of microvessel remodeling and, along with the reduced compliance of pulmonary arteries deprived of NO, is a primary contributor to increasing pulmonary vascular resistance (PVR) and clinical PAH. In early PAH, the RV compensates for the persistent increase in PVR through thickening, proliferation, and hypertrophy of cardiac tissue. Unfortunately, the RV cannot compensate indefinitely and RV failure normally ensues in PAH and can occur within 5 years of diagnosis if left untreated [170]. Hemodynamically, RV failure in PAH is observed as a sharp increase in ESPVR and RV pressure, indicative of greater contractility [190]. Inhibitors of ROS sources are expected to reduce proliferation and/or lower pulmonary vascular remodeling, leading to lower PVR and improved prognosis for patients with PAH. Despite the great potential of ROS inhibitors, no effective antioxidant treatment for this disease has yet been identified.

1.3.3 *In Vitro* Cellular Models Applicable to Pulmonary Arterial Hypertension

In attempting to model vasculature pathology in PAH using isolated cellular models, it is essential to consider that the primary vascular etiological factors of clinical PAH are hypoxia, angiogenic growth factors, and vascular remodeling [170]. To best mimic these etiological factors, hypoxia or angiogenic growth factors can be used to perturb the phenotype of pulmonary

vascular cells followed by phenotypic measurements of ROS production, protein expression, proliferation, or migration, as *in vitro* indications of PAH physiology. Of particular importance are *in vitro* models utilizing hypoxia as this is both a causative agent and an indicator of disease severity in PAH [170, 171]. Blood oxygen tension *in vivo* can vary widely from 1.0-10.0%, depending on the tissue bed. Typically, smaller vessels and those more distal from conduit arteries have lower oxygen saturation [191, 192]. Emerging from these *in vivo* measurements and clinical data from PAH patients is the current practice of using *in vitro* oxygen tensions from 1-5.0% as an *in vitro* approximation of severe pulmonary hypertension [189, 193]. In addition to hypoxia, other factors observed in clinical PAH that are useful for *in vitro* approximations include endothelin-1, estrogen metabolites, free heme, and angiogenic growth factors [194-197]. While each of these stimuli bears important implications in the pathogenesis of PAH, angiogenic growth factors merit further discussion due to their clear role in vessel remodeling and probable interactions with Nox.

The overexpression of angiogenic molecules in diseased pulmonary vessels supports the hypothesis that PAH is driven in part by disordered angiogenesis and has led to investigations on the role of angiogenic factors as contributors to PAH, in particular, HIF1α, EGF, VEGFR2, and Tie2 [174, 175, 181, 198]. As such, assays monitoring cell proliferation, mitogenic potential, migratory ability, and/or potential sprouting of pulmonary artery smooth muscle cells, endothelial cells, and/or fibroblasts are all widely used as *in vitro* approximations of pulmonary vasculature remodeling [84, 199, 200]. During the progression of PAH, the endothelium is a key player in the remodeling of pulmonary vessels, with additional contributions by the medial and adventitial layers both in composition of remodeled arteries and enhancement of remodeling via paracrine signaling factors [172, 173, 175]. While smooth muscle and fibroblast components of

pulmonary vessels cannot be ignored and remain critically important in the pathogenesis of PAH, many *in vitro* assessments pulmonary vessel remodeling utilize endothelial cells for their sensitivity to hypoxia and close relationship with the regulation of vessel tone.

Hypoxia and angiogenic growth factors are key factors for perturbing vascular phenotypes in *in vitro* approximations of PAH with major phenotypic outcomes including increased ROS production, cellular proliferation and migration which are major contributors to increased pulmonary vascular tone and remodeling. Pulmonary endothelial cells are a key component of vascular remodeling and represent a significant portion of PAH pathology. However, the endothelium is not alone in PAH pathology and it is appropriate to also consider utilizing smooth muscle cells and fibroblasts. These stimuli, phenotypes, and cell types are reasonable representations of pulmonary vascular function *in vivo* and provide a reductionist perspective of PAH pathology.

1.3.4 *In Vivo* Models of Pulmonary Arterial Hypertension

Ongoing attempts to model PAH *in vivo* include the aforementioned major clinical characteristics of PAH including elevated mPAP, hypoxia, and vascular remodeling. Current *in vivo* models of PAH utilize a variety of toxicological agents, surgical modifications, hypoxic environments, and combinations of these to generate multiple competing models of PAH that all attempt to model this complex human disease. While no model is clearly superior to all others in every situation, there remain consistent advantages and disadvantages for each model.

Pulmonary artery banding of mice using a 27-gauge surgical clip is a useful surgical model of PAH and results in an immediate pressure overload of the right ventricle with concomitant increases in RV end systolic pressure of ~35mmHg [58, 201]. This increase in pressure is chronic so long as the surgical clip remains on the pulmonary artery. The

simultaneous advantage and disadvantage of this model is the ability to dissect the effect of pressure-overload on RV function independently of pulmonary vascular effects. Incidentally, RV dysfunction without accompanying vasculopathies is observed in some cases of PAH.

In addition to pulmonary artery banding, chronic mouse hypoxia at 10% O_2 for at least 3 weeks also remains a consistently popular method to model human PAH [202]. Similar to the human condition, mice in the hypoxic environment experience a sharp rise in mPAP and RV hypertrophy that are both reversible when oxygen tension is returned to normoxia [177]. Importantly, this model of PAH does not display the extent of vascular remodeling that is prevalent in humans.

Moving beyond mice in hypoxia, extensive research in PAH physiology has been also performed in rats where PAH is induced by a single subcutaneous injection of monocrotaline, which causes functional alterations in pulmonary endothelial cells without apoptosis [203]. Following monocrotaline injection, at least two weeks of rodent maintenance are necessary to allow for the disease to develop. The monocrotaline model of PAH is characterized by a sustained increase in mPAP, RV hypertrophy, and significant pulmonary vasculature remodeling. This model has been reported to be different from human PAH as it is caused independent of hypoxia [204]. In addition, monocrotaline injections also induce significant lung fibrosis, thus further complicating the pathophysiology of PAH in this model and hampering the ability to dissect precise roles of the vasculature [205].

The most recently developed rodent model of PAH utilizes the combination of the VEGFR2 antagonist SU5416 and chronic hypoxia (SUCH) in rats to induce elevated mPAP as well as RV hypertrophy and pulmonary arteriolar remodeling [206]. Of the *in vivo* models of PAH, SUCH bears the greatest similarities to human PAH with respect to vessel remodeling. A

reported disadvantage of the SUCH model is that inhibition of VEGFR2 by SU5416 causes endothelial damage distinct from potential endothelial insults in human PAH.

The advantages and disadvantages of each model as well as the desired endpoint of study are key components that the investigator has to consider to determine which animal model of PAH is the most appropriate for the proposed experiments. In the present study, the SUCH model of PAH was chosen to test the effect of Nox1 inhibition in PAH as SUCH disease severity correlates with severe lung vessel remodeling, a process that was postulated to be attenuated via Nox1 inhibition.

1.3.5 Clinical Treatment Options for Pulmonary Arterial Hypertension

In the past quarter-century, PAH has progressed from a virtually untreatable disease with rapid mortality to a disease which can be carefully managed through three main classes of pharmacological agents. These three classes include prostacyclin analogs, agents that increase nitric oxide (NO) bioavailability, and endothelin receptor antagonists. Historically, the benefits of prostacyclin in reducing pulmonary vascular resistance were observed as early as the 1970s in dogs with human studies occurring later in the early 1980s [207]. Later, increasing NO bioavailability through inhaled NO or nitrates was developed as an additional treatment for PAH after demonstrations of clinical efficacy in the early 1990s through drugs enhancing NO signaling cascades (PDE5 inhibitors) [71, 208-210]. A relatively new class of treatments acts by preventing endothelin-mediated vasoconstriction, with one of the primary endothelin receptor antagonists (bosentan) gaining U.S. Food and Drug Administration approval for the treatment of PAH in 2001.

Each of these treatments individually or in combination is eventually overcome by unsatisfactory clinical responses. Although highly effective at treating PAH, prostacyclin analogs

are also dangerously capable of causing pulmonary edema, leading to patient death [211]. In the case of NO donors and signal enhancers, unsatisfactory clinical responses may be a result of desensitization to NO or a reduced capacity of cells to endogenously generate NO, yet a more gradual and continual delivery may be beneficial [210, 212]. Additionally, the efficacy of NO is greatly reduced in conditions of increased adiposity and hypercholesterolemia [111, 213]. In the case of bosentan, about 10% of patients experience mild liver reactions with a portion of these patients experiencing severe hepatotoxicity [214]. Recent studies implicating endothelin in the preservation of RV contractility and compensation in response to increased afterload may contraindicate ET receptor antagonists in a subset of patients [190]. Each treatment option provides a viable means to treat PAH, yet no treatment is without its significant side effects or patients who are resistant to that particular therapy. Inasmuch as renin, aldosterone and angiotensin II, *per se*, are well-established promoters of reactive oxygen species production in the lung that are likely to impede and/or or exacerbate the effects of NO, prostacyclin, or endothelin blockade, the AngII type I receptor antagonists, sartans, could become an important adjuvant therapy in PAH [36, 58]. Moreover, angiotensin II type 1 receptor antagonist could serve to enhance NO bioactivity in obese and aging populations.

The most recently approved therapy for PAH is riociguat (Adempas®), a novel stimulator of soluble guanylate cyclase (sGC) which acts through sensitizing the heme core of sGC to NO [215, 216]. Following riociguat's 2013 FDA approval, increased energy has been directed towards the identification of therapies for PAH that act on ROS-dependent mechanisms. Despite these advances in the treatment of PAH, no treatment has been developed that acts through inhibition of angiogenic signaling or ROS production. To date, no Nox inhibitors have been tested as potential therapeutics for PAH, despite their great potential to improve PAH prognosis

through increasing NO biovailability, inhibiting angiogenic signaling pathways, and attenuating pathological pulmonary vascular remodeling.

Species	Mouse/Rat	Mouse	Mouse/Rat	Rat
Toxicological Stimuli	none	none	monocrotaline 40mg/kg	SU5416 20mg/kg
Surgical Stimuli	Pulmonary artery banding	None	None	None
Hypoxia Dependent	No	Yes, 10% Oxygen	No	Yes, 10% Oxygen
Disease Progression	Causes immediate and sustained elevation of mPAP	Phenotype apparent after 3 weeks, reversible in normoxia	Severe disease 2 weeks post injection, not reversible	Severe disease after 6 weeks, not reversible
Pulmonary Artery Pressure	Immediate elevation, ~35mmHg	Gradual elevation, ~35mmHg	Gradual elevation, ~60mmHg	Gradual elevation ~35mmHg
Degree of RV Remodeling	Moderate	Moderate	Severe	Severe
Degree of Pulmonary Vascular Remodeling	none	Minimal	Moderate	Severe
Advantages	Independently dissects RV function in pressure overload	Very good model for human altitude induced PAH, ease of use	Ease of use, greatest pulmonary pressures	Severity of lung vessel remodeling
Disadvantages	Independent of pulmonary vasculature	Reversible, not a good model for idiopathic PAH	Extensive fibrosis complicates pathology	Confounding factors resulting from VEGFR2 inhibition

Table 1-3: *In vivo* models of PAH

1.4 OVERVIEW AND SPECIFIC AIMS

1.4.1 Overview

NADPH Oxidases (Nox) are a family of enzymes that are professional producers of reactive oxygen species (ROS) including superoxide ($O_2^{\cdot -}$). Multiple Nox isoforms are expressed in pulmonary vessels, of which Nox1 is the most poorly studied. Hypoxia and growth factors have been shown to promote Nox1 activity in systemic vascular cells leading to cellular proliferation and invasion, however it is unknown whether Nox1 mediates proliferative cell phenotypes in the pulmonary vasculature. The role of Nox1 in the development of pulmonary disorders remains unknown. Furthermore, despite its well characterized association with cardiovascular morbidity and mortality, there previously has been no specific inhibitor of Nox1 with an established mechanism of action. We postulated that the putative activation domain of NOXA1 plays a key role in Nox1 activation. We tested whether a peptide sequence targeting this region specifically inhibits Nox1, and used it as a tool to investigate the relative role of Nox1 in pulmonary vascular disorders, and its potential to attenuate the development of PAH.

Pulmonary arterial hypertension (PAH) is a debilitating disease characterized by abnormal proliferation in pulmonary arterioles, tissue hypoxia, and elevated pulmonary artery pressures leading to right heart failure. Angiogenic markers in diseased pulmonary vessels exhibiting endothelial and smooth muscle proliferation imply angiogenic signaling, that contribute to vessel occlusion and progression of PAH. The roles of Nox2-derived ROS have been demonstrated in systemic as well as pulmonary artery vascular cell proliferation. Significantly less is known about the role of other Nox isoforms in angiogenic signaling in the pulmonary vasculature.

While both Nox1 and Nox2 are expressed in pulmonary vessels, their relative roles in pulmonary vascular physiology and pathology are unknown. It is unknown whether hypoxic induction of Nox-derived ROS plays a role in the development of PAH.

The overarching hypothesis of this dissertation was that **Nox1 promotes endothelial dysfunction and VEGF-stimulated pulmonary artery EC migration, and that these processes endow Nox1 with a pivotal role as a potentiator of PAH.** In order to test the hypothesis, the work described herein involved the design and characterization of the first peptidic Nox1 inhibitor (NoxA1ds). After confirming the specificity of NoxAS1ds, this peptide was utilized to inhibit Nox1 in *in vitro* approximations and *in vivo* models of PAH.

1.4.2 Specific Aim 1: Development and Characterization of NoxA1ds

Recent publications have established the primary importance of NOXA1 domain in functional Nox1 $O_2^{\cdot -}$ production. Amino acids in NOXA1 corresponding to the reported $p67^{phox}$ activation domain (residues 190-210) demonstrate a high level of homology and thus suggested its role as an activation domain in the Nox1 oxidase. We derived a peptide from this region of NOXA1 which was named "NoxA1ds" on the theory that it was a NOXA1 docking sequence for Nox, thus NoxA1ds. NoxA1ds' potency, efficacy and specificity were tested using heterologous cell-free assays prepared from whole cells transfected with each of the individual vascular Nox isoforms. NoxA1ds' activity was tested by measuring $O_2^{\cdot -}$ production in HT29 colon carcinoma cells exclusively expressing Nox1.

1.4.3 Specific Aim 2: To determine the relative contribution of Nox1 vs Nox2 to endothelial $O_2^{\cdot-}$ production and cell migration

While ROS have been correlated with endothelial dysfunction and PAH, the contribution of Nox1 and Nox2 in these pathways is unclear. Pharmacological inhibitors of Nox1 and Nox2 will be tested for their isoform specificity and utilized to determine the Nox isoform responsible for hypoxia-induced $O_2^{\cdot-}$ production and endothelial dysfunction as well as VEGF-stimulated wound healing. Crosstalk between HPAEC and HPASMC will be investigated by hypoxic conditioning of each cell type to stimulate cytokine production followed by transfer of conditioned media to naïve HPAEC/SMC. The relative role of Nox1/2 in HPAEC/SMC proliferation in this conditioned media will be evaluated by MTT assay.

1.4.4 Specific Aim 3: To investigate the role of Nox1 in Pulmonary Arterial Hypertension using NoxA1ds

We will evaluate the role of Nox1 in an *in vivo* model of PAH by injecting rats subcutaneously with SU5416 and exposing the rats to 3wks of chronic hypoxia to induce severe PAH. Throughout this study, the role of Nox1-derived O_2^- in PXL formation will be tested by aerosolized delivery of NoxA1ds to rat lungs or Nox1 morpholino injection, *i.v.*, at 0, 1, and 3 wks. Measures of PAH (Fulton Index and RV pressure) will be taken followed by *ex vivo* quantification of ROS production (EPR, cytochrome *c*) in tissue homogenates.

2.0 MATERIALS AND METHODS

2.1.1 Reagents

Cytochrome c, superoxide dismutase (SOD), lithium dodecyl sulfate (LiDS), catalase, diphenyleneiodonium chloride (DPI), horseradish peroxidase (HRP), hypoxanthine, and rhodamine B were purchased from Sigma-Aldrich (St. Louis, MO, USA). Xanthine Oxidase was obtained from Calbiochem (Merck, KGaA, Damstadt, Germany). Amplex Red was purchased from Invitrogen (Eugene, OR, USA). Protease inhibitor cocktail was purchased from Roche Diagnostics GmbH (Mannheim, Germany). NoxA1ds and scrambled NoxA1ds were synthesized by the Tufts University Core Facility (Boston, MA, USA). The sequence of NoxA1ds is as follows: [NH3] E-P-V-D-A-L-G-K-A-K-V [CONH2]. The scrambled NoxA1ds sequence (SCRMB) is as follows: [NH3] L-V-K-G-P-D-A-E-K-V-A [CONH2]. The sequence of Nox2ds is [NH3] C-S-T-R-I-R-R-Q-L[CONH2]. The scrambled Nox2ds sequence (scrmb) is [NH3] C-L-R-I-T-Q-S-R [CONH2]. The sequence of the cell penetrating peptide “tat” is [NH3] R-K-K-R-R-Q-R-R-R [CONH2] and, if used, was added to the amino end of the peptide. In all cases the [NH3] group represents the amino end and [CONH2] represents the amide of the carboxy terminus, a consequence of the synthetic procedure. Each peptide was prepared in several batches, with no batch having purity less than 90%. FITC-labeled NoxA1ds was also synthesized by Tufts University and is identical in sequence to NoxA1ds with FITC linked to the N-terminus of NoxA1ds via an alpha hydroxyl acid. Rhodamine-labeled NoxA1ds was synthesized by Fisher Scientific GmbH (Schwerte, Germany) and is identical in sequence to NoxA1ds with Rhodamine B linked to the N-terminus of NoxA1ds via an alpha hydroxyl acid.

2.1.2 Cell Lines

COS-22 (COS-7 cells stably expressing human $p22^{phox}$) and COS-Nox2 (a.k.a. COS-^{phox}) cells (COS-7 cells stably expressing human $p22^{phox}$, Nox2, $p47^{phox}$ and $p67^{phox}$) were kindly provided by Dr. Mary C. Dinauer (Indiana University, School of Medicine). COS-22 cells were maintained in Dulbecco's Modified Eagle Medium (Cellgro) with 4.5 g/l glucose, L-glutamine and sodium pyruvate containing 10% heat-inactivated fetal bovine serum (FBS, Invitrogen), 100 units/ml penicillin and 100 µg/ml streptomycin (Invitrogen) supplemented with 1.8 mg/ml G418 (Calbiochem/EMB Bioscience, Gibbstown, NJ). COS-Nox2 cells were maintained in otherwise-identical media supplemented with 1 µg/ml puromycin (Sigma, St Louis, MO) and 0.2 mg/ml hygromycin B (Invitrogen, Carlsbad, CA). HEK-Nox5 (HEK-293 cells stably expressing human Nox5) were kindly provided by Dr. David Fulton (Georgia Health Sciences University) and were maintained in DMEM with 4.5 g/l glucose, L-glutamine and sodium pyruvate containing 10% FBS, 100 units/ml penicillin and 100 µg/ml streptomycin. HT-29 cells were purchased from ATCC and cultured in McCoy's 5a Medium Modified (Manassas, VA). HEK-293 cells were purchased from ATCC and cultured Dulbecco's Modified Eagle Medium (Manassas, VA). HPAEC, HPASMC and their growth medium (EBM-2 or SmGM, respectively) were purchased from Lonza (Basel, Switzerland). HPAF and their growth medium were purchased from ScienCell Laboratories (Carlsbad, CA). COS, HEK, and HT-29 cells were used within 7-10 passages for all experiments while HPAEC were used within 5-8 passages.

2.1.3 Plasmid Preparation, Amplification and Purification

Plasmids encoding full-length human cDNAs for Nox1 (pcDNA3.1-hNox1), NOXO1 (pcDNA3.1-hNOXO1), NOXA1 (pCMVsport 6-hNOXA1), and Nox4 (pcDNA3-hNox4) were kindly provided by Dr. David Lambeth (Emory University, GA) [108, 217]. Plasmids encoding full-length human cDNA's for Nox1-YFP and NoxA1-CFP were custom subclones purchased from OriGene (Rockville, MD). Nox1-YFP was subcloned into the pCMV6-AC-mYFP plasmid and NOXA1-CFP was subcloned into the pCMV6-AC-mCFP plasmid. Both plasmids placed the fluorophore at the C-terminus of the Nox-protein sequence. A membrane-targeted CFP with extensive N-terminal myristoylation (CFP^m) was kindly provided by Dr. Jean-Pierre Vilardaga (Pittsburgh, PA) [218]. Plasmids encoding Nox1, NOXO1, NOXA1, Nox1-YFP, NOXA1-CFP, or CFP^m were transformed and amplified into Escherichia coli strain TOP10 (Invitrogen, Carlsbad, CA). Plasmids were purified using a QIAfilter plasmid purification kit (QIAGEN Inc., Valencia, CA.).

2.1.4 Detection of Nox1/2/5-derived Superoxide Anion ($O_2^{\bullet -}$)

Separate populations of COS-22 cells were transfected with pcDNA3.1-hNox1 (COS-Nox1) or a co-transfection of pcDNA3.1-hNOXO1 and pCMVsport 6-hNOXA1 (COS-NOXO1/A1). Adherent cells were harvested by incubating with 0.05 % trypsin /EDTA for 5 min at 37°C. Following addition of DMEM/10%FBS to neutralize the trypsin, the cells were pelleted by centrifugation at 1000 x g for 5 min at 4°C and subsequently resuspended at 5 x 10^7 cell/ml in lysis buffer (8 mM potassium, sodium phosphate buffer pH 7.0, 131 mM NaCl, 340 mM sucrose,

2 mM NaN_3, 5 mM $MgCl_2$, 1mM EGTA, 1 mM EDTA, 1 mM DTT and protease inhibitor cocktail) [219]. The cells were lysed by freeze/thaw cycles (5 cycles), and passed through a 30-gauge needle 5 times to further lyse the cells and then centrifuged at 1000 x g for 10 min at 4°C to remove unbroken cells. The supernatant was then centrifuged at 160,000 x g for 60 min at 4°C to yield a membrane-enriched pellet (membrane fraction). The membrane fraction from COS-Nox1 was resuspended in lysis buffer and retained whereas the COS-NOXO1/A1 cytosolic fraction was retained. $O_2^{\cdot -}$ generation was measured in oxidase assay buffer (OAB) (65 mM sodium phosphate buffer (pH 7.0), 1 mM EGTA, 10 μM FAD, 1 mM $MgCl_2$, 2 mM NaN_3, and 0.2 mM cytochrome *c* with added 1000 U/ml catalase to prevent H_2O_2-mediated oxidation of cytochrome *c* [219]). The components of the cell-free system were added in the following order: oxidase assay buffer, COS-Nox1 cell membrane fraction (5 x 10^5 cell equivalents/well, approximately 5 μg protein/well), NoxA1ds/SCRMB peptides followed by 10-min incubation on ice, after which COS-NOXO1/A1-containing cytosolic fractions were added (5 x 10^5 cell equivalents/well). Plates were placed on an orbital shaker for 5 min at 120 movements/min at room temperature before addition of 180 μM NADPH to initiate $O_2^{\cdot -}$ production. The production of $O_2^{\cdot -}$ was calculated from the initial linear rate (over 15 min) of SOD-inhibitable cytochrome c reduction quantified at 550 nm using an extinction coefficient of 21.1 mM^{-1} cm^{-1} (Biotek Synergy 4 Hybrid Multi-Mode Microplate Reader). The concentration of NoxA1ds peptide that caused 50% inhibition of $O_2^{\cdot -}$ production (IC_{50}) in COS-Nox1 cell lysates was calculated by Prism 5 (GraphPad Software, Inc. La Jolla, CA, USA).

To measure Nox2-derived $O_2^{\cdot -}$ production, COS-Nox2 cells were separated into membrane and cytosolic fractions as described above. The production of $O_2^{\cdot -}$ was measured using identical methods with the addition of 130 μM LiDS after incubation with NoxA1ds or SCRMB. HEK-

Nox5 $O_2^{\cdot -}$ production was determined using methods as described previously with NoxA1ds and SCRMB peptides being added to HEK-Nox5 membrane lysates prior to the addition of calcium (final concentration 20 μM) [54]. Throughout these procedures, extreme care was taken to maintain the lysate at a temperature close to 0 $^{\circ}$C.

2.1.5 Detection of Nox4-derived hydrogen peroxide (H_2O_2)

H_2O_2 production was quantified in COS-Nox4 cell lysates as described previously [220]. It is important to note that COS-Nox4 cells do not produce measureable amounts of $O_2^{\cdot -}$ [130]. COS-Nox4 and COS-22 cells were suspended to a concentration of 5×10^7 cells/ml in ice-cold disruption buffer (PBS containing 0.1 mM EDTA, 10 % glycerol, protease inhibitor cocktail, and 0.1 mM PMSF). The cells were lysed by five freeze/thaw cycles and passed through a 30-gauge needle five times to further lyse the cells. Incubation of COS-Nox4 cell lysate (10 μg/100 μl) with NoxA1ds was performed in assay buffer (25 mM Hepes, pH 7.4, containing 120 mM NaCl, 3 mM KCl, 1 mM $MgCl_2$, 25 μM FAD, 0.1 mM Amplex Red, and 0.32 U/ml of HRP) for 15 min at room temperature on an orbital shaker (120 movements/min), before the addition of 36 μM NADPH, to initiate H_2O_2 production. This relatively low concentration of NADPH was used because it was found that higher concentrations interfered with Amplex Red fluorescence. Fluorescence measurements were made using a Biotek Synergy 4 Hybrid Multi-Mode Microplate Reader (excitation wavelength: 560 nm; emission wavelength: 590 nm). A standard curve of known H_2O_2 concentrations was developed using the Amplex Red assay (per the manufacturer's instructions, manufacturer: Life Technologies, Carlsbad, CA), and was used to quantify H_2O_2 production in the COS-Nox4 cell free system. The reaction was monitored at

room temperature for 60 min. The emission increase was linear during this interval. The effect of NoxA1ds on Nox4-derived H_2O_2 production was expressed as percent inhibition of Nox4, which was calculated by designating the amount H_2O_2 production by control mixtures in the absence of peptide as 100%.

2.1.6 $O_2^{\cdot -}$ generating activity in HEK 293 cells

In order to test the effect of Nox2ds on inducible Nox1 activity we used Nox1/NOXO1/NOXA1-transfected HEK 293 cells (hereafter referred to as HEK-Nox1) as it was shown previously that $O_2^{\cdot -}$ production in HEK-Nox1 cells was significantly stimulated by phorbol myristate acetate (PMA) treatment[117]. The effect of Nox2ds on inducible Nox1 activity was tested on LiDS-stimulated $O_2^{\cdot -}$ in HEK-Nox1 cell-free system. HEK 293 cells were separately transfected with either Nox1, NOXO1 or NOXA1. Nox1-containing membranes, and NOXO1 and NOXA1 cytosolic extracts from each preparation were prepared as described above. The Nox1 organizer subunit NOXO1 was preincubated with 10 μM Nox2ds for 10 min, and then NOX1 and NOXA1 were added consecutively. After the preincubation period, LiDS (130 μM) was added to induce the assembly of the oxidase by permitting membrane reorganization. LiDS was followed by initiation of $O_2^{\cdot -}$ production by 180 μM NADPH. Superoxide production was measured using cytochrome c.

2.1.7 Xanthine oxidase-derived $O_2^{\cdot-}$ production

The nitroxide spin probe 1-hydroxy-3-methoxycarbonyl-2,2,5,5-tetramethylpyrrolidine hydrochloride (CPH; Alexis Corp., San Diego, CA) was used to examine $O_2^{\cdot-}$ production using a Bruker eScan Table-Top EPR spectrometer (Bruker Biospin, USA). $O_2^{\cdot-}$ production in semi-purified preparations of xanthine oxidase initiated by the addition of 100μM xanthine was measured in Krebs HEPES buffer (100 mM NaCl, 5 mM KCl, 2.5 mM $CaCl_2$, 1.2 mM $MgSO_4$, 25 mM $NaHCO_3$, 1.0 mM KH_2PO_4, 5.6 mM D-Glucose, 20 mM Na-HEPES) supplemented with 50 μM CPH. Purified xanthine oxidase was incubated with NoxA1ds or SCRMB for 5 min at room temperature. Analyses of the CPH up-field spectra peak amplitude from peak to nadir were used to quantify the amount of $O_2^{\cdot-}$ produced by the lysates and were compared with buffer-only control spectra or spectra in the presence of NoxA1ds, SCRMB, or 200 U/ml SOD. To minimize the deleterious effects of contaminating metals, the buffers were treated with Chelex resin and contained 25 μM deferoxamine (Noxygen Science Transfer, Germany). The EPR instrument settings were as follows: field sweep, 50 G; microwave frequency, 9.78 GHz; microwave power 20 mW; modulation amplitude, 2 G; conversion time, 327 ms; time constant, 655 ms; receiver gain, 1 x 10^5, DETC (Noxygen Science Transfer, Germany).

2.1.8 Detection of $O_2^{\cdot-}$ Production by Whole Cells Treated with NoxA1ds

HT-29 cells at 80% confluence were serum starved in media containing 0.5% FBS for 12 hrs and NoxA1ds (final concentrations of 0.1, 0.3, 1, 3, or 5μM) was added directly to the growth media for one hour prior to cell lysis and membrane preparation for cytochrome *c* assay.

To measure HPAEC $O_2^{\cdot-}$ production, cells were grown to 80% confluence prior to 12 hr serum starvation (0.2 % FBS). Cells were placed in normoxic (20% O_2) or hypoxic (1% O_2) conditions for 23 hrs and then treated with 10 µM NoxA1ds, SCRMB NoxA1ds, Nox2ds-tat, or SCRMB Nox2ds-tat for 1 hr. For both HT-29 and HPAECs, cells were lysed in lysis buffer by 5 freeze/thaw cycles and 5 passages through a 30 gauge needle. Membrane fractions were collected by centrifugation (28,000 xg, 20 min). Membranes were suspended in OAB and NADPH-dependent $O_2^{\cdot-}$ production was determined using cytochrome c reduction.

2.1.9 Enzyme-Linked Immunosorbent Assay (ELISA)

ELISA was first used to determine whether NoxA1ds binds Nox1. Neutravidin-coated plates (Thermo Scientific, Rockford, IL, USA) were incubated with 10 µM biotinylated NoxA1ds or 10 µM biotinylated SCRMB (Tufts University Core Facility, Boston, MA, USA) for 2 hr at room temperature. The plates were washed 3 times with wash buffer (25 mM Tris, 150 mM NaCl, and 0.05% Tween-20, pH 7.2). After 1 hr incubation at room temperature, 50 µg of membrane fractions prepared from either COS-22 or COS-Nox1 cells were added to plates in phosphate buffered saline (pH 7.2) at room temperature and allowed to incubate for 1 hr. Rabbit polyclonal Nox1 antibody (1:500; Santa Cruz Biotechnology, Santa Cruz, CA, USA) was added to detect Nox1 bound to NoxA1ds or SCRMB, respectively. After 1 hr incubation and extensive washing, bound primary antibodies were detected by the addition of FITC-labeled goat anti-rabbit IgG antibody (1:1000; 30 min Sigma-Aldrich, St. Louis, MO, USA). The fluorescence of each well was measured using a Biotek Synergy 4 Hybrid Multi-Mode Microplate Reader (Excitation:488 nM, Emission:518 nM- BioTek, Winooski, VT, USA).

A second set of ELISA experiments were performed to test the mechanism by which Nox2ds could inhibit $O_2^{\cdot-}$ production in COS-Nox2 and not in the COS-Nox1 cell-free system. Neutravidin-coated plates (Thermo Scientific, Rockford, IL, USA) were incubated with biotinylated Nox2ds (Biotin-Nox2ds, 6 μM) or biotinylated scrmb Nox2ds (Biotin-scrmb, 6 μM) (Tufts University Core Facility, Boston, MA, USA) for 2 hr at room temperature. The plates were washed 3 times using wash buffer (25 mM Tris, 150 mM NaCl, 0.1% BSA, 0.05% Tween-20, pH 7.2). After 1 hr incubation at room temperature with COS-22, COS-22-p47^{phox} (COS-22 cells transfected with p47^{phox}) or COS 22-NOXO1 (COS-22 cells transfected with NOXO1) cytosolic fraction, rabbit polyclonal p47^{phox} (1:500; Santa Cruz Biotechnology, Santa Cruz, CA, USA) or rabbit NOXO1 (1:500; Rockland Immunochemicals Inc., Gilbertsville, PA, USA) antibodies were used to detect p47^{phox} or NOXO1 bound to Nox2ds or its scrambled control, respectively. After 1 hr incubation and extensive washing, bound primary antibodies were detected by the addition of FITC-labeled goat anti-rabbit IgG antibody (1:500; Sigma-Aldrich, St. Louis, MO, USA). The fluorescence of each well was measured using a Biotek Synergy 4 Hybrid Multi-Mode Microplate Reader and expressed as relative fluorescence units (Excitation:488 nM, Emission:518 nM- BioTek, Winooski, VT, USA).

2.1.10 Fluorescence Recovery After Photobleaching (FRAP)

FRAP was performed using an Olympus FV1000 confocal microscope with minor modifications from studies by Wheeler *et al*[221]. Briefly, circular regions of interest (1.0 μm^2) were selected and bleached with a 400 ms pulse from a 488-nm (YFP) and a 559-nm (Rhodamine) laser line using the SIM scanner; recovery data were acquired using the instrument's main scanner and the

488 and 559-nm lines of an argon gas laser. This short pulse was selected to ensure a Gaussian bleaching spot. To maximize reproducibility of the experimental conditions, all data were acquired in the photon-counting mode of the instrument. Thirty-five images were then collected at intervals of ~7 s. Average fluorescence intensities of the bleached and control regions in other cells or far-removed regions of the same cell were obtained and used to account for bleaching resulting from image acquisition. Fluorescence was normalized to time = 0 and monitored for ~ 250 s. Mobile fraction was calculated using equation 1:

$$\text{Mobile Fraction} = \frac{\text{End Fluorescence Intensity}}{\text{Fluorescence Intensity Before Photobleaching}}$$

2.1.11 Fluorescence Resonance Energy Transfer (FRET)

COS-22 cells seeded at 20% density on glass-bottomed tissue culture plates were co-transfected with Nox1-YFP and NOXA1-CFP or Nox1-YFP and CFP^m. After 24 h, cells were washed with PBS and fixed in 2 % paraformaldehyde. The interaction between Nox1 or CFP^m and NOXA1 was then detected using a combination laser scanning microscope system (Nikon A1 confocal) and quantified by acceptor photobleaching. To achieve excitation, the 458 nm line of an argon ion laser was focused through the Nikon ×60 oil differential interference contrast objective. Emissions of YFP (the FRET acceptor) and CFP were collected through 530–575 nm and 475–500 nm barrier filters, respectively, over a segment of the cell ~5 microns in diameter. Photobleaching was performed with 50 iterations and 100% intensity of a 514-nm laser. Using methods described previously, average fluorescence intensities/pixel was calculated following

background subtraction [222]. To determine the effect of NoxA1ds on Nox - NOXA1 association, cells transfected with Nox1-YFP and NOXA1-CFP were incubated with 10 μM NoxA1ds or SCRMB 24 hrs post transfection for 1 hr before fixing the cells. FRET efficiency was calculated using Equation 2.

Equation 2:

$$\text{FRET Efficiency} = \text{E} = 1 - \frac{\text{CFP}_{\text{post-bleach intensity}}}{\text{CFP}_{\text{pre-bleach intensity}}} * 100 = 1 - \frac{\text{CFP}_{\text{post}}}{\text{CFP}_{\text{pre}}} * 100$$

2.1.12 Cell Migration Assay

Scratch assay was performed as described by Liang *et al.* with minor modification [223]. Briefly, HPAECs were grown to 90% confluence in 35-mm dishes before growth media was replaced with starvation media (1:10 dilution of growth media). Before cell seeding, each dish was marked on its bottom with ink bisecting the dish into two halves. HPAEC were starved for 16 hours before the cell monolayer was disrupted with a P1000 pipet tip in one stroke that passed through both halves of the dish. The scratch was photographed as positions immediately above and below the halfway mark, cells were treated with +/- 20 nM VEGF, +/- 10 μM NoxA1ds, +/- 10 μM SCRMB NoxA1ds, +/- 10 μM Nox2ds-tat, +/- 10 μM SCRMB Nox2ds-tat and placed in either 1.0% O_2 or 20% O_2 environment at 37° for 24 hours. VEGF was added only at time 0 whereas peptides were added at time 0 and each 4 hrs thereafter. After 24 hours, the cells were again photographed immediately above and below the halfway mark on the dish. ImageJ software was used to calculate the change in distance between the cell fronts as compared to the

time 0 photograph. Distance between the cell fronts was calculated as the width of the rectangular are between the cell fronts containing 16 cells.

2.1.13 Quantification of *in vitro* VEGF Production

Human pulmonary artery endothelial cells (HPAEC), human pulmonary artery smooth muscle cells (HPASMC), or human pulmonary artery fibroblasts (HPAF) were seeded as 40,000 cells/well in a 96 well plate in 100µl of their respective culture media. After 24hrs, cells were conditioned at either normoxia (20% O_2) or hypoxia (1.0% O_2) for 24 hrs. After normoxic or hypoxic conditioning, media was removed from the cells and VEGF quantified in the supernatant using an ELISA kit and a SECTOR Imager 2400 from Meso Scale Discovery (Rockville, MD). Data were expressed as pg/ml VEGF.

2.1.14 MTT (Methylthiazolyldiphenyl-tetrazolium bromide) Assay of Cell Proliferation

HPAF were seeded as 40,000 cells/well in a 96-well plate in 100 µl of their respective culture media. HPAF were conditioned at either normoxia (20% O_2) or hypoxia (1.0% O_2) for 24 hrs. During HPAF hypoxic conditioning, HPAEC were seeded as 10,000 cells/well in a 96 well plate in 100µl of their respective culture media. After HPAF oxygen conditioning, media was aspirated from HPAEC and replaced with HPAF-conditioned media. After 24 hrs, 10µl of MTT reagent (final concentration 0.5mg/ml) was added to each well containing HPAEC cultured in HPAF-conditioned media. After 2 hrs, media was aspirated from the HPAEC and replaced with 100µl DMSO to solubilize metabolized MTT reagent as per manufacturer's (Sigma Aldrich)

protocol. After 15-minute incubation with mild agitation, absorbance of the DMSO solution was read at 570nm. Absorbance is an indication of cellular respiration and the data were expressed as relative absorbance.

2.1.15 Rodent Model of Pulmonary Arterial Hypertension (PAH)

To induce a rodent model of PAH, the protocol described by Abe et al. was followed with minor modification [206]. Briefly, female Sprague-Dawley rats (Charles River) weighing between 210-225 grams were injected with 100mg/kg SU5416 and housed in either room air (21% O_2) or hypoxic air (10% O_2) for three weeks, at which point all animals housed in hypoxic air were removed from hypoxia and housed in room air for an additional one week. This treatment course is referred to here as SU5416 with chronic hypoxia (SUCH). Control animals were housed in the same room as hypoxic animals for the same time, yet in room air. During the entire four-week course of the experiment, rats were treated with 10mg/kg NoxA1ds or SCRMB via aerosol inhalation for 30 minutes twice a week. The concentration of NoxA1ds/SCRMB for aerosol preparation was calculated to deliver 10μM peptide to the lung epithelium. Pressure-volume loop analysis of the left and right ventricles of the heart was performed through the apex of the heart in an open chest cavity, as described by Pacher et al. using catheters provided by Transonic (Ithaca, NY) [64]. After RV and LV hemodynamic phenotyping, animals were sacrificed by exsanguination immediately followed by tissue collection and Fulton index calculation. All animal experiments were performed in accordance with the University of Pittsburgh Institutional Animal Care and Use Committee regulations.

2.1.16 Measurement of ROS in Tissue Homogenates

Tissues from female SUCH-treated rats were flash frozen in liquid nitrogen immediately after sacrifice. Cryopreserved tissues were homogenized in phosphate buffered saline followed by centrifugation at 5,000xg for 10 minutes to remove debris. Homogenates were passed through a 30ga needle 5 times to completely lyse remaining cells before suspension in OAB. NADPH-dependent $O_2^{\cdot -}$ production was determined using cytochrome c reduction as described above, using 5ug protein per sample.

2.1.17 Statistical Analysis

All results are expressed as means ± S.E. A Student's t-test was used for simple comparisons between two data sets. Two-way ANOVA with replication followed by a Bonferroni post-test was used to discern point differences in data sets with more than one group and with multiple treatments in each group, e.g. measurements from 2-3 treatment regimens over various time points. Statistical analyses and IC_{50} determinations were performed using GraphPad Prism 5 software. A p value of <0.05 was considered statistically significant.

3.0 DEVELOPMENT AND CHARACTERIZATION OF AN ISOFORM-SPECIFIC NOX1 INHIBITOR

3.1 INTRODUCTION

The production of ROS by Nox enzymes is achieved through a conserved catalytic mechanism contained within the enzyme's transmembrane domain that causes the transfer of electrons from NADPH through FAD and two heme groups to molecular oxygen to form $O_2^{\cdot -}$ and/or H_2O_2 [224]. While this catalytic core is conserved among Nox isoforms, it alone is insufficient for activity in a subclass of Noxes including Nox1. Indeed, key interactions between Nox1 and its co-activating cytosolic subunits play a major role in activation of this enzyme domain by forming a heterodimeric complex essential for ROS generation [36, 115]. Canonical Nox2 oxidase, the closest homologue of Nox1 and for which much more is known, requires the GTPase Rac, organizer subunit $p47^{phox}$ and activator subunit $p67^{phox}$ for activation [54, 132, 225] whereas canonical Nox1 requires interaction with homologous organizer NOXO1 and activator NOXA1 [226]. Nox1 also requires the small GTPase Rac and the transmembrane protein $p22^{phox}$ [36]. The assembled complex of subunits (Nox1, NOXO1, NOXA1, Rac, $p22^{phox}$) comprises the functional Nox1 oxidase. The biochemical structure and function of NOXA1 and NOXO1 are largely unknown due to their more recent discovery. That said, $p67^{phox}$ contains an "activation domain" spanning amino acids 190-210 that participates in the catalytic reduction of FAD [127]. This domain shares 50% and 80% homology with corresponding residues 191-211 and 198-208 of NOXA1, respectively [116]. Targeted and specific inhibition of Nox1 has long been desired and prior to the design of NoxA1ds, there was an absence of Nox1-specific inhibitors with a

validated target and established mechanism. We hypothesized that residues 191-211 of NOXA1 serve a function similar to that of the activation domain of p67^{phox} and, in turn, that a peptide derived from this domain could serve as a viable inhibitor of NOXA1-Nox1 binding and activation. With the knowledge that mutagenesis of a phenylalanine for an alanine at residue 199 of NOXA1 reduces Nox1-derived $O_2^{\cdot -}$ production by > 95% [129], we postulated that the same substitution would render this truncated peptide a highly-effective inhibitor of Nox1-derived $O_2^{\cdot -}$ production. In addition, by including amino acids that are homologous (residues 200 to 205) and non-homologous between NOXA1 and p67^{phox} (residues 195-198), we surmised that the peptide would bind to Nox1, rather than Nox2. The peptide representing amino acids 195-205 of NOXA1 with a F199A substitution is heretofore referred to as NOXA1 docking sequence (NoxA1ds) and was tested for its efficacy as a Nox1 inhibitor (Figure 3-1).

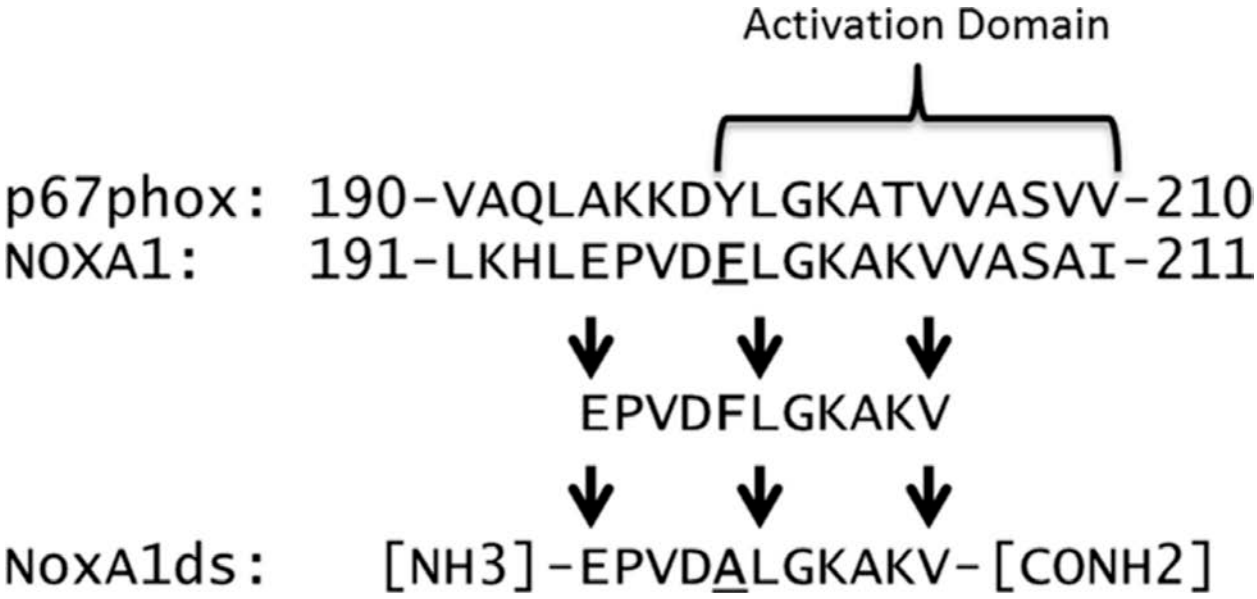

Figure 3-1: Design of NoxA1ds.

Alignment of $p67^{phox}$ and NOXA1 indicates a highly homologous region between the two sequences within the activation domain. Phe-199 (F199) in NOXA1 was previously shown to be critical for enzymatic activity of Nox1. We selected an 11-mer sequence that contained critical portions of the activation domain (i.e. Phe-199), substituted Phe-199 to Ala, and used the resulting peptide as NoxA1ds.

3.2 RESULTS

3.2.1 NoxA1ds is a Potent Inhibitor of Nox1-Derived $O_2^{\cdot-}$ in Cell-Free Preparations

To investigate the ability of NoxA1ds ([NH_3]-E-P-V-D-A-L-G-K-A-K-V-[$CONH_2$]) to inhibit Nox1, $O_2^{\cdot-}$ production was assessed in a reconstituted canonical COS-Nox1 oxidase system expressing Nox1, $p22^{phox}$, NOXA1, and NOXO1. Previous reports suggested that a related previously ascribed "activation domain" in NOXA1 homolog $p67^{phox}$ interacts with FAD sites on Nox2's C-terminal tail [128]. To maximize the potential for NoxA1ds and Nox1 to interact in this manner, membrane-integrated fractions from COS-Nox1 cells containing holoprotein Nox1 with its C-terminal tail, were incubated with cumulative concentrations of NoxA1ds (10^{-12} – 10^{-5} M) before adding cytosolic fractions containing NOXA1 and NOXO1. NoxA1ds concentration-dependently inhibited $O_2^{\cdot-}$ production with an IC_{50} of 20 nM (Fig. 3-2A). Maximal inhibition of Nox1 was achieved at 1.0 µM NoxA1ds. In concert with these experiments, we designed a scrambled control peptide consisting of an identical amino acid composition in randomized order (SCRMB, [NH_3]-L-V-K-G-P-D-A-E-K-V-A-[$CONH_2$]) and verified that minimal to no matches were found in protein database (i.e. BLAST). Multiple variations of SCRMB with different amino acid sequences were initially considered as control peptides. This sequence was chosen as the control peptide as it did not preserve the order of charged residues nor the central key amino acid sequence of the activation domain (V-D-A-L). SCRMB did not inhibit Nox1 (Fig. 3-2B).

3.2.2 NoxA1ds is an Isoform-Specific Nox1 Inhibitor

Isoform-specificity was explored by testing the ability of NoxA1ds to inhibit Nox2, Nox4, and Nox5. Cell lysates were prepared from COS-Nox2, COS-Nox4, or HEK-Nox5 cells and $O_2^{\cdot-}$

(Nox2/Nox5) or H_2O_2 (Nox4) production was measured using the reduction of cytochrome *c* or Amplex Red fluorescence, respectively. NoxA1ds was applied to prepared membrane fractions before addition of fractions containing cytosolic subunits (absent in Nox4 and 5 preparations) to maximize its ability to inhibit the oxidase. NoxA1ds did not inhibit Nox2-derived $O_2^{\cdot-}$ production, Nox4-derived H_2O_2 production, or Nox5-derived $O_2^{\cdot-}$ production (Fig. 3-2C-E). Additionally, the ability of NoxA1ds to inhibit $O_2^{\cdot-}$ production by xanthine oxidase (XO), a molybdenum-dependent enzyme that produces $O_2^{\cdot-}$, was investigated. XO produces $O_2^{\cdot-}$ as a result of purine catabolism where electrons from the substrate (hypoxanthine) are transferred to oxygen as the enzyme produces xanthine and uric acid [227, 228]. The hydroxylamine EPR spin probe CPH was used to detect $O_2^{\cdot-}$ produced by XO in the presence or absence of $O_2^{\cdot-}$ scavenger SOD or the XO-specific inhibitor allopurinol (measuring $CP^{\cdot}$ signal intensity). Concentrations of NoxA1ds up to 1 μM did not inhibit XO-derived $O_2^{\cdot-}$ (Fig. 3-2F) as compared to SOD and allopurinol controls which abolished the signal. Each Nox and XO was also tested for to the effect of SCRMB control peptide; and no effect on ROS production by any of these oxidases was observed (Figure 3-3). These data indicate that NoxA1ds does not inhibit Nox2-, Nox4-, Nox5-, or XO-derived ROS. In addition, the data indicate that NoxA1ds does not scavenge either $O_2^{\cdot-}$ from XO or H_2O_2 from Nox4.

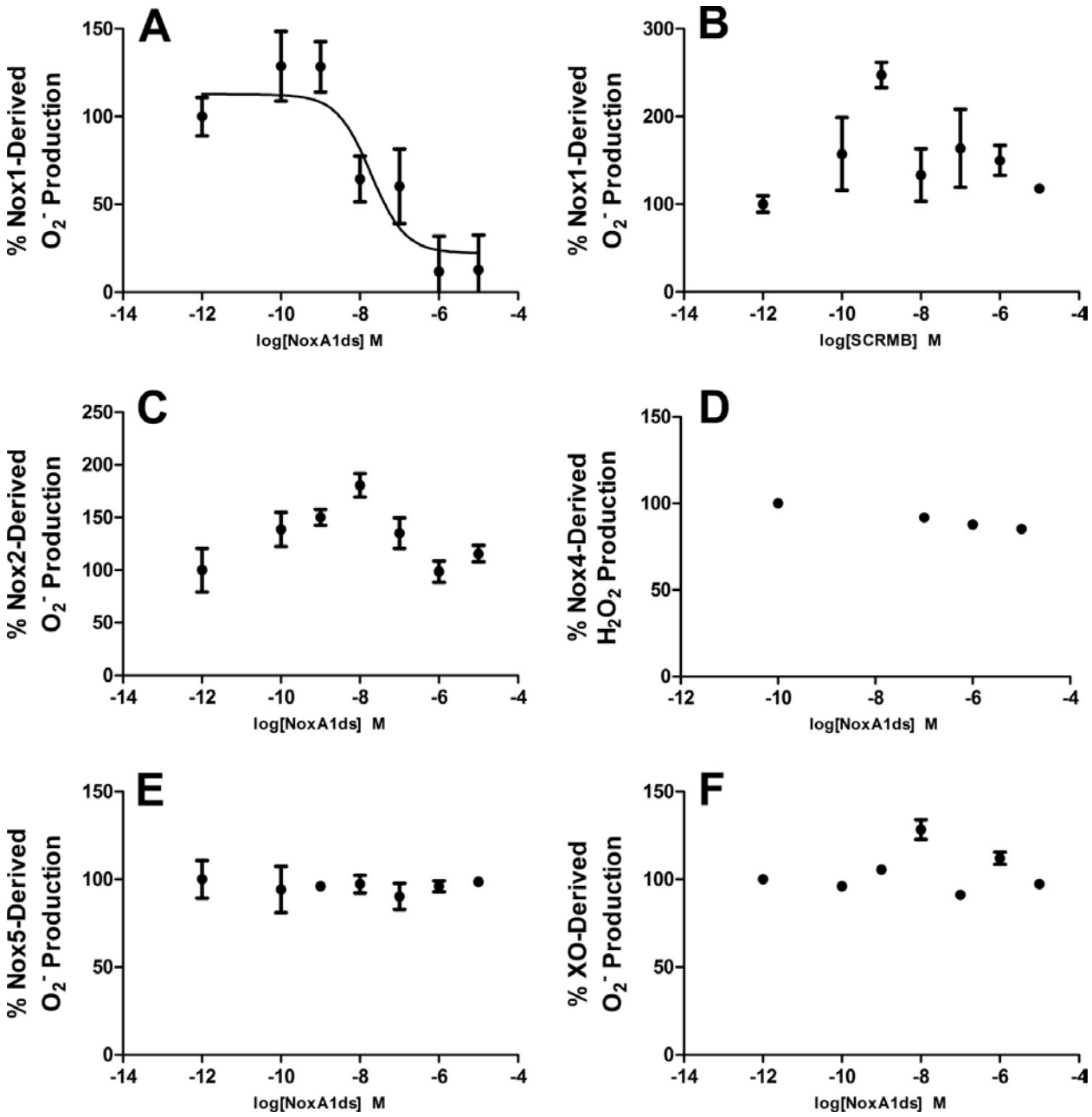

Figure 3-2: NoxA1ds inhibits Nox1-derived $O_2^{\cdot-}$ but not related enzymes.

Production of $O_2^{\cdot-}$ was calculated by monitoring the reduction of cytochrome *c* for 15 minutes post NADPH addition and subtracting baseline cytochrome *c* reduction occurring in the presence of SOD. **A)** Production of $O_2^{\cdot-}$ as measured by the reduction of cytochrome *c* by cell lysates from COS cells transiently transfected with the Nox1 oxidase. Increasing concentrations (from 0.1 nM to 10,000 nM) of NoxA1ds caused a dose dependent inhibition of $O_2^{\cdot-}$ production with an IC_{50} of 20nM. Maximal

inhibition of 88% of total $O_2^{\cdot -}$ production was achieved at a dose of 1.0 μM NoxA1ds. **B)** Increasing concentrations of SCRMB did not inhibit Nox1-derived $O_2^{\cdot -}$. **C)** Production of $O_2^{\cdot -}$ as measured by the reduction of cytochrome *c* by cell lysates from COS cells transiently transfected with the Nox2 oxidase. Lysates were treated with increasing concentrations of NoxA1ds (from 0.1 nM to 10,000 nM) prior to stimulation of enzyme assembly with 130 μM LiDS and enzyme activation with 180 μM NADPH. **D)** Production of H_2O_2 as measured by Amplex red fluorescence 15 min minutes post NADP addition by membrane fractions prepared from COS cells transiently transfected with the Nox4 oxidase. Lysates were treated with increasing concentrations of NoxA1ds (from 100 nM to 10,000 nM). **E)** Production of $O_2^{\cdot -}$ as measured by the reduction of cytochrome *c* by cell lysates from HEK293 cells stably transfected with the Nox5 oxidase stimulated with Ca^{2+} as described by Banfi et al (Ref. 13), and treated with increasing concentrations of NoxA1ds (from 0.1 nM to 10,000 nM). **F)** Production of $O_2^{\cdot -}$ as measured by Electron Paramagnetic Resonance from pure xanthine oxidase enzyme preparations, stimulated with hypoxanthine and pre-treated with increasing concentrations of NoxA1ds (from 0.1 nM to 10,000 nM). In all panels, enzyme activity was evaluated 15 min post enzyme activation with substrate (20 min post NoxA1ds treatment) and no inhibition of the signal was observed. n = 9-12, three to four separate experiments.

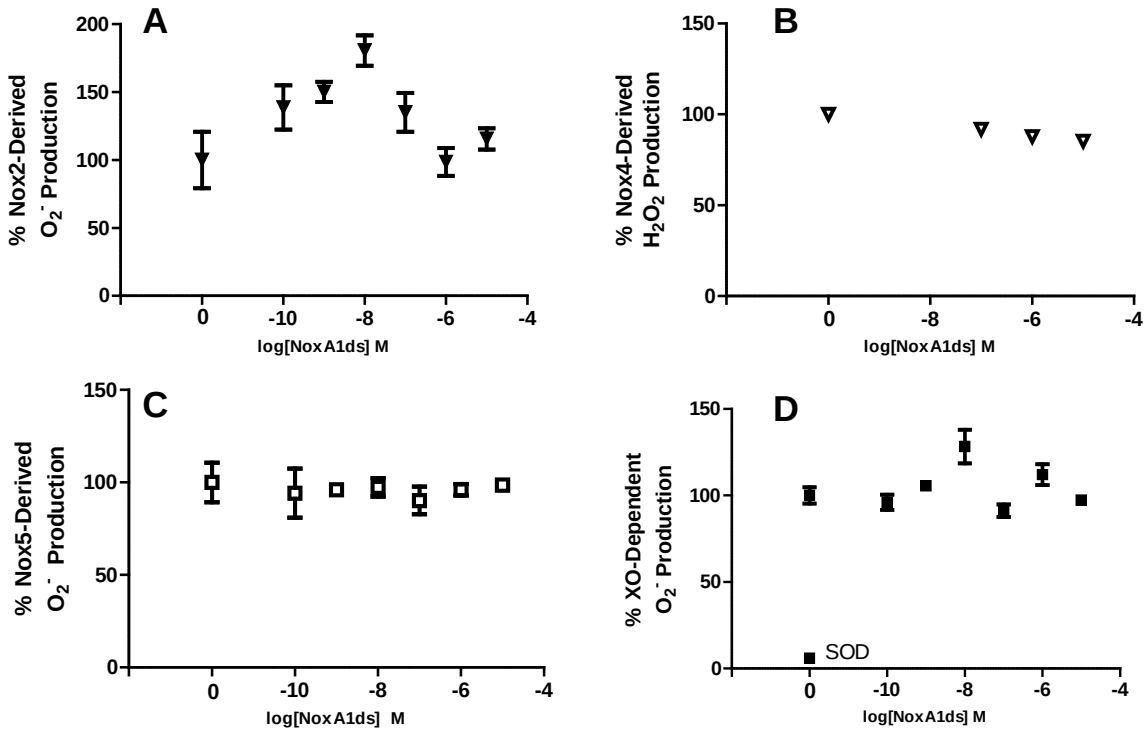

Figure 3-3: SCRMB NoxA1ds does not inhibit Nox2, Nox4, Nox5 or XO.

A) Production of $O_2^{\cdot-}$ as measured by the reduction of cytochrome c by cell lysates from COS cells transiently transfected with the Nox2 oxidase, stimulated with LiDS, and treated with increasing concentrations of NoxA1ds (from 0.1 nM to 10,000 nM). **B)** Production of H_2O_2 as measured by Amplex red fluorescence by COS cells transiently transfected with the Nox4 oxidase and treated with increasing concentrations of NoxA1ds (from 100 nM to 10,000 nM). **C)** Production of $O_2^{\cdot-}$ as measured by the reduction of cytochrome c by cell lysates from HEK293 cells stably transfected with the Nox5 oxidase stimulated with Ca2+, and treated with increasing concentrations of NoxA1ds (from 0.1 nM to 10,000 nM). **D)** Production of $O_2^{\cdot-}$ as measured by Electron Paramagnetic Resonance from pure xanthine oxidase enzyme preparations, stimulated with hypoxanthine and treated with increasing concentrations of NoxA1ds (from 0.1 nM to 10,000 nM). In all panels, no inhibition of the signal was observed. *n* = 9-12, three to four separate experiments.

3.2.3 NoxA1ds Inhibits $O_2^{\cdot-}$ in Whole Cells

We used HT-29 cells to explore whether NoxA1ds could be used as a viable pharmacological inhibitor in intact cells. HT-29 are a unique population of colon carcinoma cells that solely express Nox1 without expression of any other Nox isoform [229]. To test for permeability, HT-29 cells were treated with a FITC-labeled NoxA1ds variant for 1 hr before imaging. Confocal microscopy revealed that NoxA1ds permeated the cell membrane of HT-29 cells and localized to the cytoplasm (Fig. 3-4A-D). To test whether NoxA1ds inhibits Nox1-derived $O_2^{\cdot-}$ production in intact cells containing Nox1, HT-29 cells were incubated with increasing NoxA1ds concentrations and $O_2^{\cdot-}$ was measured in membrane fractions using cytochrome c. Fig. 3-4E illustrates concentration-dependent inhibition of HT-29 $O_2^{\cdot-}$ that was absent in cells treated with SCRMB control peptide. In whole HT-29 cells, the IC_{50} was 1.0 μM with maximal inhibition at 5.0 μM NoxA1ds. As measured in intact HT-29 cells via EPR, Nox1 inhibition in HT-29 cells by NoxA1ds was matched by Nox1 siRNA control (Fig 3-4F). As an additional control, we investigated whether NoxA1ds inhibited $O_2^{\cdot-}$ production in cells that do not express Nox1. Peritoneal macrophages isolated from Nox1-null mice were pretreated with NoxA1ds for 1 hr before addition of PMA to stimulate $O_2^{\cdot-}$ production. No inhibition of $O_2^{\cdot-}$ production was observed using L-012 luminescence (Figure 3-4H).

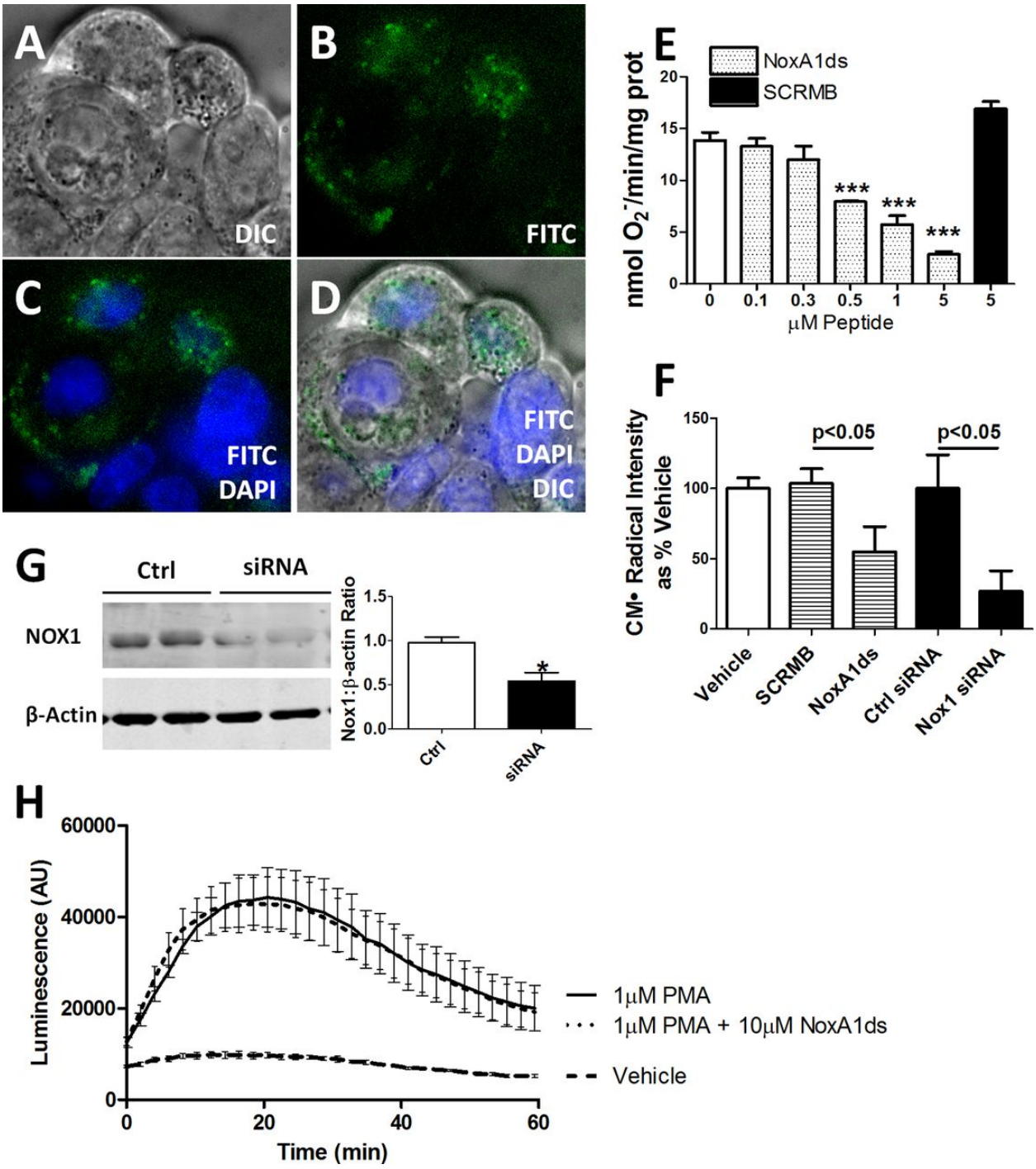

Figure 3-4: NoxA1dsis cell-permeant and effective in whole colon adenocarcinoma cells yet ineffective in Nox1$^{-/y}$ cells.

FITC-labeled NoxA1ds and native NoxA1ds were incubated with HT-29 colon adenocarcinoma cells. HT-29 cells bear the distinction of having abundant Nox1 expression while not expressing Nox2, Nox4,

or Nox5. **A-D)** FITC-labeled NoxA1ds was incubated with HT-29 colon adenocarcinoma cells for 1hr prior to imaging. Confocal microscopy of these cells indicates that FITC-NoxA1ds penetrated the extracellular membrane and that its distribution is cytosolic and perinuclear. **E)** As measured by SOD inhibitable reduction of cytochrome c, increasing doses of NoxA1ds caused dose-dependent inhibition of $O_2^{\cdot -}$ production by HT-29 cells. SCRMB peptide did not inhibit $O_2^{\cdot -}$ production, *** $p<0.05$ for 0.5, 1, and 5 μM NoxA1ds vs 0μM NoxA1ds by one-way ANOVA. **F)** As measured by EPR, 10 μM NoxA1ds and Nox1 siRNA both significantly inhibited $O_2^{\cdot -}$ production by HT29 cells, p values determined by one-way ANOVA **G)** Western blot analysis of Nox1/β-actin protein from Nox1 siRNA or control treated HT29 cells. **H)** Peritoneal macrophages were isolated from Nox1 null mice and $O_2^{\cdot -}$ production was measured by L-012 chemiluminescence after 2 hr incubation with NoxA1ds and subsequent PMA stimulation. No difference was observed between NoxA1ds treated and untreated samples. All values are expressed as n = 9, except for H which was quantified via three separate experiments n = 10-12, cells from four individual mice.

3.2.4 NoxA1ds Binds to Nox1

An ELISA-based assay was used to test whether NoxA1ds binds to Nox1. Biotin-tagged NoxA1ds (B-NoxA1ds) applied to neutravidin-coated 96-well plates was added membrane fractions from Nox1-transfected or non-transfected COS-22 cells followed by treatment with fluorescent secondary antibodies. After repeated washing, a 30% increase in fluorescence was observed in wells treated with membrane fractions of Nox1-transfected cells *vs.* untransfected cells. This increase was not observed in wells treated with Nox1-transfected cell membranes added to wells containing biotin-tagged SCRMB control peptide (Fig. 3-5A). A similar ELISA-based assay indicated that Nox2 from COS-Nox2 membrane fractions did not bind NoxA1ds (Fig 3-5B).

To corroborate these results, Fluorescence Recovery After Photobleaching (FRAP) of a Rhodamine-labeled NoxA1ds (R-NoxA1ds) in untransfected cells and those transfected with Nox1-YFP was quantified. As seen in Fig. 3-5C, R-NoxA1ds completely recovered after 250 s in untransfected cells while R-NoxA1ds recovery was significantly slower and markedly attenuated in cells transfected with Nox1-YFP, i.e. by 250 s, R-NoxA1ds had recovered less than 50% in Nox1-YFP-transfected cells. The significant decrease in the mobile fraction of R-NoxA1ds and Nox1-YFP-transfected *vs.* non-transfected cells corroborates the ELISA data, indicating binding between Nox1 and NoxA1ds (Fig. 3-5)

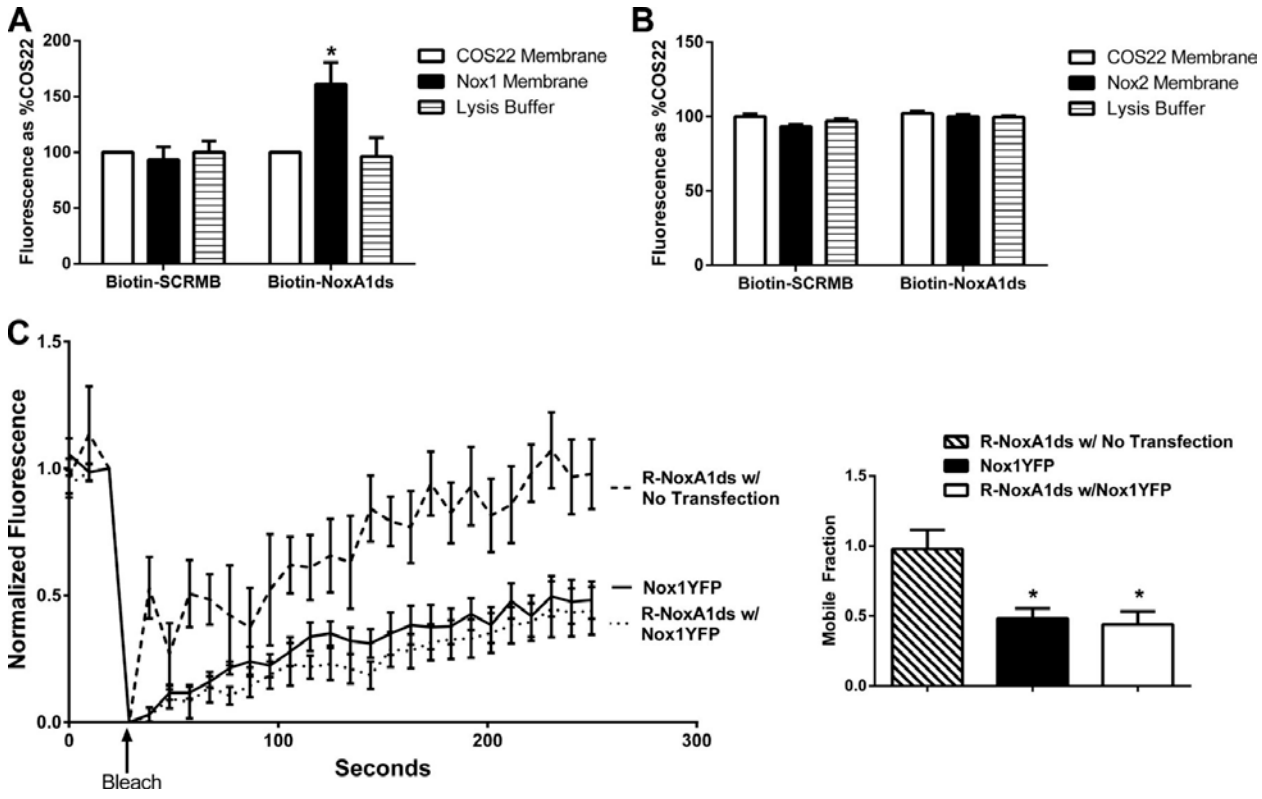

Figure 3-5: NoxA1ds binds to Nox1 but does not detectably bind Nox2.

A) Neutravidin coated plates were incubated with biotin-tagged NoxA1ds (Biotin-NoxA1ds) or biotin-tagged SCRMB (Biotin-SCRMB) before addition of cell membranes prepared from cells transfected with Nox1 (Nox1 membrane) or transfected with an empty vector (COS22 membrane). Bound Nox1 was detected through a FITC conjugated secondary antibody bound to the Nox1 primary antibody. FITC fluorescence was expressed as binding as % COS22 membranes on each experimental day. There was no difference in binding between COS22 membranes and Nox1 membranes incubated with Biotin-SCRMB whereas membranes incubated with Biotin-NoxA1ds showed a significant increase in binding when transfected with Nox1. n = 10-12, three separate experiments, *$p<0.05$, two-way ANOVA with Bonferroni post-hoc t-test. **B)** Neutravidin coated plates were incubated with biotin-tagged NoxA1ds (Biotin-NoxA1ds) or biotin-tagged SCRMB (Biotin-SCRMB) before addition of cell membranes prepared from cells transfected with Nox2 (Nox2 membrane) or transfected with an empty vector (COS22 membrane). Bound Nox2 was detected through an Alexa 488 conjugated secondary antibody bound to

the Nox1 primary antibody. Fluorescence was expressed as binding as % COS22 membranes on each experimental day. There was no difference in binding between COS22 membranes and Nox2 membranes incubated with Biotin-SCRMB or Biotin-NoxA1ds, **C)** Fluorescence Recovery After Photobleaching (FRAP) of COS22 cells treated with 70nM Rhodamine B-labeled NoxA1ds (R-NoxA1ds) in the absence and presence of Nox1YFP transfection and FRAP of Nox1YFP alone. Panel to the right represents mobile fraction of these groups after 250 sec, *$p<0.05$, one-way ANOVA with Bonferroni post-hoc t-test.

3.2.5 NoxA1ds Interrupts Nox1 : NOXA1 Association

Upon observation of NoxA1ds-Nox1 binding, we proposed that NoxA1ds would interrupt association of Nox1 and NOXA1. To test this, we employed a FRET-based assay in which COS-22 cells were transfected with Nox1-YFP and NOXA1-CFP. Cells were analyzed by fixing followed by irreversible YFP-photobleaching to determine if FRET was occurring between YFP and CFP. FRET is observed indicating protein interaction between two partners when the donor emission (CFP) signal increases after a nearby acceptor fluorophore (YFP) is inactivated by irreversible photobleaching. In these cells, photobleaching of the YFP label resulted in a concomitant increase in CFP fluorescence, together with a decrease in YFP signal intensity, indicating a direct interaction between Nox1-YFP and NOXA1-CFP (Fig. 3-6A). Hence, photobleaching effectively prevented dipole-dipole coupled acceptor (YFP-Nox1) from accepting a quantum energy transfer from the donor (CFP), thus enhancing CFP fluorescence. We used a myristolated CFP (CFP^m) which is exclusively targeted to the cell membrane as a negative control [25]. In cells expressing CFP^m and Nox1-YFP, photobleaching of YFP did not result in an increase in CFP fluorescence, indicating FRET was not a result of coincidental membrane abundance and co-localization of these proteins (Fig 3-7).

COS-22 cells transfected with Nox1-YFP and NOXA1-CFP were then incubated with 10 μM SCRMB NoxA1ds or NoxA1ds for 1 hr before imaging. The SCRMB control peptide had no effect on CFP/YFP FRET coupling (Fig. 3-6B, D). On the other hand, NoxA1ds significantly reduced FRET efficiency (Fig. 3-6C, D). These results indicate that Nox1 and NOXA1 directly interact and that this interaction is disrupted by NoxA1ds, but not by control peptide.

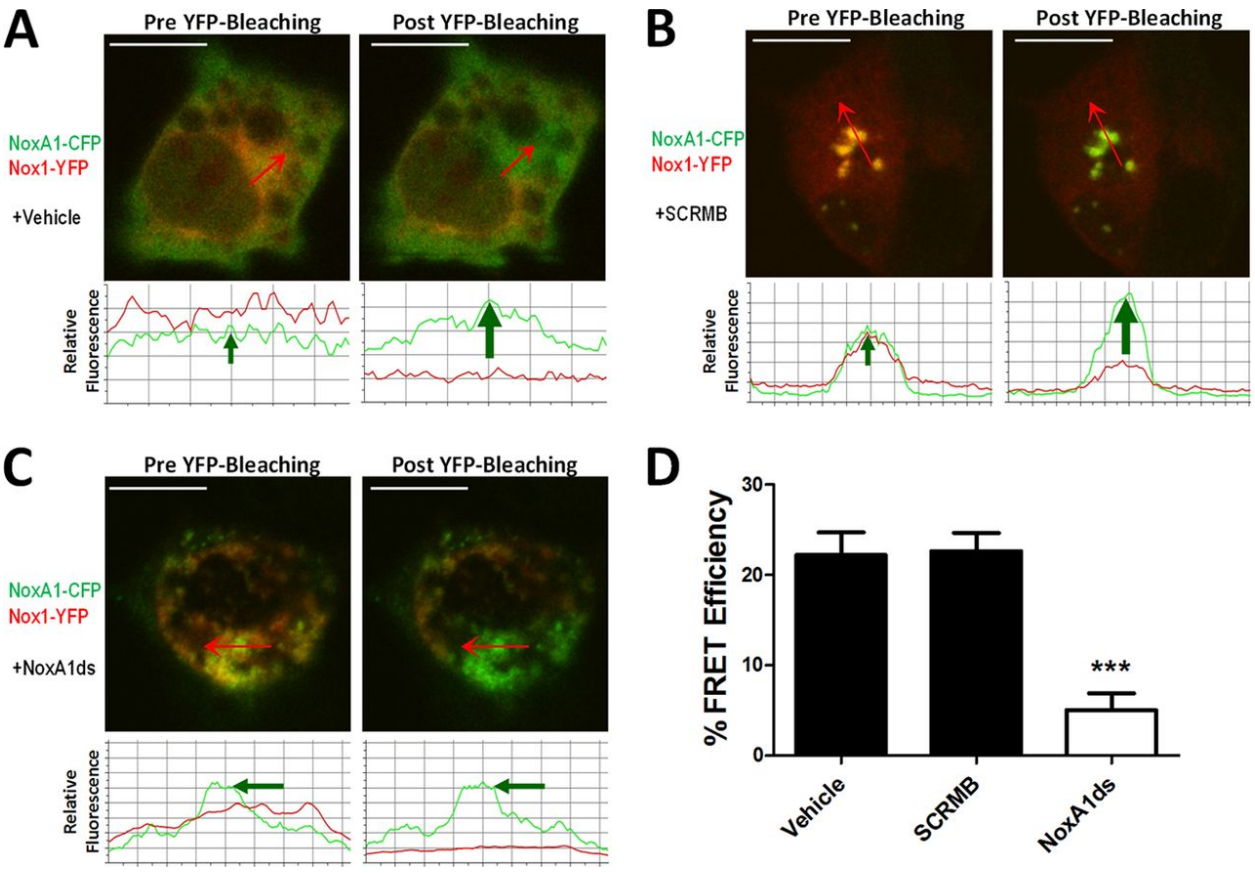

Figure 3-6. NoxA1ds disrupts Nox1-NOXA1 interaction.

FRET between Nox1-YFP and NoxA1-CFP transfected COS22 cells in the presence or absence of 10µM NoxA1ds or SCRMB was evaluated. Relative fluorescence of CFP is green while YFP is red. Traces underneath the images indicate fluorescent intensities of CFP and YFP underneath the arrow overlaid on each cell. **A)** Transfected COS22 cells were treated with vehicle for one hour prior to imaging cells, photobleaching of Nox1-YFP was complete and resulted in a concomitant increase in CFP fluorescence. **B)** Transfected COS22 cells were treated with 10µM SCRMB peptide for one hour prior to imaging cells, photobleaching of Nox1-YFP was complete and also resulted in a concomitant increase in CFP fluorescence. **C)** Transfected COS22 cells were treated with 10µM NoxA1ds peptide for one hour prior to imaging cells, photobleaching of Nox1-YFP was complete but did not result in a concomitant increase in CFP fluorescence. **D)** Quantification of FRET efficiency from images A-C. Values expressed as n= 8, three separate experiments ***$p<0.001$ by one-way ANOVA and Bonferroni post-test

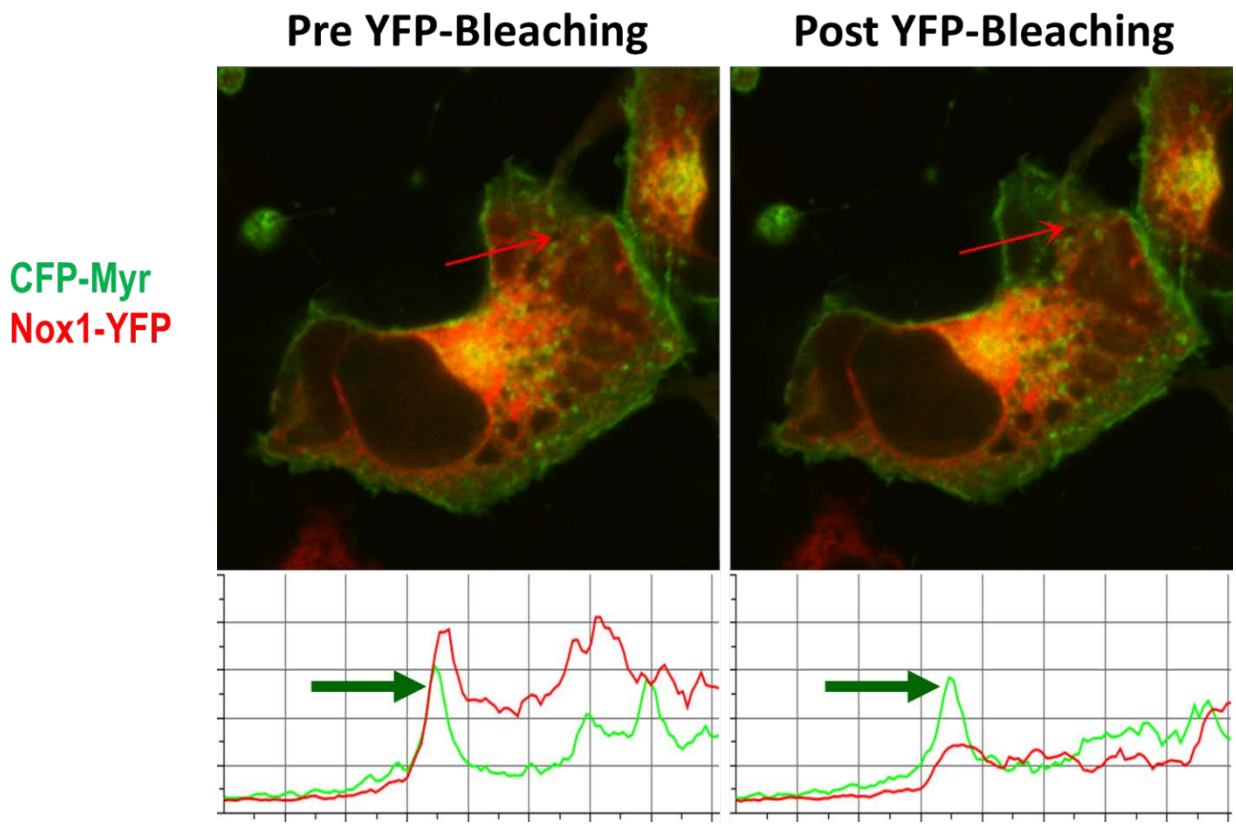

Figure 3-7: Nox1:NOXA1 FRET interaction is not a result of CFP and YFP proximity in the membrane.

Potential FRET between Nox1-YFP and a myristolated-CFP (CFP-Myr) transfected COS22 cells was evaluated. Relative fluorescence of CFP is green while YFP is red. Traces underneath the images indicate fluorescent intensities of CFP and YFP underneath the arrow overlaid on each cell. Photobleaching of Nox1-YFP was complete but did not result in a concomitant increase in CFP fluorescence.

3.3 DISCUSSION

We report here on the design, mechanism, and target validation of a specific Nox1 inhibitor (NoxA1ds) that is cell permeant and highly potent [230]. NoxA1ds was derived from a peptide whose structure is based on a short sequence of an essential Nox subunit; in this case, a putative activation domain of NOXA1. We demonstrate here that NoxA1ds binds directly to NOX1 and displaces NOXA1 to inhibit enzymatic activity and biological function.

NoxA1ds recapitulates a putative activation subdomain of NOXA1 with a F199A substitution in the sequence of NOXA1 stretching from residues 195 to 205 (^{195}EPVD(F→A)LGKAKV^{205}). This modification mimics a point mutation first created in the holoprotein by Maehara *et al.* [129] that caused a 75% loss in activity in the reconstituted canonical Nox1 oxidase system. Although the function of this domain in NOXA1 is unclear, a related domain exists in p67^{phox}, the activator of Nox2 [128]. The activation domain of p67^{phox} is known to be critical for catalytic Nox2 oxidase activity [128]. In designing NoxA1ds as a potential competitive and specific inhibitor of Nox1-NOXA1 binding, we selected a *sub*domain in NOXA1 containing residues that are both conserved and non-conserved between NOXA1 and p67^{phox}.

The defined p67^{phox} activation domain (amino acids 190–210) and corresponding region in NOXA1 share 50% homology. NoxA1ds was intentionally derived from a corresponding portion of this region in which 46% of the amino acids are dissimilar between p67^{phox} and NOXA1, i.e. NoxA1ds is derived from amino acids 195 to 205, in which the first four amino acids are EPVD as opposed to AKKD in p67^{phox}. We postulated that this difference confers isoform specificity of NoxA1ds for Nox1. The lack of observed inhibition in Nox4 or Nox5

systems is likely a result of these Nox systems having no cytosolic activator subunit requirement. Finally, the lack of inhibition of XO by NoxA1ds is further confirmation that its inhibitory effect is not germane to all oxidases and is not a consequence of ROS scavenging.

NoxA1ds could potentially mimic functional sites in other proteins and thus interfere with their function. We used BLAST to compare the sequence of NoxA1ds to the National Institutes of Health translated nucleotide database to determine potential nonspecific protein interactions with NoxA1ds. We were surprised to observe that fewer than five mammalian proteins outside of the NADPH oxidase family shared significant homology with NoxA1ds. These hits were hypothetical proteins based on isolated DNA sequences. As such, we believe nonspecific actions of NoxA1ds should be negligible.

When NoxA1ds was added to cell-free preparations of the canonical Nox1 oxidase, composed of catalytic subunit Nox1, activating subunit NOXA1 and organizing subunit NOXO1 along with Rac, NoxA1ds inhibited Nox1-derived $O_2^{\cdot -}$ production with an IC_{50} of 20 nM achieving maximum inhibition of 90% at 1.0 μM. In addition, we showed that NoxA1ds does not scavenge either $O_2^{\cdot -}$ or H_2O_2 and does not inhibit Nox2, Nox4, Nox5, or XO activity. These results support NoxA1ds as an isoform-specific inhibitor of Nox1.

We extended our studies to determine the *in vitro* efficacy of NoxA1ds and observed that fluorescent analogues of NoxA1ds (Noxa1ds-FITC) are capable of crossing the plasma membrane and localizing to the cytosol. Many short peptides require the small HIV “tat” peptide moiety to penetrate cell membranes [112, 231]. In contrast, our findings herein demonstrated that “tat” is unnecessary for NoxA1ds to cross the plasma membrane, and we attribute this in part to the positively charged lysines in the C terminus of NoxA1ds and the alternating hydrophobic/hydrophilic amino acid structure of NoxA1ds. Indeed, other short peptides with

similar hydropathy patterns have proven highly cell permeant and thus support our findings [232]. Upon demonstrating its permeability in whole cells, we tested whether NoxA1ds is an effective inhibitor of $O_2^{\cdot -}$ production in a primary cancer cell line (HT-29) that exclusively expresses Nox1 oxidase [229]. We observed that NoxA1ds significantly attenuated $O_2^{\cdot -}$ production in HT-29.

ELISA and FRAP data revealed that NoxA1ds binds to the catalytic Nox1 subunit, and FRET demonstrated that NoxA1ds disrupted the critical association of Nox1 with NOXA1 and that this binding is specific to Nox1 in HPAEC. Our FRET data support the notion that not only is this domain an activation domain critical for enzyme activity in Nox1 but that this domain is also a key binding region in Nox1-NOXA1 complexes [129].

Notwithstanding the broadly-demonstrated effectiveness of related peptides by parenteral, peritoneal, subcutaneous, and direct application to blood vessels using gene therapy [159, 232], the limitations in the use of peptides as “druggable” therapeutics are obvious. These include a very limited oral bioavailability due to peptide degradation in the gut. As mentioned earlier, however, these issues are being circumvented by novel technologies, including the use of nanotechnologies such as microbubble mediated drug delivery [233, 234]. Beyond targeted peptide delivery, there are a number of peptide modifications that can support bioavailability by reducing protease degradation. These include hydrocarbon stapling and partial substitution of d-amino acids [235, 236].

Maehara et al. [129] first reported that the NOXA1 F199A mutation that we incorporated into NoxA1ds interferes with FAD reduction in the enzyme complex and thus may prevent catalytic $O_2^{\cdot -}$ production. While it is plausible that NoxA1ds inhibits Nox1 through a similar mechanism, our data are more in line with NoxA1ds preventing Nox1-NOXA1 binding and

inhibiting $O_2^{\cdot-}$ production. Thus, we propose that this domain is crucial for the binding and activation of Nox1. Taken together, our data indicate that the peptide NoxA1ds is a specific inhibitor of Nox1 in cell-free and whole cell preparation and that this inhibition occurs via binding to the catalytic Nox1 subunit and blockade of Nox1-NOXA1 binding (Figure 3-8). It stands to reason that this site-specific binding is important for subsequent FAD reduction. However, whether the domain somehow catalyzes or facilitates FAD reduction either directly or *via* an allosteric change in the Nox1 C-terminus is still an open question.

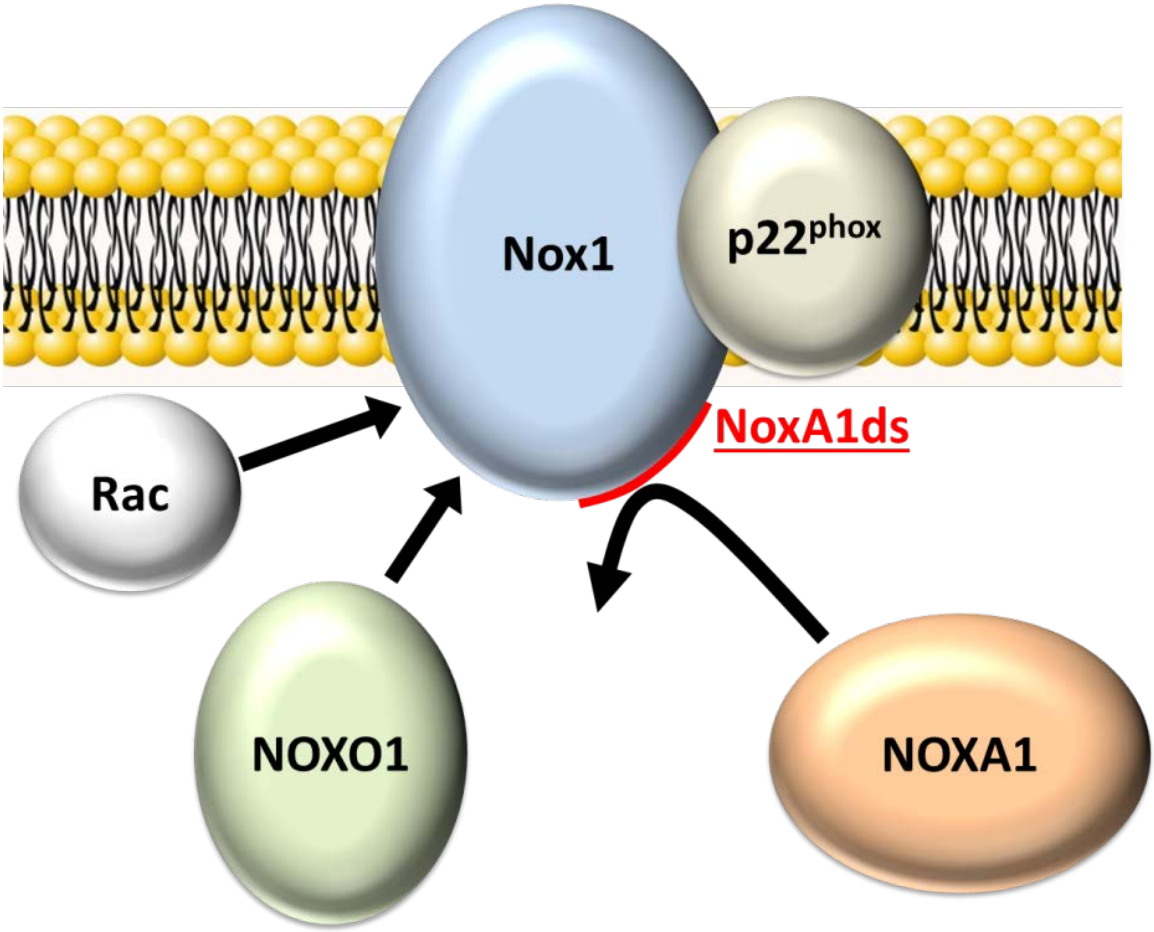

Figure 3-8: Schematic of NoxA1ds Mechanism of Action.

The data presented here indicate that NoxA1ds is a specific Nox1 inhibitor that binds to Nox1 and prevents its interaction with NOXA1.

4.0 DETERMINE RELATIVE ROLES OF NOX1 VS NOX2 IN ENDOTHELIAL $O_2^{\cdot-}$ PRODUCTION AND CELL MIGRATION

4.1 INTRODUCTION

The first rationally-designed, peptidic Nox inhibitor, Nox2ds-tat (Nox2 docking sequence-tat; Nox2ds-tat a.k.a. gp91ds-tat), was identified by the Pagano laboratory in 1999 and published in 2001 as a compound that decreased angiotensin II-induced vascular $O_2^{\cdot-}$ generation and attenuate systemic blood pressure elevation in hypertensive mice [112]. Nox2ds-tat was designed as a peptide mimicking the second intracellular loop of Nox2, with the "tat" sequence added to the C-terminus to facilitate cell permeation [112]. Since its development, the utility of Nox2ds-tat has been demonstrated as a Nox inhibitor in a wide variety of cell and organ systems representing different disease phenotypes, including cardiovascular and neurodegenerative manifestations of disease consistent with the expression of Nox2 [151, 167, 237, 238]. However, despite the widespread efficacy and utility of Nox2ds-tat, specificity of Nox2ds for the Nox2-oxidase had not been fully tested. This gap in knowledge was in part a result of the development of Nox2ds-tat prior to or simultaneous with the discovery of new Nox homologues. Indeed, Nox1 was discovered in prostate cancer cells in 1999 [100] while Nox4 was discovered in kidney cells in 2001 [131] and Nox5 was discovered in testis in 2001 [53]. At the time of Nox2ds-tat's discovery, vascular expression, physiological roles, and genetic data of these Noxes was completely lacking, thereby precluding investigation of the specificity of Nox2ds-tat against these novel Nox isoforms [108]. What's more, heterologous systems (i.e., COS or HEK cell preparations) were not generally available.

The significant homology between Nox1 and Nox2 has raised a possibility that Nox2ds may also inhibit Nox1 despite its derivation from components of the Nox2 oxidase. Since its discovery in 2001, Nox2ds-tat has seen continued use as a generic Nox inhibitor and an untested bias that it would be effective at inhibiting other Noxes. As the major vascular isoforms of Nox are Nox1, Nox2, and Nox4 (with the specificity of Nox2ds vs Nox4 being tested elsewhere), our laboratory proceeded to characterize the specificity of Nox2ds-tat for Nox2 vs Nox1 and Nox4 and to determine the relative roles of various isoforms of Nox in endothelial cell biology. The group long postulated that Nox2ds preferentially inhibits Nox2 rather than Nox1 and 4 by virtue of its design. Furthermore, elucidation of the primary Nox isoform responsible for ROS production in HPAEC and subsequent effect on cell physiology was sought in this dissertation. Here, as part of a comprehensive study performed by Drs. Csanyi and Pagano (and co-workers), I performed a subset of experiments using cell-free biochemical assays of Nox activity to determine the pharmacological profile of Nox2ds against Nox1, Nox2 and Nox4. Nox2ds' specificity was tested without the "tat" conjugation as these assays were performed in cell-free systems. Following certification of Nox2ds specificity, I utilized NoxA1ds and Nox2ds-tat to investigate the relative contribution of Nox1 and Nox2 to hypoxia-induced $O_2^{\cdot-}$ production and VEGF-mediated migration of endothelial cells. The "tat" cell penetrating peptide leader sequence was added to Nox2ds and used for our endothelial cell migration experiments.

4.2 RESULTS

4.2.1 Nox2ds inhibits $O_2^{\bullet -}$ production from Nox2-oxidase

To investigate whether Nox2ds inhibits $O_2^{\bullet -}$ production in the Nox2 oxidase system, SOD-inhibitable cytochrome *c* reduction was measured in Nox2ds-pretreated COS-Nox2 cell lysates. Addition of LiDS to lysates derived from COS-Nox2 cells stimulated $O_2^{\bullet -}$ production in a reaction that was dependent on the presence of NADPH (1.33±0.1 and 0.40±0.1 nmol $O_2^{\bullet -}$ /min/10^7 COS-Nox2 lysate-cell equivalents for LiDS- and vehicle-treated COS-Nox2 lysates, respectively, $p < 0.05$). $O_2^{\bullet -}$ production in non-transfected COS-22 cell lysates (control) was 0.16±0.1 nmol $O_2^{\bullet -}$/min/10^7 COS-22 lysate-cell equivalents (Fig. 4-1). As demonstrated in Fig. 4-1, preincubation of COS-Nox2 cell lysates with Nox2ds (before LiDS-treatment) concentration-dependently inhibited $O_2^{\bullet -}$ production, displaying an IC_{50} of 0.74 μM. In contrast, preincubation of COS-Nox2 cell lysates with scrmb Nox2ds did not inhibit Nox2-oxidase. Note: Experiments described in Sections 4.2.1 through 4.2.3 are part of a larger study performed by Dr. Gabor Csanyi et al. in the Pagano laboratory and are germane to this dissertation. The candidate's specific experimental contributions to this body of work are noted below.

4.2.2 Nox2ds does not inhibit $O_2^{\bullet -}$ production from Canonical or Hybrid Nox1-oxidase

The series of experiments described in this subsection were personally carried out by the candidate and are directly relevant to the validation of Nox2ds for the purposes of this dissertation. In contrast to the COS-Nox2 cell-free system and in line with the constitutive activity of COS-Nox1/NOXO1/NOXA1 cells, the cytochrome *c* assay of COS-Nox1/NOXO1/NOXA1 cell free system revealed that the canonical COS-Nox1 oxidase does not

require LiDS for activation (nmol $O_2^{\cdot-}$/min/10^7 cell equivalents were: 1.30±0.3 and 0.16±0.1 for COS-Nox1 and COS-22 cell lysates, respectively, $p < 0.05$). Preincubation of COS-Nox1 cell lysates with different concentrations of Nox2ds did not inhibit $O_2^{\cdot-}$ production (Fig. 4-2).

In separate experiments, we tested whether the lack of an inhibitory effect of Nox2ds on the Nox1 system is due to the stable interaction of NOXO1 and NOXA1 with Nox1. The Nox1 organizer subunit NOXO1 was preincubated with vehicle (control) or 10 μM Nox2ds for 10 min, and then NOX1 and NOXA1 were added consecutively. After the preincubation period, LiDS was added and $O_2^{\cdot-}$ production was measured. Our results demonstrate that preincubation of NOXO1 with Nox2ds did not inhibit the canonical Nox1 oxidase (Table 4-1). Previous studies reported that Nox1 can be activated by not only NOXO1 and NOXA1 but also by $p47^{phox}$ and $p67^{phox}$ [226]. We therefore tested the effect of Nox2ds on $O_2^{\cdot-}$ production on all possible combinations of Nox1 oxidase system. As shown in Table 4-1, Nox2ds did not inhibit $O_2^{\cdot-}$ production in either the canonical or the hybrid Nox1 system.

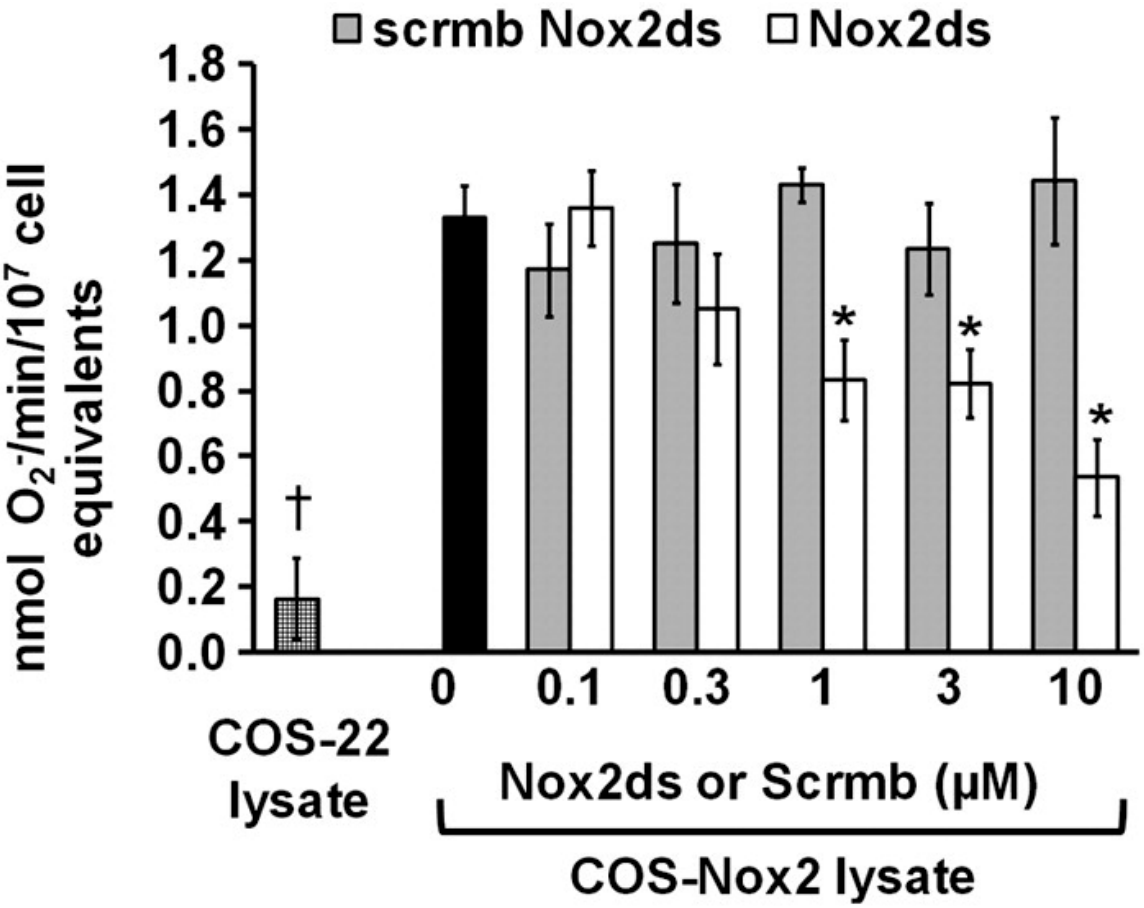

Figure 4-1. Nox2ds dose-dependently inhibits $O_2^{\bullet-}$ production from Nox2-oxidase.

COS-Nox2 cell lysate was preincubated with various concentrations of Nox2ds (from 0.1 μM to 10 μM) and Scrmb Nox2ds (from 0.1 μM to 10 μM) for 5 min at 25°C. After the addition of 130 μM LiDS, $O_2^{\bullet-}$ production was initiated by the addition of 180 μM NADPH and measured by the initial linear rate of SOD-inhibitable cytochrome *c* reduction. $O_2^{\bullet-}$ production is expressed as nmol $O_2^{\bullet-}$/min/10^7 cell equivalents. Data represent the mean ± SEM of 7-16 experiments. For comparison, $O_2^{\bullet-}$ production in non-transfected COS-22 cell lysate is shown. $^{*}p < 0.05$ indicates significant differences in $O_2^{\bullet-}$ production between Nox2ds- and scrmb Nox2ds-treatment. $^{\dagger}p < 0.05$ indicates significant difference between COS-Nox2 and COS-22 cell lysate activity.

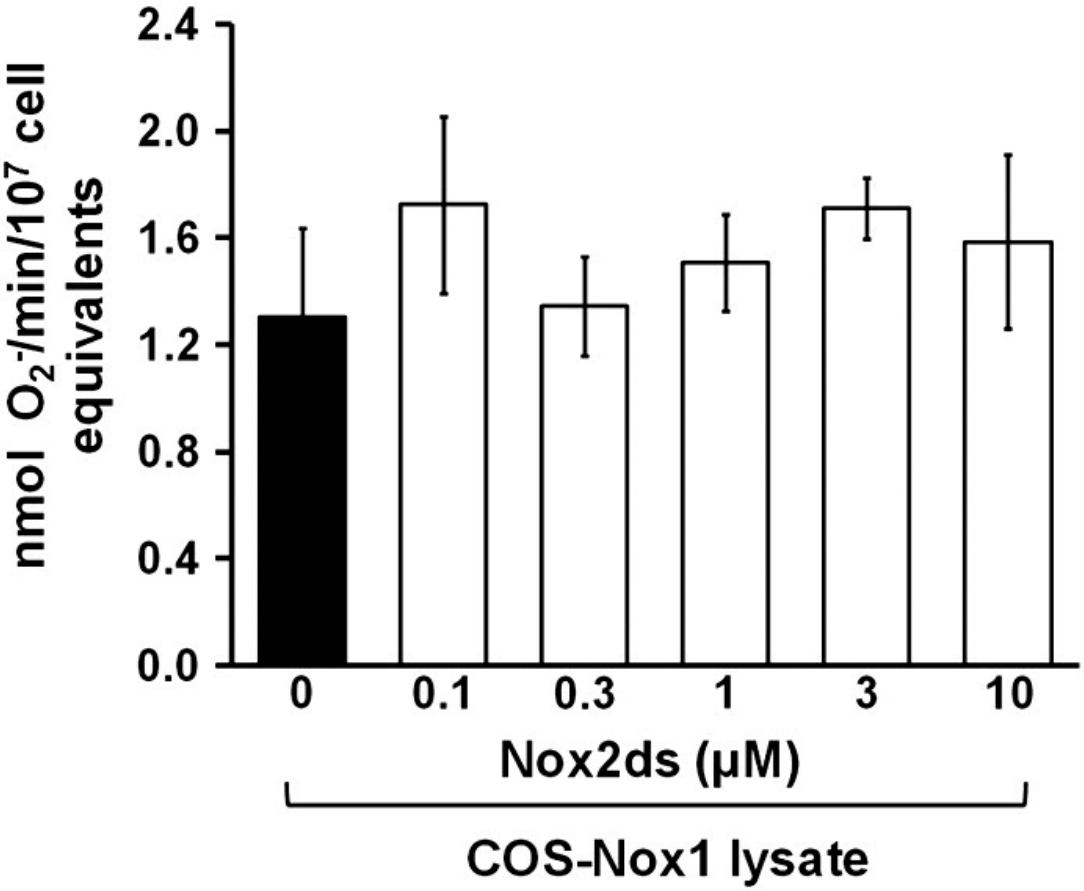

Figure 4-2. Nox2ds does not inhibit $O_2^{\cdot-}$ production from Nox1-oxidase.

COS-Nox1 cell lysate was preincubated with various concentrations of Nox2ds (from 0.1 μM to 10 μM) for 5 min at 25 °C. $O_2^{\cdot-}$ production was initiated by the addition of 180 μM NADPH and measured by the initial linear rate of SOD-inhibitable cytochrome *c* reduction. $O_2^{\cdot-}$production is expressed as nmol $O_2^{\cdot-}$ /min/10^7 cell equivalents. Data represent the mean ± SEM of three experiments. The series of experiments described in this figure were conducted by the candidate and Dr. Csanyi and are directly relevant to the validation of Nox2ds for the purposes of this dissertation.

HEK293 Cells:

Nox system	Control (no LiDS)	LiDS	10 μM Nox2ds + LiDS
Nox1/NOXO1/NOXA1	0.53 ± 0.01	0.98 ± 0.2*	1.2 ± 0.2

COS22 Cells:

Nox system	Control (no LiDS)	LiDS	10 μM Nox2ds + LiDS
Nontransfected COS-22	0.16 ± 0.10	–	–
Nox1/NOXO1/NOXA1	0.53 ± 0.02*	0.49 ± 0.02	0.43 ± 0.04
Nox1/NOXO1/p67^{phox}	0.58 ± 0.04*	0.66 ± 0.18	0.80 ± 0.20
Nox1/p47^{phox}/NOXA1	0.45 ± 0.03*	0.41 ± 0.02	0.66 ± 0.20
Nox1/p47^{phox}/p67^{phox}	0.96 ± 0.03*	1.52 ± 0.18#	1.29 ± 0.20

Table 4-1. Effect of Nox2ds on $O_2^{\bullet-}$ generating activity of Nox1 oxidase.

COS-22 cells were separately transfected with Nox1, NOXO1, p47^{phox}, NOXA1 or p67^{phox}, lysed and the Nox1 membrane component, as well as the NOXO1, p47^{phox}, NOXA1 and p67^{phox} cytosolic extracts were separately prepared. The respective organizer subunit (NOXO1 or p47^{phox}) was preincubated with vehicle (control) or 10 μM Nox2ds for 10 min, and then Nox1-containing membrane and NOXA1/p67^{phox} were added consecutively. After the preincubation period, LiDS (130 μM) was added to induce the assembly of the oxidase and $O_2^{\cdot-}$ production was initiated by 180 μM NADPH. $O_2^{\bullet-}$ was measured by the initial linear rate of SOD-inhibitable cytochrome *c* reduction. $O_2^{\cdot-}$ production is expressed as nmol $O_2^{\cdot-}$/min/10^7 cell equivalents. Data represent the mean ± SEM of 3–6 experiments. The series of experiments described in this subsection were personally carried out by the candidate and are directly relevant to the validation of Nox2ds for the purposes of this dissertation.

4.2.3 p47^{phox}, but not NOXO1, binds to Nox2ds

Nox2ds was designed to selectively inhibit the interaction between the cytosolic B-loop of Nox2 and p47^{phox} by binding to p47^{phox} and preventing its translocation to the membrane. To confirm this binding and to rule out binding of Nox2ds to NOXO1, ELISA experiments were performed on lysates from p47^{phox}- or NOXO1-transfected COS-22 cells incubated in ELISA plates with neutravidin-immobilized biotinylated Nox2ds or its scrambled control. As shown in Fig. 4-3A, using p47^{phox} antibody to detect binding (followed by fluorescently tagged secondary antibody), fluorescence intensity in biotinylated Nox2ds-bound wells was significantly higher when cytosolic fractions of COS-22-p47^{phox} vs. COS-22 were added. These data indicate that p47^{phox} binds to Nox2ds. Binding of p47^{phox} was sequence specific as p47^{phox} binding to the scrambled sequence produced significantly less fluorescence (Fig. 4-3A). In contrast, there was no difference in fluorescence intensity when cytosolic fractions of COS-22 NOXO1 vs. COS-22 cytosol were added to plates bound with Nox2ds, followed by incubation with NOXO1 antibody (Fig. 4-3B).

4.2.4 Nox1, but not Nox2-derived $O_2^{\bullet-}$ Mediates Endothelial Cell Migration

To test the role of this key Nox1-NOXA1 interaction in a pathophysiologically relevant vascular cell phenotype, we investigated whether Nox1-NoxA1ds binding and inhibition was effective in HPAEC as these cells express abundant Nox1 and Nox2 with Nox4 being the most highly expressed (Fig. 4-4B). ELISA data indicated that NoxA1ds bound to Nox1 but not Nox2 or -4 in HPAEC (Fig. 4-4A). HPAEC were exposed to 1.0% oxygen for 24 h and treated with 10 μm NoxA1ds or SCRMB for 1 h before measuring $O_2^{\cdot-}$ production. Hypoxia caused a 3-fold increase in $O_2^{\cdot-}$ production that was completely inhibited by preincubation with NoxA1ds but not

with SCRMB or by Nox2ds-tat (Fig 4-4C,F). The effect of NoxA1ds was partially replicated using Nox1 siRNA, with detectable yet statistically insignificant inhibition of $O_2^{\cdot -}$ production. The incomplete inhibition of $O_2^{\cdot -}$ production was likely due to incomplete knockdown of Nox1 by the siRNA (Fig. 4-4E). To determine the effect of NoxA1ds on migration, we performed a wound assay on VEGF-stimulated HPAEC migration under hypoxic conditions (1.0% O_2). NoxA1ds caused a significant reversion in endothelial cell migration to vehicle control levels, an effect that was not observed in cells treated with SCRMB or Nox2ds-tat (Fig. 4-5). Additionally, HPAEC transfected with Nox1-YFP and NOXA1-CFP showed an increase in FRET when treated with 20 nm VEGF that was inhibitable by NoxA1ds, indicating that VEGF promotes Nox1-NOXA1 association (Fig.4-6).

4.2.5 Fibroblasts are a Potential *in vivo* Source for VEGF during Hypoxia

To determine potential sources for VEGF and thus Nox1 activation in the vessel, HPAEC, HPASMC and HPAF were cultured at either 20% O_2 or 1.0%O_2 for 24 hrs before quantification of VEGF in the cell culture media. HPAEC consumed nearly all VEGF initially present in the media while HPASMC produced substantial VEGF, yet in a hypoxia independent manner. Interestingly, HPAF were the only tested vascular cell type to exhibit enhanced VEGF production during hypoxia (Figure 4-7). This VEGF-enriched media derived from hypoxia conditioned HPAF was then used to culture HPAEC and was observed to support HPAEC mitogenic propensity significantly more than media derived from normoxia conditioned HPAF as measured by MTT assay. This stimulation of mitogenic propensity was inhibited by NoxA1ds, confirming a role for Nox1 in VEGF stimulated HPAEC proliferation (Figure 4-7D).

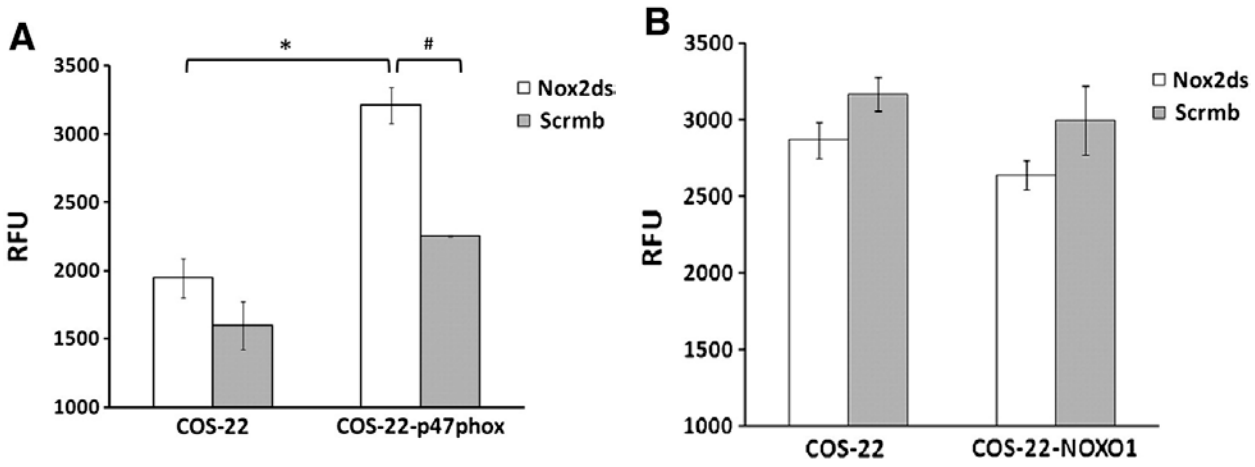

Figure 4-3: p47^{phox}, but not NOXO1, binds to Nox2ds.

ELISA experiments were performed to test whether p47^{phox} (A) and NOXO1 (B) bind to Nox2ds and/or scrmb Nox2ds. Biotinylated Nox2ds and scrambled peptides were first bound to neutravidin-coated plates and then incubated with COS-22, COS-22-p47^{phox} (COS-22 cells transfected with p47^{phox}) or COS-22-NOXO1 (COS-22 cells transfected with NOXO1) cytosolic extracts for 1 hr at room temperature. Rabbit polyclonal p47^{phox} or rabbit NOXO1 antibodies were used to detect Nox2ds-bound p47^{phox} or NOXO1, respectively. After 1 hr incubation and extensive washing, bound primary antibodies were detected by FITC-labeled goat anti rabbit IgG antibody. The fluorescence of each well was measured using a Biotek Synergy 4 Hybrid Multi-Mode Microplate Reader (Excitation:488 nM, Emission:518 nM). Data represent the mean ± SEM of 3–4 experiments. *p<0.05 between COS-22 and COS-22-p47^{phox} cytosolic extracts in Nox2ds wells. $^{\#}p$<0.05 between Nox2ds and Scrmb Nox2ds wells incubated with COS-22-p47^{phox} extracts

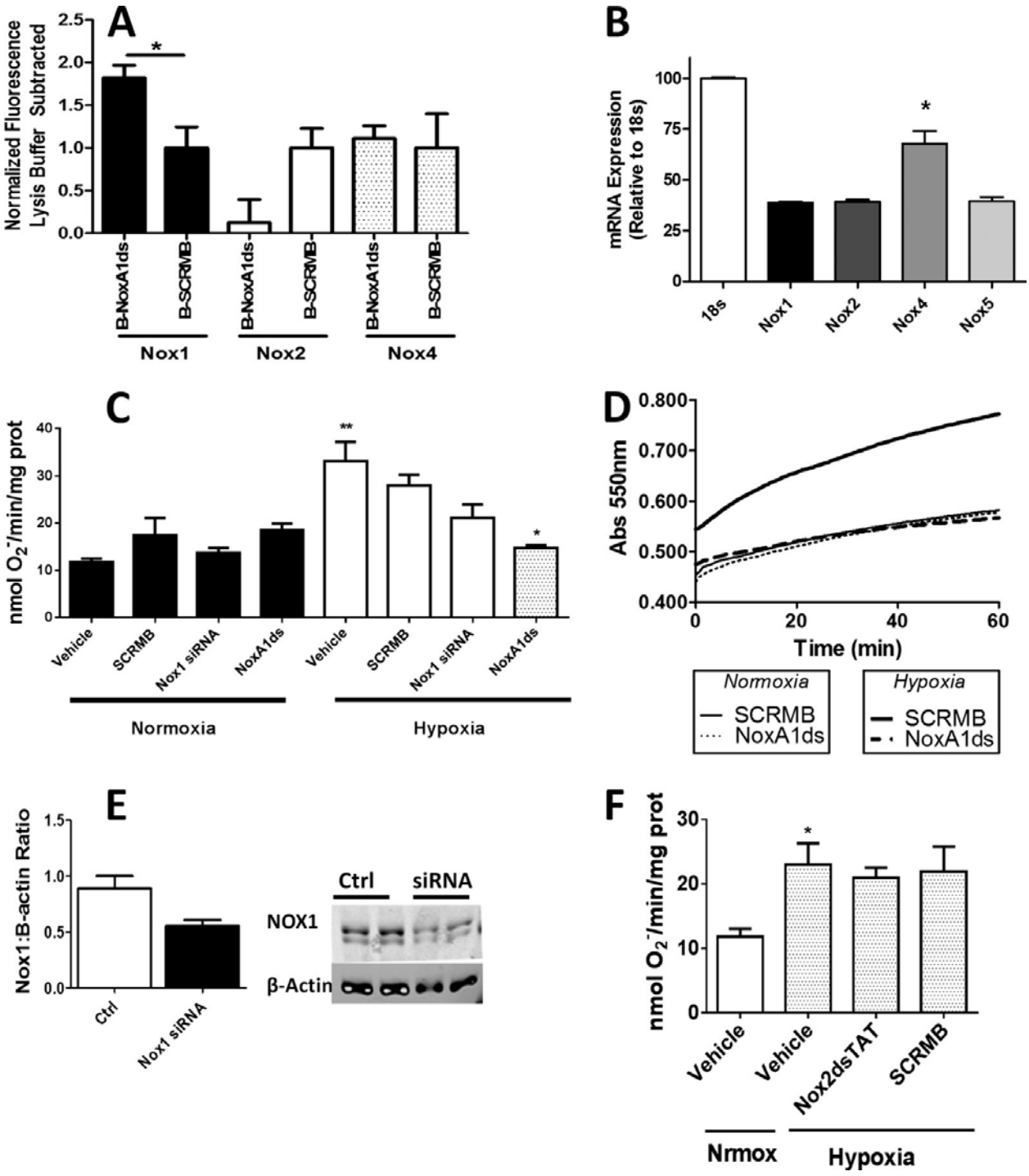

Figure 4-4: NoxA1ds attenuates hypoxia-induced $O_2^{\cdot-}$production.

A) NoxA1ds binds to Nox1 but not Nox2 or Nox4 in HPAEC. Neutravidin coated plates were incubated with biotin-tagged NoxA1ds (B-NoxA1ds) or biotin-tagged SCRMB (B-SCRMB) before addition of HPAEC cell membranes. Captured Noxes were detected through a Alexa-488 conjugated secondary

antibody bound to the Nox1,2 or 4 primary antibody. Fluorescence was expressed with background lysis buffer fluorescence subtracted. When fluorescence was detected via Nox1 primary antibody, there was a significant increase in binding as compared to B-SCRMB. *n* = 4, *p<0.05, unpaired t-test. **B)** Relative Nox expression in HPAEC quantified by qPCR. **C)** In hypoxia and normoxia, SCRMB and NoxA1ds peptides were added to cells at 10uM for 1hr prior to cell lysis and quantification of enzyme activity. Cells were transfected with Nox1 siRNA 24hrs prior to 24hr normoxic/hypoxic treatment followed by cell lysis and quantification of enzyme activity. SCRMB, NoxA1ds, and Nox1 siRNA had a negligible effect on $O_2^{\cdot -}$production under normoxic conditions. Hypoxia (1.0% O_2, 24hrs) treatment resulted in a three-fold increase in $O_2^{\cdot -}$ production that was unaffected by SCRMB. Upon treatment with NoxA1ds, $O_2^{\cdot -}$production by cells subjected to hypoxia returned to the amount observed under normoxia. **D)** Representative experimental trace for enzyme activity in "B" shown as the SOD-inhibitable reduction of cytochrome c over time. n = 9, three separate experiments. **E)** Western blot analysis of Nox1/β-actin protein from Nox1 siRNA or control treated human pulmonary artery endothelial cells (HPAEC). Nox1 knockdown was incomplete and approximates the degree of knockdown observed as $O_2^{\cdot -}$ production **F)** Hypoxia (1.0% O_2, 24hrs) treatment resulted in a two-fold increase in HPAEC (Human Pulmonary Artery Endothelial Cells) $O_2^{\cdot -}$ production that was unaffected by Nox2ds-tat or its control (SCRMB). *n* = 9, three separate experiments. *p<0.05, **p<0.01, one-way ANOVA with Bonferroni post-hoc t-test.

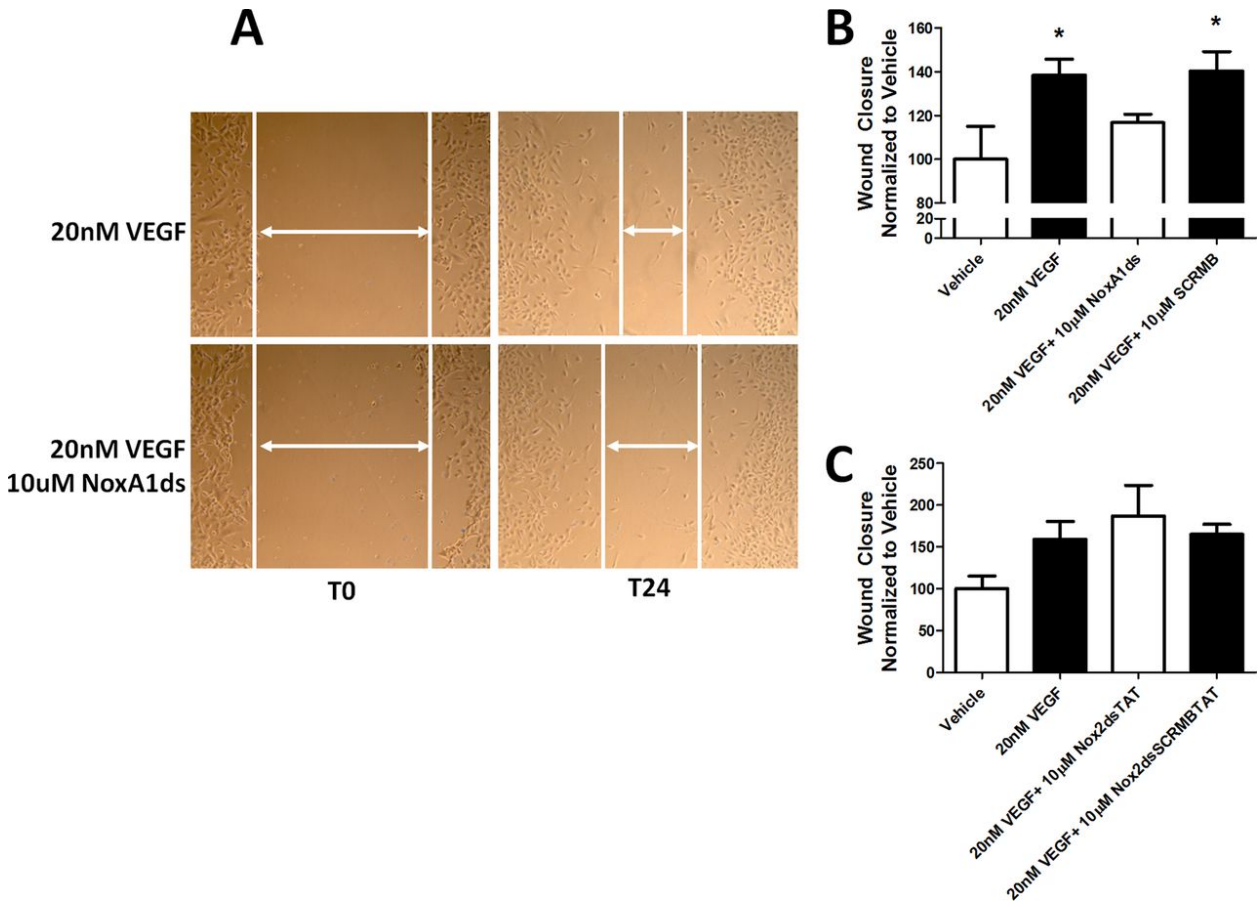

Figure 4-5: Nox1, but not Nox2, is responsible for VEGF-stimulated wound healing.

Confluent HPAEC were scratched with P1000 pipet tip, photographed, treated with 20nM VEGF +/- 10μM NoxA1ds, and photographed again after 24 hours. **A)** Representative images of HPAEC immediately after scratch wounding and 24hrs post scratch wound. **B)** Quantification of HPAEC wound closure VEGF +/- 10μM NoxA1ds **C)** Quantification of HPAEC wound closure treated with VEGF +/- 10μM Nox2ds-tat. Values represent n=6-8, three to four separate experiments, *$p<0.05$ one-way ANOVA with Bonferroni post-test as compared to vehicle treatment.

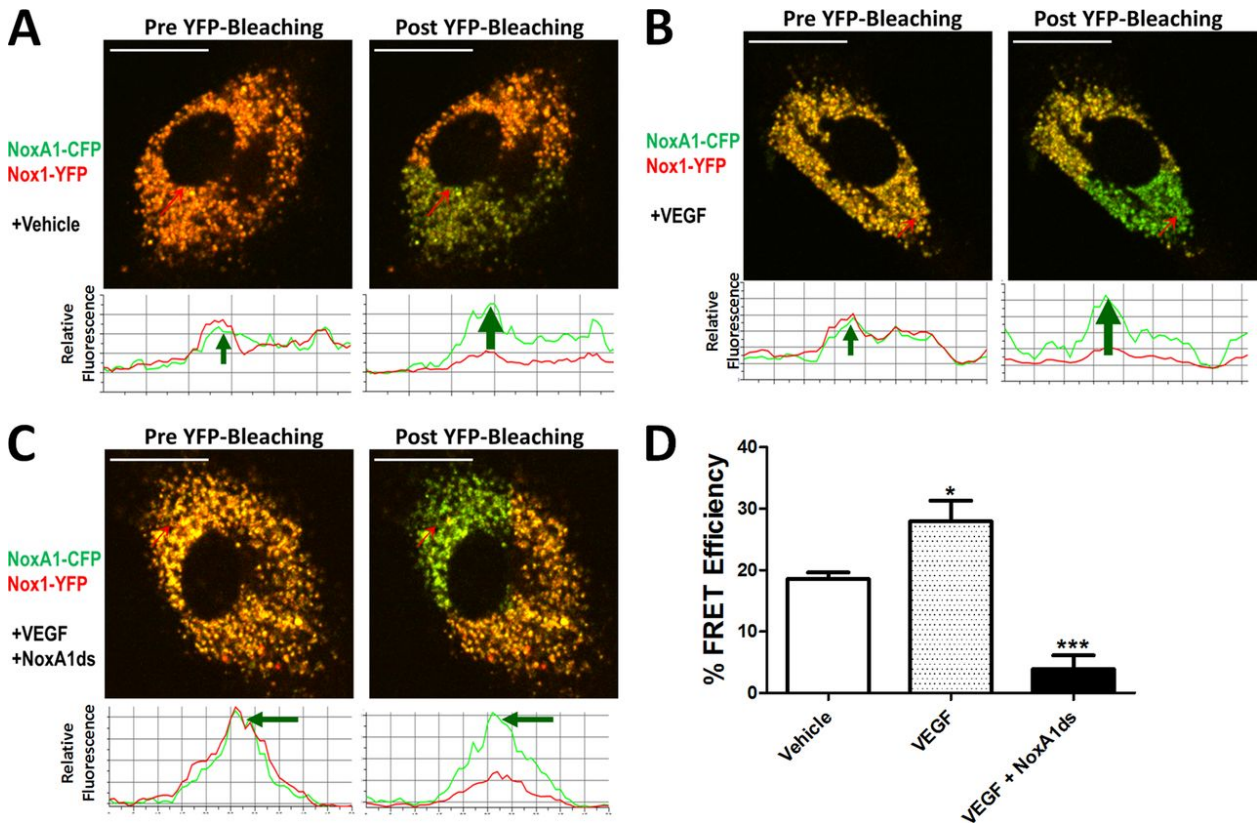

Figure 4-6: NoxA1ds disrupts VEGF-stimulated Nox1-NOXA1 interaction.

FRET between Nox1-YFP and NoxA1-CFP transfected HPAEC in the presence or absence of 20 nm VEGF and/or 10 μM NoxA1ds. Relative fluorescence of CFP is *green*, and YFP is *red. Traces* below the images indicate fluorescent intensities of CFP and YFP below the *arrow* overlaid on each cell. **A)** transfected HPAEC were treated with vehicle for 1 h prior to imaging cells; photobleaching of Nox1-YFP was complete and resulted in a concomitant increase in CFP fluorescence. **B)** transfected HPAEC were treated with 20 nm VEGF for 1 h prior to imaging cells; photobleaching of Nox1-YFP was complete and resulted in an increase in CFP fluorescence of greater magnitude than without VEGF. **C)** Transfected HPAEC were treated with 10 μM NoxA1ds peptide for 1 h prior 20 nm VEGF for 1 h. Cells were then imaged after VEGF treatment. Photobleaching of Nox1-YFP was complete but did not result in a concomitant increase in CFP fluorescence. **D)** Quantification of FRET efficiency from images A-C. Values expressed as $n = 6$, two separate experiments; *, $p < 0.05$ *versus* vehicle; ***, $p < 0.001$ *versus* VEGF, one-way ANOVA and Bonferroni post-test.

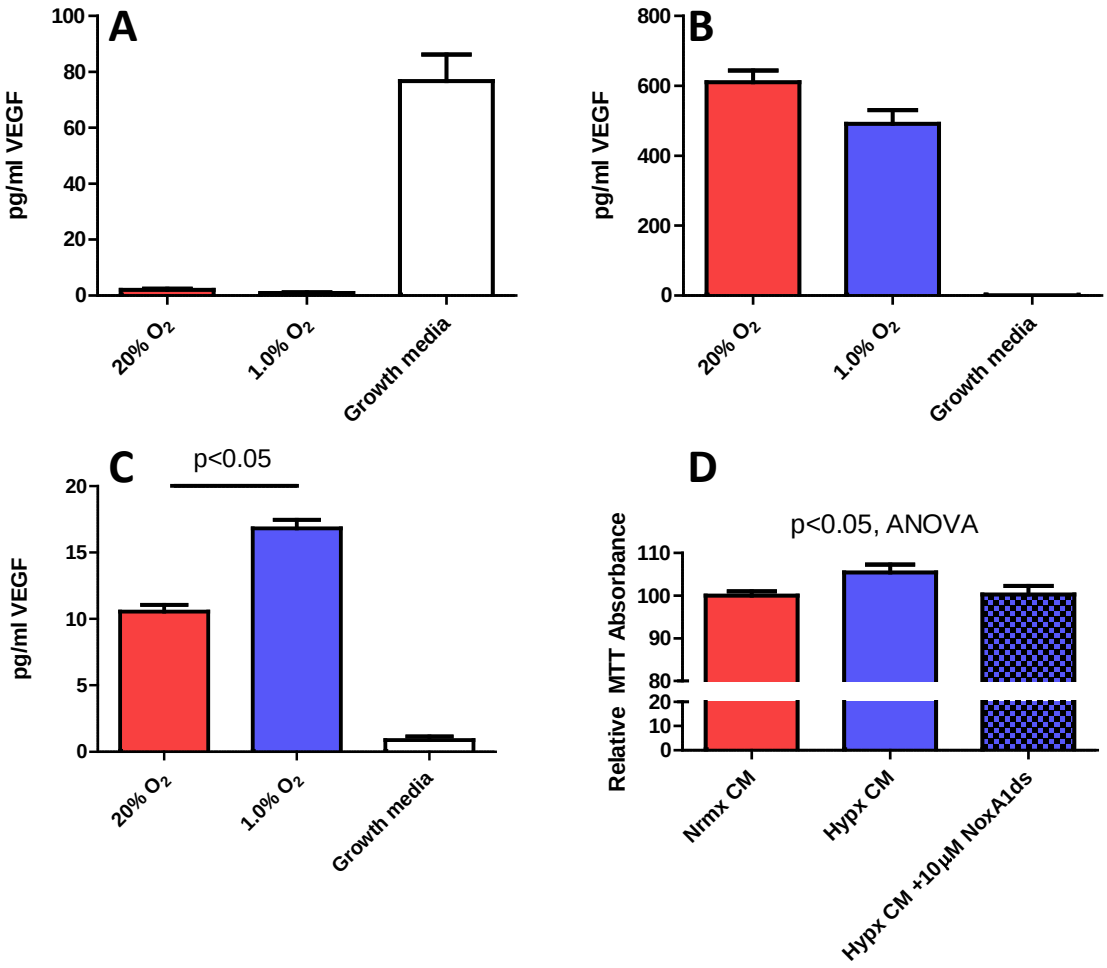

Figure 4-7: VEGF Production by HPAF is enhanced by hypoxia.

A) VEGF production by HPAEC measured by MSD ELISA indicated that HPAEC consumed most VEGF present in the media after 24hrs in either hypoxic (1.0% O_2) or normoxic (20% O_2) media, *n*=3. **B)** HPASMC produce VEGF with respect to naïve media without cells but in an oxygen-insensitive manner, *n*=3. **C)** VEGF production by HPAF measured by MSD ELISA indicated that HPAF produce VEGF with respect to naïve media without cells and that this is enhanced by 1.5 fold in hypoxic media versus normoxic media, D) Normoxic HPAF conditioned media (Nrmx CM) or hypoxic HPAF-conditioned media (Hypx CM) was used to culture HPAEC for 24 hrs ±NoxA1ds, after which cellular proliferative propensity was determined by MTT assay. Hypx CM potentiated HPAEC proliferative propensity in a Nox1 dependent manner. *n*=3.

4.3 DISCUSSION

Numerous studies have established the ability of Nox2ds-tat to inhibit Nox activity *in vitro* and *in vivo* [46, 122, 139, 197]. However, until now the specificity of inhibition of Nox2ds (non-chimeric B-loop peptide) between Nox1 and Nox2 had not been investigated. To test the specificity of Nox2ds, we examined its potential inhibitory activity in cell-free assays using reconstituted systems of Nox1 while others demonstrated that Nox2ds does not inhibit Nox4 [130]. Our data demonstrate that Nox2ds concentration-dependently inhibited $O_2^{\cdot-}$ production in a COS-Nox2 cell-free system and that Nox2ds is a potent and efficacious inhibitor of Nox2 NADPH oxidase with an IC_{50} of 0.74 μM. Furthermore, our results demonstrated that Nox2ds does not inhibit ROS production in the COS-Nox1 system with others determining that Nox2ds does not inhibit ROS production by COS-Nox4 or XO. The results of the present study demonstrate selectivity of Nox2ds peptide in differentiating the contribution of Nox2- vs. Nox1-oxidase to Nox-derived ROS production. Furthermore, it was also determined that Nox2ds does not inhibit hybrid Nox1 systems where either NOXO1 or NOXA1 is replaced with $p47^{phox}$ or $p67^{phox}$, respectively. These findings are of particular importance as we showed that $p47^{phox}$, which is present in Nox1 hybrid systems in vascular smooth muscle cells, is the binding target of Nox2ds. These findings have broad implications for distinguishing the role of Nox2 in a wide range of disease processes and support its potential use as a Nox2-targeted therapeutic agent.

We next conjugated Nox2ds to the cell penetrating peptide sequence "tat,"[169] thus enabling us to use Nox2ds-tat and NoxA1ds to comparatively analyze the role of Nox1 vs Nox2 in whole HPAEC $O_2^{\cdot-}$ production in response to hypoxia and VEGF-induced HPAEC migration in a scratch wound healing assay. *In vitro* experiments determined that Nox2 plays an

insignificant role in hypoxia-induced $O_2^{\cdot-}$ production as well as VEGF-induced HPAEC migration. These observations are largely in agreement with those made by Garrido-Urbani *et. al*. showing that Nox1 rather than Nox2 plays a greater role in angiogenesis [98]. Finally, the data presented here establish that Nox1 can be directly activated by VEGF and present a new pathway through which Nox1 can directly influence vascular (patho)physiology.

To investigate potential sources of VEGF in the pulmonary vasculature, HPAEC, HPASMC, and HPAF were incubated under normoxic and hypoxic conditions for 24 hrs and VEGF was quantified in the media. Relative to naïve media devoid of cells, HPAEC consumed nearly all VEGF present, regardless of the oxygen tension. HPASMC produced a substantial amount of VEGF relative to naïve media, but in an oxygen independent manner. Normoxic HPAF produced a significant quantity of VEGF versus naïve media, and this was enhanced by 1.5 fold through hypoxic conditioning (10.56 vs 16.81 pg/ml VEGF), with values comparable to physiological human serum VEGF concentrations (between 10 and 200pg/ml) [239]. When hypoxic HPAF conditioned media enriched in VEGF was used to culture HPAEC, the mitogenic propensity of the HPAEC significantly increased in a Nox1-dependent manner, suggesting that hypoxic HPAF may contribute to HPAEC Nox1 activation *in vivo* through paracrine VEGF signaling in addition to myriad other factors present in the extracellular milieu. While HPAF conditioned media enriched in VEGF was capable of enhancing the mitogenic potential of HPAEC in a Nox1-dependent manner, the magnitude of this 5% increase is minor when compared to the 100% increase in Nox1 activity when HPAEC were treated with hypoxia alone. These data suggest that hypoxia, rather than HPAF-mediated paracrine signaling, is the primary insult that potentiates Nox1 activation in HPAEC.

In collaboration with Drs. Csanyi and Pagano, I observed that Nox2ds is a Nox2 specific inhibitor that does not inhibit canonical, induced, or hybrid Nox1 systems. By using NoxA1ds and Nox2ds-tat to specifically inhibit Nox1 and Nox2, respectively, we determined that Nox1, but not Nox2, is responsible for hypoxic induction of $O_2^{\cdot -}$ production and VEGF-stimulated cell migration of HPAEC. Furthermore, we identified a novel pathway where VEGF can directly activate Nox1:NOXA1 assembly. Our data also demonstrated that HPAF are a potential source for VEGF under hypoxic conditions, although HPAF-sourced VEGF seems to play a minor role in HPAEC physiology when compared to hypoxia alone. These data indicate that targeting Nox1 with NoxA1ds may provide effective therapy for diseases of the pulmonary vasculature, including pulmonary arterial hypertension.

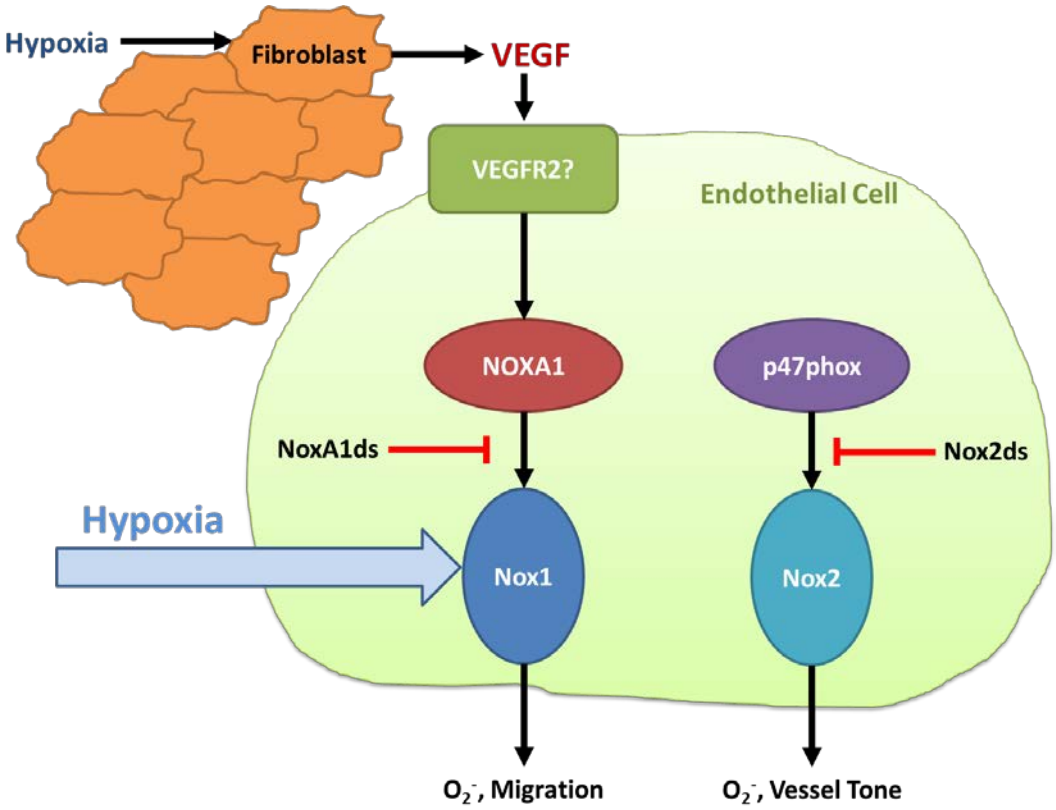

Figure 4-8: Vascular Nox signaling pathways identified

NoxA1ds was developed as a specific Nox1 inhibitor preventing Nox1:NOXA1 binding while Nox2ds was validated as a specific Nox2 inhibitor acting at the site of $p47^{phox}$:Nox2 interaction. Fibroblasts produce VEGF in response to hypoxia. VEGF promotes Nox1:NOXA1 assembly while hypoxia stimulated Nox1 activity. Through VEGF and hypoxia, Nox1 promotes endothelial cell migration and proliferation. Receptor-mediated activation of VEGF stimulated Nox1:NOXA1 assembly is potentially mediated by VEGFR2, although further work is needed to establish this. Further research may establish the stimuli necessary to invoke Nox2 in pulmonary endothelial migration and proliferation, as neither hypoxia nor VEGF treated HPAECs responded in a Nox2-dependent manner.

5.0 INTERROGATE A ROLE FOR NOX1 IN PULMONARY ARTERIAL HYPERTENSION

5.1 INTRODUCTION

5.1.1 Etiology of Pulmonary Arterial Hypertension

Pulmonary arterial hypertension (PAH) is a debilitating disease with high mortality characterized by a mean pulmonary artery pressure (mPAP) greater than 25 mmHg, in part a consequence of abnormal pulmonary vessel intimal remodeling as well as reduced NO bioavailability [170]. In many patients, vessel remodeling often partially or completely occludes the lumen, increasing pulmonary vascular resistance and pulmonary pressure eventually leading to right heart failure [170]. Hypoxia stimulates Nox-derived ROS production, causing reduced NO bioavailability, vascular cell proliferation and vessel remodeling [94, 179]. In addition to hypoxia, mitogenic factors promoting vascular cell proliferation, including EGF and VEGF, have been implicated in the development of PAH [174, 181]. Despite this association with hypoxia and growth factors, no cause for idiopathic PAH has been identified and current treatment regimens symptomatically treat the disease [170]. These treatments include prostacyclin, nitrates, beta-blockers, and sartans [240]. Unfortunately, all of these treatments fail to cure PAH and are eventually overcome by desensitized responses, leading to disease progression. Inhibitors of ROS sources, including Nox1, have shown promise in promoting NO bioavailability, attenuating intimal and medial remodeling, thus lowering PVR and providing an alternative and potentially curative therapy for PAH [241, 242]. Despite their potential, no specific Nox inhibitor or antioxidant therapy has yet been identified for PAH.

5.1.2 Pulmonary Vascular Hemodynamics in PAH

The defining hemodynamic phenotype in PAH is a mean pulmonary artery pressure (mPAP) greater than 25 mmHg, causing chronically increased afterload on the right ventricle [170, 243]. This chronic pressure overload results in compensatory right heart hypertrophy associated with preserved contractility eventually leading to decompensation and right heart failure [170]. Indicative of right heart hypertrophy, the Fulton index is a key indicator of PAH that quantifies the relative size of the right heart versus the left heart + interventricular septum (Equation 2) [71]. Beyond simple increases in mPAP and consequent RV hypertrophy, substantial changes in the hemodynamic profile of the RV follow, with each parameter providing a portion of a more detailed picture on the pathology of PAH.

Equation 2:

$$\text{Fulton index} = \frac{\text{Right Ventricle Mass}}{\text{Left Ventricle Mass} + \text{Septum Mass}}$$

Pressure-volume catheterization and the resulting pressure-volume loops (PV loops) is the primary method of evaluating hemodynamic function within the RV or LV in both clinical and scientific cardiology settings. The PV loop quantifies simultaneous pressure and volume changes in the ventricle of the heart though which the catheter is inserted during the cyclical beating of the heart through both systole and diastole. These loops quantitatively describe the filling, contraction, ejection, and relaxation of the ventricle into which the catheter is inserted (Figure 5-1) [65, 67]. Hemodynamic criteria evaluated by PV loop analysis include, but are not limited to, pressure within each ventricle of the heart, the volume of a full ventricle (end diastolic volume, EDV), the amount of blood pumped by the ventricle in unit time (cardiac output), and

the volume of the contracted heart (systolic volume). Perhaps the most important values obtained from PV loop analysis are the end systolic pressure volume relationship (ESPVR) and end diastolic pressure volume relationship (EDPVR) (Figure 5-2). ESPVR indicates the maximum pressure the heart can achieve at any given volume and is a key indicator of ventricular contractility while EDPVR indicates the maximum volume the heart can achieve at any given pressure is a key measure of ventricular compliance. Deviation of either parameter from the ideal slope is an indication of different cardiologic abnormalities, depending on the direction of the shift. In PAH, RV EDPVR remains unchanged while ESPVR increases as a result of the increase in RV pressure with minimal change in volume (Figure 5-1). ESPVR and EDPVR are obtained creating a series of descending PV loops where the volume of the ventricle is reduced by preventing blood return to the heart via vena cava occlusion. ESPVR and EDPVR are then calculated as the slope of a line connecting either the top-left (ESPVR) or bottom-right (EDPVR) inflection points of these descending PV loops (see Figure 1-3).

The nature of closed system of the vasculature as well as the heart's structure, (i.e. the shared septum of the RV and LV) allows for both ventricles to perform separately, but still in a tightly coordinated manner. In performing these independent functions, each ventricle is susceptible to pathologies linked to either the systemic (LV) or pulmonary vasculature (RV). Despite the independent roles of the LV and RV, the closed system of blood flow and shared RV/LV anatomy can cause RV pathologies to directly influence LV function, and vice versa. This concept is of particular importance when considering left heart dysfunction and failure in the context of PAH. While many cases of PAH are restricted to the RV and pulmonary vasculature, a significant portion are also associated with left heart failure. As such, no phenotypic analysis of PAH is complete without both RV and LV hemodynamic consideration.

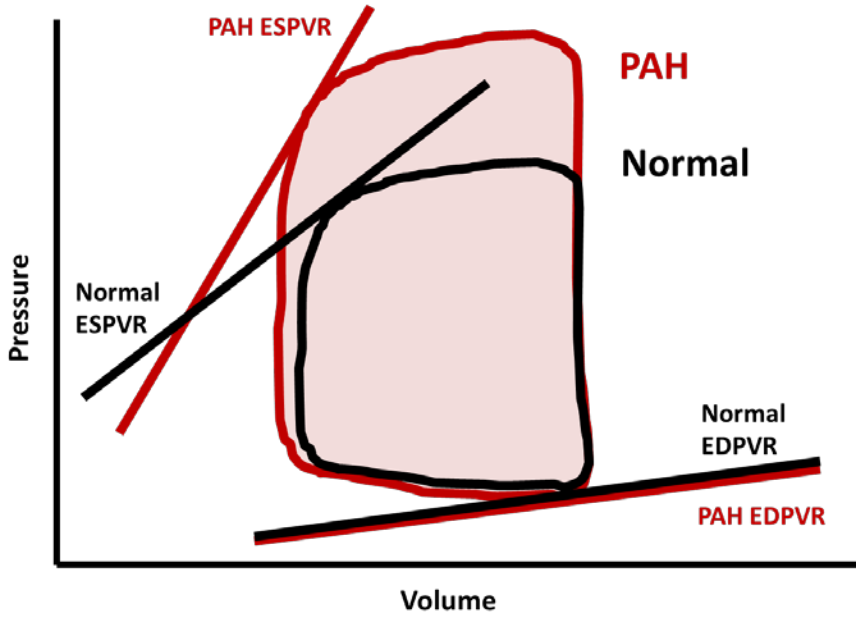

Figure 5-1: Normal vs PAH RV PV-loops.

Normal RV PV-loop with corresponding EDPVR and ESPVR is shown in black. PAH diseased PV loop with corresponding EDPVR and ESPVR is shown in red. EDPVR is unchanged between normal and diseased RV PV-loops while ESPVR increases in PAH.

In this study we quantified RV and LV hemodynamic function in a SU5416 and chronic hypoxia (SUCH) rat model of PAH. As Nox1 was previously shown to be the major Nox isoform responsible for HPAEC migration and hypoxia-induced $O_2^{\cdot-}$ production, we tested whether Nox1 inhibition by aerosolized NoxA1ds can prevent the decline of RV and LV cardiological function in the severe SUCH model of PAH.

5.2 RESULTS

5.2.1 Aerosolized NoxA1ds inhibits SUCH induced RV $O_2^{\cdot-}$ production and insignificantly reduces RV hypertrophy

Female Sprague-Dawley rats injected with 100mg/kg subcutaneous injection of SU5416 followed by a 3 wk course of hypoxia at 10% O_2 (SUCH) to induce severe PAH. After this time, rats were sacrificed and tissues harvested. Cytochrome c detection of $O_2^{\cdot-}$ in RV homogenates indicated that SUCH treatment potentiated $O_2^{\cdot-}$ production in the RV and that this increase was inhibitable by twice weekly treatment with aerosolized NoxA1ds (Figure 5-3). Aerosolization was used for NoxA1ds delivery to bypass potential degradation of orally administered peptides. Additionally, SUCH treatment caused a significant increase in the Fulton index (0.22±.02 vs 0.59±0.05, control vs SUCH). Twice a week treatment with NoxA1ds aerosol had a statistically insignificant effect on the Fulton index (0.59±0.05 vs 0.50±0.03, SUCH vs SUCH+NoxA1ds) (Figure 4-4). These experiments were conducted as part of a collaboration with Dr. Imad Al Ghouleh, Dr. Stevan Tofovic and coworkers in the Vascular Medicine Institute.

5.2.2 Nox1 inhibition does not improve RV hemodynamic dysfunction in severe PAH

Female Sprague-Dawley rats at the completion of SUCH treatment were phenotyped by *in vivo* PV loop analysis of the right heart. SUCH treated rats exhibited a marked increase in mPAP, RV max pressure, and ESPVR vs control rats (mPAP: 15.5±1.2 vs 38.0±2.4mmHg, 23±1.8mmHg vs 57.6±3.7mmHg, ESPVR: 0.094±0.02 vs 0.67±.22 all values control vs SUCH) and a mild but insignificant increase in RV end diastolic volume (186±38µl vs 295±109µl,

control vs SUCH). Twice weekly delivery of NoxA1ds aerosol had no significant effect on any hemodynamic parameters of RV dysfunction (Fig. 5-4 & Fig. 5-5).

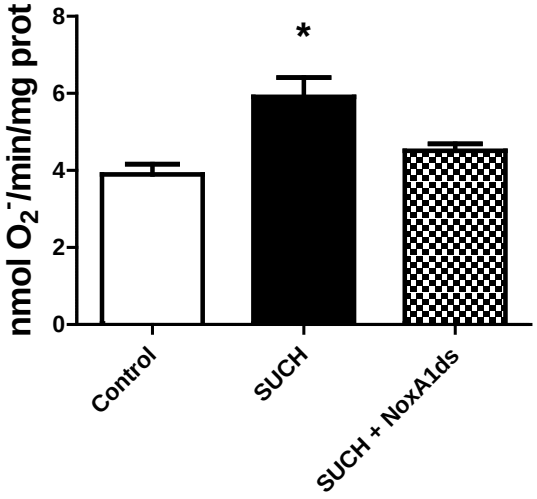

Figure 5-2: SUCH treatment enhances Nox1 mediated $O_2^{\cdot-}$ production in the RV.

RV tissue homogenates from SUCH treated rats produced significantly more $O_2^{\cdot-}$ than RV tissue homogenates from either untreated control animals or SUCH animals treated with aerosolized NoxA1ds, n= 4 rats per group, *p<0.05 via ANOVA followed by Bonferroni post-test compared to control.

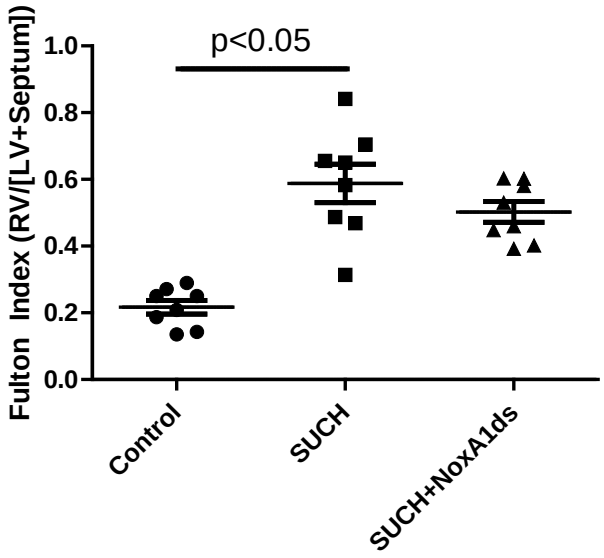

Figure 5-3: SUCH treatment causes RV hypertrophy with a marginal, but insignificant, effect of NoxA1ds.

Fulton index of rat heats indicate a significant increase in RV hypertrophy resulting from SUCH treatment with an insignificant effect of NoxA1ds on RV hypertrophy in SUCH treatment (n=8).

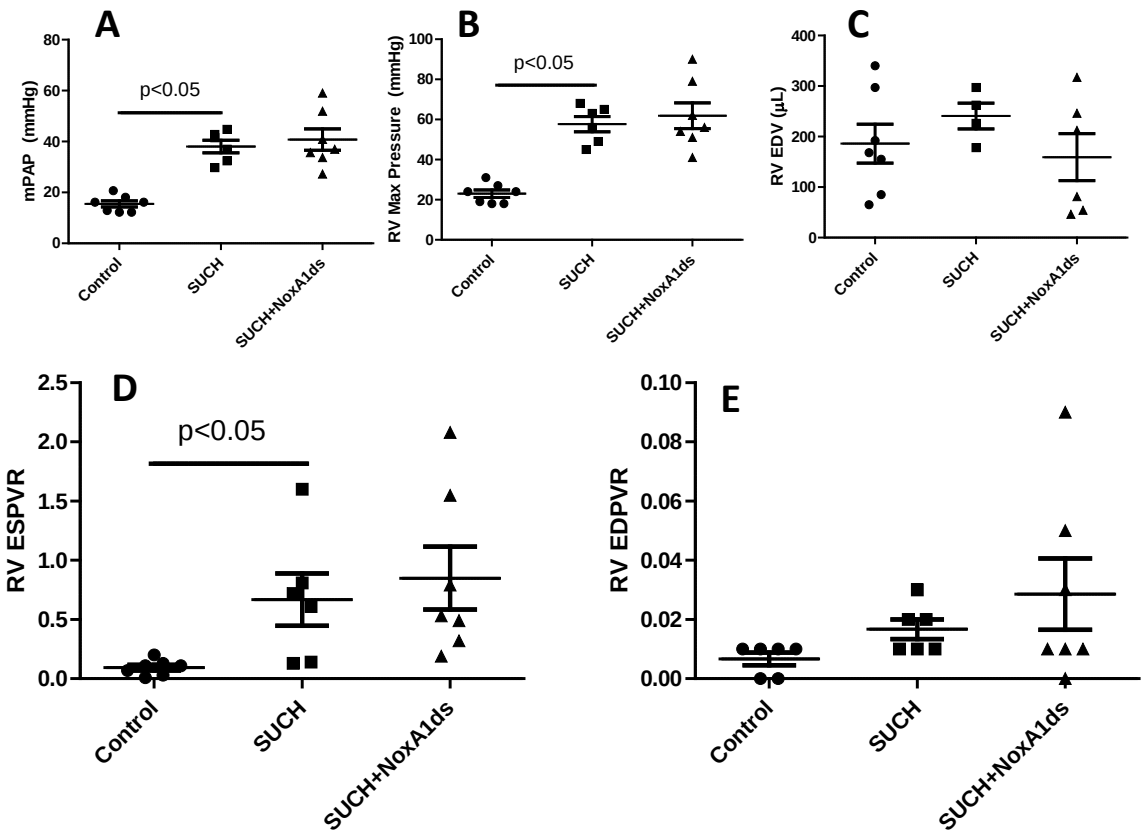

Figure 5-4: Minimal therapeutic benefit of aerosolized NoxA1ds in RV hemodynamic dysfunction. SUCH treatment significantly increased rat **A)** mPAP, **B)** RV Max Pressure and **D)** ESPVR with mild but insignificant increases in **C)** RV EDV and **E)** EDPVR. In no phenotypic measurement did NoxA1ds aerosol attenuate the effects of SUCH treatment, in all panels n = 6-7 rats per treatment.

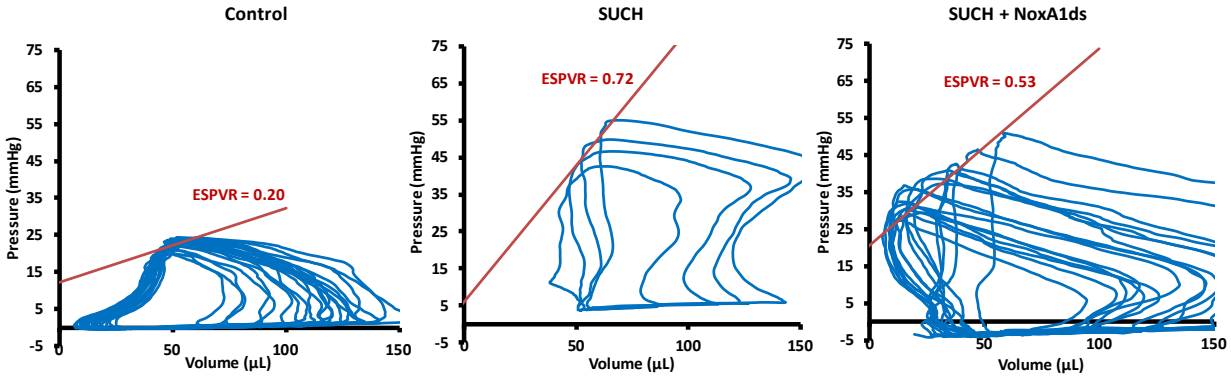

Figure 5-5: Representative Right Ventricle PV-loops.

5.2.3 Nox1 inhibition prevents LV dilatory cardiomyopathy

Immediately after subjecting rats to RV catheterization and PV loop analysis, the LV was catheterized and PV loops from the LV were subsequently recorded. SUCH treatment had no detectable effect on LV pressures or LV ESPVR. Unexpectedly, SUCH caused a significant increase in EDV and a corresponding increase in LV cardiac output. SUCH rats treated with twice weekly NoxA1ds via aerosol did not display an increase in either LV EDV or cardiac output (Fig. 5-7 & Fig. 5-8). Considering both LV pressures and volumes, the LV EDPVR was decreased by SUCH treatment and this decrease was prevented by NoxA1ds aerosol. Statistical analysis was not performed on LV EDPVR as there was no detectable difference between the LV EDPVRs of SUCH treated animals.

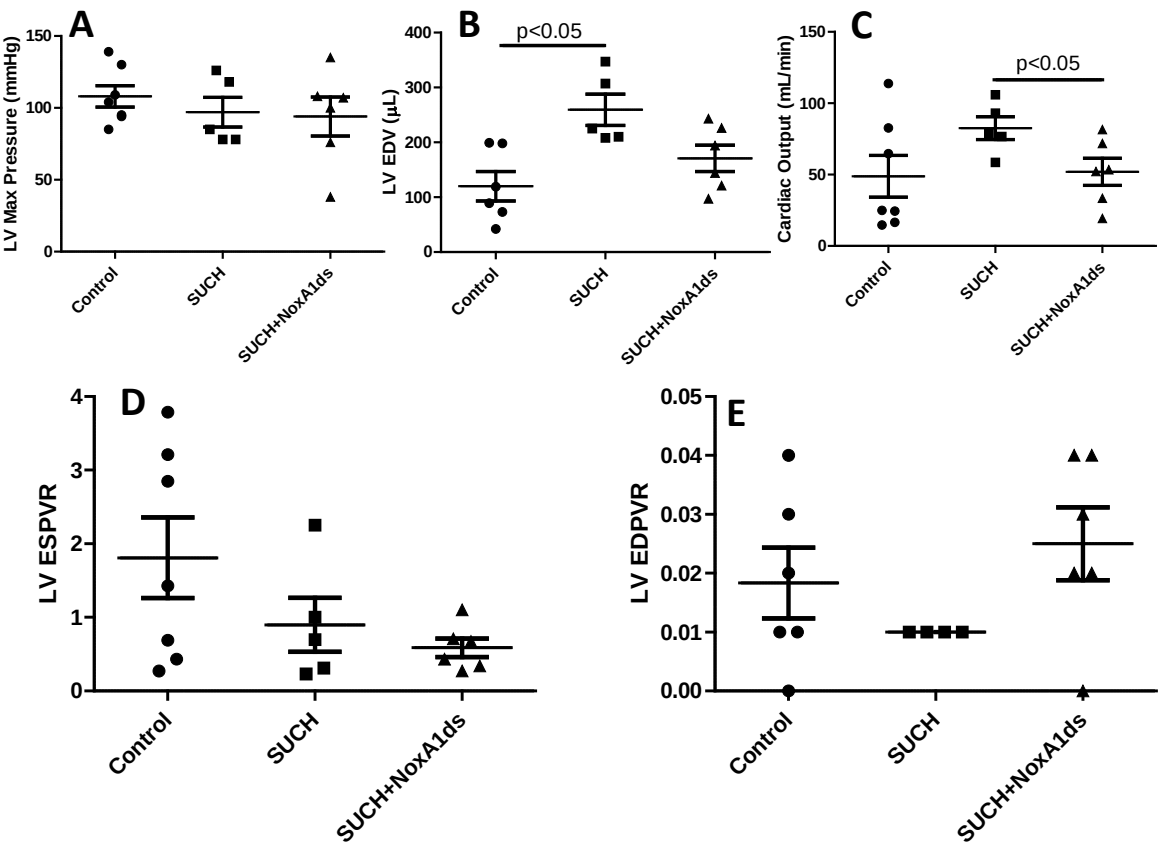

Figure 5-6. SUCH causes LV dysfunction that is prevented by NoxA1ds.

SUCH treatment had no significant effect on **A)** LV max pressure or **D)** LV ESPVR but significantly increased **B)** LV EDV and **C)** LV cardiac output with a corresponding decrease in **E)** LV EDPVR. NoxA1ds prevented the effect of SUCH treatment on LV EDV, cardiac output, and LV EDPVR. Statistical analysis was not performed on the data in "E" as all animals with SUCH treatment exhibited an identical LV EDPVR (0.01), in all panels n=6-7 rats per treatment.

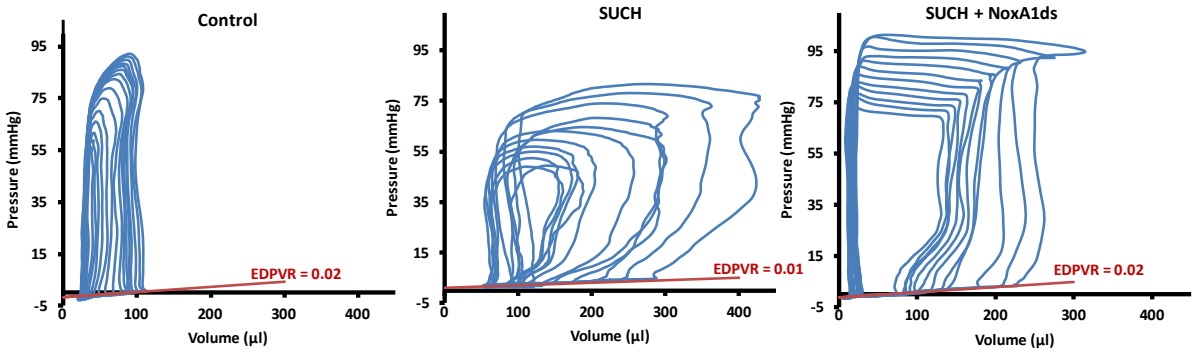

Figure 5-7: Representative Left Ventricle PV-loops.

5.3 DISCUSSION

In this study, we tested the therapeutic potential of Nox1 inhibition in a rodent model of PAH utilizing the combination of SUCH. Of the current leading rodent models of PAH, SUCH was utilized as it exhibits the greatest severity of pulmonary vessel remodeling among rodent models of PAH [206]. Reduced NO bioavailability and endothelial remodeling are both major contributors to increased pulmonary vascular resistance and clinical PAH. Independently of clinical data and *in vivo* models, these factors have also been linked to Nox1 [9, 230]. As Nox1 is more closely linked with endothelial pathophysiology in PAH, we therefore hypothesized that Nox1 inhibition, reduces PAH progression and leading to corresponding changes in pulmonary vascular resistance, RV hemodynamics, and RV remodeling. Beyond its effects on endothelial remodeling, secondary benefits of Nox1 inhibition in PAH likely include potentiation of vasodilation through reduced NO scavenging by Nox1-derived $O_2^{\cdot-}$. Together, these provide ample rationale for investigating the therapeutic potential of Nox1 inhibition in PAH.

Through the established SUCH model of PAH [206], female rats were treated with twice weekly aerosol delivery of either PBS or 10 mg/kg/day NoxA1ds as calculated to deliver 10 μM NoxA1ds to the lung epithelia. Female rats were utilized to as PAH is predominately observed in human female patients. Biweekly aerosolized NoxA1ds effectively inhibited $O_2^{\cdot -}$ produced in RV tissue homogenates, indicating favorable pharmacokinetics and pharmacodynamics of NoxA1ds. Despite the clear effect of NoxA1ds on RV $O_2^{\cdot -}$ production, PV loop analysis of the right ventricle revealed that NoxA1ds treatment had no therapeutic benefit on RV hemodynamics of PAH rats while the Fulton index displayed a marginal, but insignificant, effect of NoxA1ds on RV hypertrophy.

These data displaying a minimal therapeutic benefit of Nox1 inhibition on RV hypertrophy/hemodynamics in the SUCH model of PAH indicate that Nox1 may not be the primary protein responsible for RV dysfunction in PAH. Among the many established contributors to the progression, other likely contributors to RV dysfunction PAH aside from Nox1 include Nox2, Nox4, XO, uncoupled eNOS, and estradiol metabolites [6, 196, 244, 245]. Indeed, at the time of writing, a current publication indicates that PAH in SUCH treated rats is not only Nox4 dependent, but that all of the activating/organizing subunits of Nox1 and Nox2 ($p47^{phox}$, $p67^{phox}$, NOXO1, and NOXA1) are significantly downregulated during SUCH, likely precluding enzyme activity [246]. These data, along with those in the present study, strongly suggest that the SUCH model of PAH is independent of Nox1 and Nox2 activity. Beyond simple downregulation of Nox1, SUCH instigated PAH may be independent of Nox1 also through inhibition of VEGFR2 by SU5416 and subsequent inhibition of direct signaling between VEGF and Nox1.

Simultaneous with the PV loop analysis of RV hemodynamics in SUCH treated rats, PV loop analysis of the LV of SUCH treated rats was also performed. Unexpectedly, SUCH rats demonstrated LV dilatory cardiomyopathy as indicated by increased EDV, cardiac output, and reduced EDPVR. This LV dilated cardiomyopathy was independent of left heart failure, as evidenced by unchanged LV systolic and diastolic pressures and unchanged ejection fraction and heart rate (Fig. 5-9). Interestingly, development of LV dysfunction was almost completely inhibited by NoxA1ds treatment. Nox2 has previously been identified as a contributor to LV dilatory cardiomyopathy, but prior to this study, it was previously unknown whether Nox1 played a role in this pathology [247]. Clinically, dilatory cardiomyopathy is often seen in patients displaying symptoms of heart failure with preserved ejection fraction (HFpEF). HFpEF has been suspected to be correlated with ROS production, and to our knowledge, Nox1 has not been investigated as a contributor to this disease [248]. While this study was not designed to directly investigate the role of Nox1 in HFpEF, our data present Nox1 as an interesting potential therapeutic target for HFpEF, a disease with poor treatment options and outcomes. As *in vivo* models for HFpEF are developed we may be able to test this indication for Nox1 inhibition more conclusively.

Other groups have reported that both SU5416 and hypoxia are independently associated with LV dysfunction and systemic hypertension in animals and humans [249-252]. Indeed, the initial clinical trials testing the efficacy of SU5416 against tumor progression noted systemic hypertension as well as cardiac dysfunction as significant side effects [253-255]. Unfortunately, no systemic measures of vascular tone were obtained in the present study, and the effect of Nox1 inhibition on LV dysfunction must be evaluated independently of potential systemic effects, although there is abundant evidence from other studies indicating that SU5416 and hypoxia each

contribute to LV dysfunction in part through systemic hypertension. Future studies will evaluate the effect of Nox1 inhibition in systemic models of hypertension and associated LV dysfunction.

As a whole, our results demonstrate that Nox1 plays a key role in dilatory cardiomyopathy with preserved ejection fraction and that Nox1's role in the development of PAH is likely superseded by other proteins in the SUCH model of PAH. These data indicate that other models of PAH independent of VEGFR inhibition may be better suited for evaluating the role of Nox1 in PAH and also strongly suggest further investigation concerning Nox1's role in the systemic vasculature, LV dysfunction, and HFpEF.

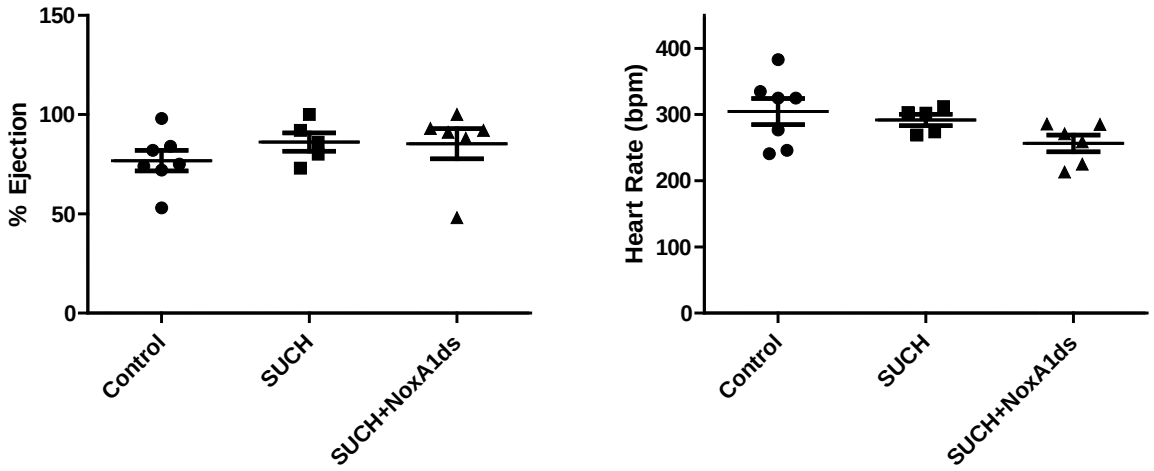

Figure 5-8: LV ejection fraction and heart rate during SUCH treatment

There was no detectable difference in LV ejection fraction or heat rate between control, SUCH, and SUCH + NoxA1ds treated rats.

6.0 GENERAL DISCUSSION AND CONCLUSION

6.1 GENERAL DISCUSSION

Nox1-derived $O_2^{\cdot-}$ is associated with morbidity and mortality of multiple diseases including atherosclerosis, systemic hypertension, inflammatory bowel disease, and cancer [9, 83, 101, 137, 256]. Specific pharmacological inhibitors of Nox1 have long been desired as potential therapeutics for these diseases and as tools to evaluate the role of Nox1 while avoiding the confounding factors inexorably tied with genetic manipulation of cellular and animal models. In a major step towards meeting this great unmet clinical and scientific need, we have developed the first specific Nox1 inhibitor with a validated target and established mechanism of action and called this inhibitor NoxA1ds. After verifying Nox2 specificity of the established Nox inhibitor Nox2ds-tat, NoxA1ds and Nox2ds-tat were then used to evaluate the role of Nox1 vs Nox2 in hypoxia stimulated $O_2^{\cdot-}$ production and VEGF-stimulated migration by HPAECs *in vitro*. As Nox1 was established as the primary contributor to pathways linked to the pathophysiology of PAH (endothelial $O_2^{\cdot-}$ production and VEGF stimulated migration), NoxA1ds was tested as a potential therapeutic in an *in vivo* model of PAH. Although limited therapeutic benefit of NoxA1ds in the RV was observed in the tested models *in vivo*, a therapeutic benefit of NoxA1ds was observed in the LV, bearing implications for left ventricular HFpEF in association with PAH and systemic cardiovascular dysfunction.

6.1.1 Specific Aim 1: Develop and Characterize an Isoform Specific Nox1 Inhibitor

The lack of specific Nox inhibitors has stymied progress into the role of these enzymes in physiology and disease. To date, major existing Nox inhibitors include diphenyleneiodonium (DPI), ML171, GKT137831, and Nox2ds-tat among others [112, 157-160]. DPI has long been considered a potent Nox inhibitor, yet it is burdened by its lack of specificity for any Nox isoform and its inhibition of other flavoproteins [157, 158]. The compound ML171 was recently reported as a specific Nox1 inhibitor with no reported inhibition of Nox2 or Nox4 activity [159]. Unfortunately, the mechanism of action and protein target of ML171 remain unanswered questions. It also remains unknown whether ML171 acts on Nox4, Nox5, or XO-derived ROS production. The compound GKT137831 is a potent Nox1/4 inhibitor and bears the distinction of being the first Nox inhibitor to have reached phase I clinical trials [160]. Of the above compounds, DPI and GKT137831 are plagued by their lack of specificity against a single Nox isoform while the reports on ML171 and GKT137831 lack mechanistic insight. However, these compounds remain potentially useful in situations where multiple Noxes contribute to a single phenotype.

The design and mechanistic clarity of the Nox1 inhibitor NoxA1ds represents a significant step forward in the investigation of NADPH oxidase roles in physiology and pathophysiology. Indeed, prior to this study, a specific Nox1 inhibitor with validated target and established mechanism did not exist. By recapitulating residues 195-205 of NOXA1 reputed to activate Nox1 and including the F199A first made by Maehara et al, we generated the peptide NoxA1ds [195-EPVD(F→A)LGKAKV-205][129]. NoxA1ds was added in increasing concentrations to cell-free preparations of vascular Nox isoforms Nox1, Nox2, Nox4, Nox5 and XO. Resulting ROS production demonstrated that NoxA1ds, but not its scrambled control,

inhibited Nox1 derived $O_2^{\cdot-}$ with an IC_{50} of 20nM. Neither NoxA1ds nor SCRMB had any inhibitory effect on Nox2, Nox4, Nox5, or XO, demonstrating that NoxA1ds is specific for Nox1 and does not scavenge either $O_2^{\cdot-}$ or H_2O_2.

All of the initial assays testing the specificity of NoxA1ds were conducted in cell-free assays to maximize our ability to identify putative Nox1 inhibitors. As such, we proceeded to verify that NoxA1ds was also effective in whole cells. We first verified the ability of NoxA1ds to penetrate cells through the observation that FITC-tagged NoxA1ds crossed the plasma membrane of intact cells within 1 hr. We next tested the effect of NoxA1ds on HT-29 cells that exclusively express Nox1 and not any other Nox isoform and determined that NoxA1ds inhibited $O_2^{\cdot-}$ production by HT-29 cells with an IC_{50} of ~100nM. Using ELISA, we demonstrated that NoxA1ds bound to Nox1, but not Nox2. Furthermore, using FRAP, we determined that fluorescently labeled NoxA1ds is less mobile in cells transfected with Nox1, further confirming that NoxA1ds either directly binds to Nox1 or it binds to an as of yet unidentified closely associating protein. Finally, a FRET assay utilizing Nox1-YFP as the energy acceptor and NOXA1-CFP as the energy donor indicated that NoxA1ds disrupted energy transfer between Nox1-YFP and NOXA1-CFP. These data provide a complete mechanistic paradigm where NoxA1ds directly binds to Nox1 and prevents Nox1:NOXA1 association and subsequent enzyme activation, and that inhibition of Nox1 by NoxA1ds is highly specific and efficacious.

Specific Aim 2: Determine Relative Roles of Nox1 vs Nox2 in Endothelial $O_2^{\cdot-}$ Production and Cell Migration

After fully characterizing the mechanism of NoxA1ds, we sought to evaluate the contribution of Nox1 vs Nox2 derived $O_2^{\cdot-}$ *in vitro* using specific pharmacological inhibitors. To this end, we

first validated that an established Nox inhibitor, Nox2ds, does not inhibit Nox1 in reconstituted cell-free heterologous Nox systems transiently expressed in either COS22 or HEK293 cells. Through our characterization of Nox2ds, we discovered that this peptide targets a cytosolic component of the Nox2 oxidase ($p47^{phox}$). Initially, this raised serious concerns as the cytosolic organizing and activating Nox subunits have the potential to activate either Nox1 or Nox2 and that these hybrid systems would not be specifically inhibited by compounds targeting the cytosolic subunits. For this reason, we confirmed that $p47^{phox}$ can substitute for NOXO1 and that $p67^{phox}$ can substitute for NOXA1 in the organization and activation of Nox1 and thus create a hybrid Nox1 system. As this hybrid Nox1 could potentially be inhibited by Nox2ds, we utilized heterologous cell-free systems to verify that Nox2ds does not inhibit any permutation of hybrid Nox1 oxidases with either $p47^{phox}$ substituting for NOXO1 or $p67^{phox}$ substituting for NOXA1. These data, as part of a larger study conducted by Csanyi et al [130], indicate that Nox2ds is a specific Nox2 inhibitor.

With newly-validated specific Nox1 and Nox2 inhibitors, we proceeded to utilize these inhibitors (NoxA1ds and Nox2ds) to determine relative signaling contribution of Nox1 and Nox2 *in vitro*. HPAEC were identified as an ideal cell type to test the relative role of Nox1 vs Nox2 *in vitro*, as both the Nox1 and the Nox2 isoforms are transcribed in equal amounts. ROS production in HPAEC incubated for 24 hrs in hypoxia (1.0% O_2) was significantly increased, as measured by cytochrome *c* reduction, and was inhibitable by NoxA1ds and Nox1 siRNA, but not Nox2ds conjugated to the cell penetrating peptide "tat". Our data indicate that Nox1 is responsible for $O_2^{\cdot -}$ produced by HPAEC in response to hypoxia and that Nox1 is also responsible for the migration of HPAEC in response to VEGF stimulation. Further investigation revealed that VEGF directly stimulates Nox1:NOXA1 assembly and that pulmonary artery

fibroblasts secrete VEGF during hypoxia and are capable of promoting Nox1-dependent endothelial cell metabolism and its associated proliferation. These data suggested that Nox1 is a more significant contributor than Nox2 to pulmonary endothelial dysfunction.

6.1.2 Specific Aim 3: Interrogate a Role for Nox in Pulmonary Arterial Hypertension

Pulmonary arterial hypertension is a debilitating disease with few effective treatment options. Historical treatment options for PAH include endothelin receptor antagonists, agents that increase NO bioavailability, and prostacyclin [240]. Endothelin receptor antagonists, such as bosentan, prevent vasoconstriction initiated by the ET1 receptor while inhaled NO, nitrates, or PDE5 inhibitors (i.e. sildenafil) are used to facilitate vasodilation via enhanced NO bioavailability. Unfortunately, each of these treatments is eventually overcome by side effects or acquired resistance to the therapy. Recent research has identified soluble guanylate cyclase (sGC) activators as effective therapies for PAH that can bypass endogenous NO scavenging, although it remains to be seen whether these compounds are eventually overcome by acquired resistance as well [195, 215]. Nevertheless, clinical management of PAH remains a difficult goal while curative treatments are completely elusive.

In this study, we tested the efficacy of a novel and specific Nox1 inhibitor (NoxA1ds) as a treatment during the development of PAH in a rodent model. Nox1 was chosen as the target molecule due to mounting evidence that Nox1, rather than Nox2, plays a greater role in endothelial phenotypes observed in PAH, including hypoxia induced $O_2^{\cdot -}$ production, VEGF-stimulated migration, and angiogenic signaling [98, 230]. We report that NoxA1ds significantly inhibited RV $O_2^{\cdot -}$ production. Despite the observed reduction in RV $O_2^{\cdot -}$, no corresponding improvement in RV hemodynamics was observed in SUCH rats treated with NoxA1ds. These

results indicate that while NoxA1ds is effective *in vivo* at preventing enzymatic $O_2^{\cdot-}$ production, Nox1 is likely not responsible for cardiomyocyte mediated RV dysfunction in SUCH PAH and that RV $O_2^{\cdot-}$ production is not the primary instigator of RV hypertrophy and dysfunction. Rather, other groups have proposed that Nox4 is the primary isoform responsible for RV dysfunction in this context. Beyond Nox4, it remains possible that other pathways, including growth receptor signaling and fibrosis contribute to the disease in this model. It remains possible that Nox1 indirectly contributes to RV dysfuction in PAH through modulation of pulmonary vascular remodeling. Future studies will elucidate Nox1's direct effect on pulmonary vascular remodeling in PAH.

As an unexpected side effect of SUCH treatment, the LV of SUCH treated rats exhibited a dilatory cardiomyopathy, as indicated by the increased LV EDV and cardiac output paired with a decreased LV EDPVR. Indeed, dilatory cardiomyopathies have previously been associated with Nox activity and hypoxia, but it was completely unknown whether Nox1 contributes to this pathology [247, 251]. Most interestingly, the LV dilatory cardiomyopathy in SUCH treated rats was prevented via NoxA1ds aerosol treatment. These data indicate that Nox1 may play a more significant pathophysiological in LV vs the RV.

Prior to this study, virtually nothing was known about the role of Nox1 in the LV or RV in the context of pulmonary hypertension. Through this study where we treated rats in the SUCH model of pulmonary hypertension with a novel Nox1 inhibitor NoxA1ds, we determined that while NoxA1ds effectively inhibits RV $O_2^{\cdot-}$ production in PAH, Nox1 inhibition is an ineffective treatment for the SUCH model of PAH as measured by the Fulton index, ESPVR, and mPAP. Surprisingly, we identified a novel role for Nox1 in LV dilatory cardiomyopathy,

indicating that Nox1 inhibition may be a potential target for the treatment of HFpEF. It remains to be seen whether Nox1 inhibition is effective in alternative models PAH.

6.2 CONCLUSION

The overarching goal of this thesis was the effort to pharmacologically test the role of Nox *in vitro* and *in vivo* through the design and characterization of a novel Nox1 inhibitor. In this respect, I was successful in designing NoxA1ds; a peptide that has proven to be a highly efficacious and specific inhibitor of Nox1that is effective *in vitro* and *in vivo*.

Following a thorough literature review and through creative insight, NoxA1ds was designed to mimic the putative activation domain of NOXA1. Progressing from the initial design of NoxA1ds we characterized its pharmacological profile and verified its specificity against Nox1 and its ability to penetrate and attenuate Nox1 activity in whole cells. Further studies showed that mechanistically, NoxA1ds inhibits Nox1 by binding Nox1 and preventing its interaction with NOXA1.

After the successful design and characterization of NoxA1ds, I then proceeded to investigate the role of Nox1 vs Nox2 in HPAECs, a cell line that transcribes Nox1 and Nox2 in equal amounts. To do this, we first validated that the established Nox inhibitor, Nox2ds, is specific for Nox2 over Nox1. Then, using NoxA1ds and Nox2ds to specifically inhibit either Nox1 or Nox2, I determined that Nox1, rather than Nox2, is responsible for $O_2^{\cdot -}$ produced by HPAEC in response to hypoxia and HPAEC migration in response to VEGF stimulation.

As Nox1 rather than Nox2 was responsible for pulmonary endothelial phenotypes associated with PAH, we proceeded to test the role of Nox1 in the development of PAH, a disease thought to be, in part, mediated by dysfunctional endothelium. Through an *in vivo* model of PAH, we demonstrated that NoxA1ds is effective at inhibiting RV $O_2^{\cdot -}$ production *in vivo*, but that this inhibition is insufficient to prevent RV dysfunction in severe PAH. Unexpectedly, this same *in vivo* model of PAH revealed that LV dilatory dysfunction in the context of PAH can be prevented through Nox1 inhibition, bearing implications for the treatment of HFpEF associated with PAH. Future studies will investigate the effect of Nox1 inhibition in other models of cardiovascular disease, including systemic hypertension and associated left heart failure.

Concerning public health, this dissertation has contributed to a greater understanding of Nox1's role in the endothelium in cardiovascular disease, potentially catalyzing the development of treatments for cardiovascular diseases driven by Nox1. Additionally, the Nox1 inhibitor described here, NoxA1ds, may be utilized as a tool to elucidate Nox1's role in cellular biology and animal physiology in any number of disease models.

APPENDIX A

ELSEVIER LICENSE
TERMS AND CONDITIONS

Aug 19, 2014

This is a License Agreement between Daniel J Ranayhossaini ("You") and Elsevier ("Elsevier") provided by Copyright Clearance Center ("CCC"). The license consists of your order details, the terms and conditions provided by Elsevier, and the payment terms and conditions.

All payments must be made in full to CCC. For payment instructions, please see information listed at the bottom of this form.

Supplier	Elsevier Limited The Boulevard, Langford Lane Kidlington,Oxford,OX5 1GB,UK
Registered Company Number	1982084
Customer name	Daniel J Ranayhossaini
Customer address	E1200 BST PITTSBURGH, PA 15213
License number	3401530058793
License date	Jun 03, 2014
Licensed content publisher	Elsevier
Licensed content publication	Free Radical Biology and Medicine
Licensed content title	Oxidases and peroxidases in cardiovascular and lung disease: New concepts in reactive oxygen species signaling
Licensed content author	Imad Al Ghouleh, Nicholas K.H. Khoo, Ulla G. Knaus, Kathy K. Griendling, Rhian M. Touyz, Victor J. Thannickal, Aaron Barchowsky, William M. Nauseef, Eric E. Kelley, Phillip M. Bauer, Victor Darley-Usmar, Sruti Shiva, Eugenia Cifuentes-Pagano, Bruce A. Freeman, et al.
Licensed content date	1 October 2011
Licensed content volume number	51
Licensed content issue number	7
Number of pages	18
Start Page	1271
End Page	1288
Type of Use	reuse in a thesis/dissertation
Intended publisher of new work	other
Portion	figures/tables/illustrations
Number of figures/tables	

/illustrations	
	1
Format	both print and electronic
Are you the author of this Elsevier article?	
	No
Will you be translating?	No
Title of your thesis/dissertation	
	RATIONAL DESIGN AND THERAPEUTIC POTENTIAL OF A NOVEL NOX1 INHIBITOR FOR THE TREATMENT OF PULMONARY HYPERTENSION: IN VITRO AND IN VIVO EFFECTS OF NOX1 INHIBITION
Expected completion date	Aug 2014
Estimated size (number of pages)	
	120
Elsevier VAT number	GB 494 6272 12
Permissions price	0.00 USD

APPENDIX B

NATURE PUBLISHING GROUP LICENSE TERMS AND CONDITIONS

Aug 19, 2014

This is a License Agreement between Daniel J Ranayhossaini ("You") and Nature Publishing Group ("Nature Publishing Group") provided by Copyright Clearance Center ("CCC"). The license consists of your order details, the terms and conditions provided by Nature Publishing Group, and the payment terms and conditions.

All payments must be made in full to CCC. For payment instructions, please see information listed at the bottom of this form.

License Number	3401521101637
License date	Jun 03, 2014
Licensed content publisher	Nature Publishing Group
Licensed content publication	Nature Reviews Drug Discovery
Licensed content title	Combating oxidative stress in vascular disease: NADPH oxidases as therapeutic targets
Licensed content author	Grant R. Drummond, Stavros Selemidis, Kathy K. Griendling and Christopher G. Sobey
Licensed content date	Jun 1, 2011
Volume number	10
Issue number	6
Type of Use	reuse in a dissertation / thesis
Requestor type	academic/educational
Format	print and electronic
Portion	figures/tables/illustrations
Number of figures/tables /illustrations	1
High-res required	no
Figures	Figure 2
Author of this NPG article	no
Your reference number	None
Title of your thesis / dissertation	RATIONAL DESIGN AND THERAPEUTIC POTENTIAL OF A NOVEL NOX1 INHIBITOR FOR THE TREATMENT OF PULMONARY HYPERTENSION: IN VITRO AND IN VIVO EFFECTS OF NOX1 INHIBITION
Expected completion date	Aug 2014
Estimated size (number of pages)	120

Total 0.00 USD

APPENDIX C

ELSEVIER LICENSE
TERMS AND CONDITIONS

Aug 19, 2014

This is a License Agreement between Daniel J Ranayhossaini ("You") and Elsevier ("Elsevier") provided by Copyright Clearance Center ("CCC"). The license consists of your order details, the terms and conditions provided by Elsevier, and the payment terms and conditions.

All payments must be made in full to CCC. For payment instructions, please see information listed at the bottom of this form.

Supplier	Elsevier Limited The Boulevard, Langford Lane Kidlington, Oxford, OX5 1GB,UK
Registered Company Number	1982084
Customer name	Daniel J Ranayhossaini
Customer address	E1200 BST PITTSBURGH, PA 15213
License number	3406561441195
License date	Jun 12, 2014
Licensed content publisher	Elsevier
Licensed content publication	Free Radical Biology and Medicine
Licensed content title	Nox2 B-loop peptide, Nox2ds, specifically inhibits the NADPH oxidase Nox2
Licensed content author	Gábor Csányi, Eugenia Cifuentes-Pagano, Imad Al Ghouleh, Daniel J. Ranayhossaini, Loreto Egaña, Lucia R. Lopes, Heather M. Jackson, Eric E. Kelley, Patrick J. Pagano
Licensed content date	15 September 2011
Licensed content volume number	51
Licensed content issue number	6
Number of pages	10
Start Page	1116
End Page	1125
Type of Use	reuse in a thesis/dissertation
Portion	figures/tables/illustrations
Number of figures/tables /illustrations	3
Format	both print and electronic
Are you the author of this Elsevier article?	Yes
Will you be translating?	No
Title of your thesis/dissertation	

	RATIONAL DESIGN AND THERAPEUTIC POTENTIAL OF A NOVEL NOX1 INHIBITOR FOR THE TREATMENT OF PULMONARY HYPERTENSION: IN VITRO AND IN VIVO EFFECTS OF NOX1 INHIBITION
Expected completion date	Aug 2014
Estimated size (number of pages)	120
Elsevier VAT number	GB 494 6272 12
Permissions price	0.00 USD
VAT/Local Sales Tax	0.00 USD / 0.00 GBP
Total	0.00 USD

BIBLIOGRAPHY

1.Kelley, E.E., et al., *Nitro-oleic acid, a novel and irreversible inhibitor of xanthine oxidoreductase.* J Biol Chem, 2008. **283**(52): p. 36176-84.

2.Rey, F.E., et al., *Perivascular superoxide anion contributes to impairment of endothelium-dependent relaxation: role of gp91(phox).* Circulation, 2002. **106**(19): p. 2497-502.

3.Kuzkaya, N., et al., *Interactions of peroxynitrite, tetrahydrobiopterin, ascorbic acid, and thiols: implications for uncoupling endothelial nitric-oxide synthase.* J Biol Chem, 2003. **278**(25): p. 22546-54.

4.Gray, B. and A.J. Carmichael, *Kinetics of superoxide scavenging by dismutase enzymes and manganese mimics determined by electron spin resonance.* Biochem J, 1992. **281**(Pt 3): p. 795-802.

5.Tarpey, M.M. and I. Fridovich, *Methods of detection of vascular reactive species: nitric oxide, superoxide, hydrogen peroxide, and peroxynitrite.* Circ Res, 2001. **89**(3): p. 224-36.

6.Tabima, D.M., S. Frizzell, and M.T. Gladwin, *Reactive oxygen and nitrogen species in pulmonary hypertension.* Free Radic Biol Med, 2012. **52**(9): p. 1970-86.

7.Noguchi, K., et al., *Increasing dihydrobiopterin causes dysfunction of endothelial nitric oxide synthase in rats in vivo.* Am J Physiol Heart Circ Physiol, 2011. **301**(3): p. H721-9.

8.Vásquez-Vivar, J., et al., *Reaction of tetrahydrobiopterin with superoxide: EPR-kinetic analysis and characterization of the pteridine radical.* Free Radical Biology and Medicine, 2001. **31**(8): p. 975-985.

9.Dikalova, A.E., et al., *Upregulation of Nox1 in vascular smooth muscle leads to impaired endothelium-dependent relaxation via eNOS uncoupling.* Am J Physiol Heart Circ Physiol, 2010. **299**(3): p. H673-9.

10.Winterbourn, C.C. and D. Metodiewa, *Reactivity of biologically important thiol compounds with superoxide and hydrogen peroxide.* Free Radic Biol Med, 1999. **27**(3-4): p. 322-8.

11.Breithaupt, J., *Summary Review of Available Literature for Hydrogen Peroxide and Peroxyacetic Acid for New Use to Treat Wastewater*, P. Office of Prevention, and Toxic Substances, Editor 2007. p. 35.

12.Neville, R.G., *The Oxidation of cysteine by Iron and Hydrogen Peroxide.* Journal of the American Chemical Society, 1957. **79**(10): p. 2456-2457.

13.Luo, D., S.W. Smith, and B.D. Anderson, *Kinetics and mechanism of the reaction of cysteine and hydrogen peroxide in aqueous solution.* J Pharm Sci, 2005. **94**(2): p. 304-16.

14.Loew, O., *A NEW ENZYME OF GENERAL OCCURRENCE IN ORGANISMIS.* Science, 1900. **11**(279): p. 701-2.

15.Jones, P. and A. Suggett, *The catalase–hydrogen peroxide system. Kinetics of catalatic action at high substrate concentrations.* Biochem J, 1968. **110**(4): p. 617-20.

16.Foster, J., et al., *Oxygenases*1962, New York: Academic Press. 588.

17.Dunford, H.B., *Peroxidases and Catalases*2010, Hoboken, NJ: John Wiley & Sons. 459.

18.Furchgott, R.F. and P.M. Vanhoutte, *Endothelium-derived relaxing and contracting factors.* FASEB J, 1989. **3**(9): p. 2007-18.

19.Griffith, T.M., et al., *The nature of endothelium-derived vascular relaxant factor.* Nature, 1984. **308**(5960): p. 645-7.

20.Castiglione, N., et al., *Nitrite and nitrite reductases: from molecular mechanisms to significance in human health and disease.* Antioxid Redox Signal, 2012. **17**(4): p. 684-716.
21.Beckman, J.S. and W.H. Koppenol, *Nitric oxide, superoxide, and peroxynitrite: the good, the bad, and ugly.* Am J Physiol, 1996. **271**(5 Pt 1): p. C1424-37.
22.Herrera, M., N.J. Hong, and J.L. Garvin, *Aquaporin-1 transports NO across cell membranes.* Hypertension, 2006. **48**(1): p. 157-64.
23.Squadrito, G.L. and W.A. Pryor, *The formation of peroxynitrite in vivo from nitric oxide and superoxide.* Chem Biol Interact, 1995. **96**(2): p. 203-6.
24.Huie, R.E. and S. Padmaja, *The reaction of no with superoxide.* Free Radic Res Commun, 1993. **18**(4): p. 195-9.
25.Tsai JH, H.T., Harrison JG, Jablowski M, van der Woerd M, Martin JC, Beckman JS, *Role of peroxynitrite conformation with its stability and toxicity.* J Am Chem Soc, 1994. **116**: p. 4115-4116.
26.Whiteman, M. and B. Halliwell, *Protection against peroxynitrite-dependent tyrosine nitration and alpha 1-antiproteinase inactivation by ascorbic acid. A comparison with other biological antioxidants.* Free Radic Res, 1996. **25**(3): p. 275-83.
27.Beckman, J.S., et al., *Apparent hydroxyl radical production by peroxynitrite: implications for endothelial injury from nitric oxide and superoxide.* Proc Natl Acad Sci U S A, 1990. **87**(4): p. 1620-4.
28.Ischiropoulos, H., et al., *Peroxynitrite-mediated tyrosine nitration catalyzed by superoxide dismutase.* Arch Biochem Biophys, 1992. **298**(2): p. 431-7.
29.Radi, R., et al., *Peroxynitrite oxidation of sulfhydryls. The cytotoxic potential of superoxide and nitric oxide.* J Biol Chem, 1991. **266**(7): p. 4244-50.
30.Pryor, W.A. and G.L. Squadrito, *The chemistry of peroxynitrite: a product from the reaction of nitric oxide with superoxide.* Am J Physiol, 1995. **268**(5 Pt 1): p. L699-722.
31.Halliwell, B., J.M.C. Gutteridge, and O.I. Aruoma, *The deoxyribose method: A simple "test-tube" assay for determination of rate constants for reactions of hydroxyl radicals.* Analytical Biochemistry, 1987. **165**(1): p. 215-219.
32.Martinez, A., et al., *Structural and molecular basis of the peroxynitrite-mediated nitration and inactivation of Trypanosoma cruzi iron-superoxide dismutases (Fe-SODs) A and B: disparate susceptibilities due to the repair of Tyr35 radical by Cys83 in Fe-SODB through intramolecular electron transfer.* J Biol Chem, 2014. **289**(18): p. 12760-78.
33.Lupidi, G., et al., *Peroxynitrite-mediated oxidation of fibrinogen inhibits clot formation.* FEBS Lett, 1999. **462**(3): p. 236-40.
34.Cassina, A.M., et al., *Cytochrome c nitration by peroxynitrite.* J Biol Chem, 2000. **275**(28): p. 21409-15.
35.Franco, M.C., et al., *Nitration of Hsp90 induces cell death.* Proc Natl Acad Sci U S A, 2013. **110**(12): p. E1102-11.
36.Al Ghouleh, I., et al., *Oxidases and peroxidases in cardiovascular and lung disease: New concepts in reactive oxygen species signaling.* Free Radic Biol Med, 2011. **51**(7): p. 1271-88.
37.Sbarra, A.J. and M.L. Karnovsky, *The biochemical basis of phagocytosis. 2. Incorporation of C14-labeled building blocks into lipid, protein, and glycogen of leukocytes during phagocytosis.* J Biol Chem, 1960. **235**: p. 2224-9.

38.Sbarra, A.J. and M.L. Karnovsky, *The biochemical basis of phagocytosis. I. Metabolic changes during the ingestion of particles by polymorphonuclear leukocytes.* J Biol Chem, 1959. **234**(6): p. 1355-62.
39.Karnovsky, M.L. and A.J. Sbarra, *Metabolic changes accompanying the ingestion of particulate matter by cells.* Am J Clin Nutr, 1960. **8**: p. 147-55.
40.Griendling, K.K., D. Sorescu, and M. Ushio-Fukai, *NAD(P)H oxidase: role in cardiovascular biology and disease.* Circ Res, 2000. **86**(5): p. 494-501.
41.Cui, X.L., et al., *Expression of NADPH oxidase isoform 1 (Nox1) in human placenta: involvement in preeclampsia.* Placenta, 2006. **27**(4-5): p. 422-31.
42.Banfi, B., et al., *A mammalian H+ channel generated through alternative splicing of the NADPH oxidase homolog NOH-1.* Science, 2000. **287**(5450): p. 138-42.
43.Miller, F.J., Jr., et al., *Cytokine activation of nuclear factor kappa B in vascular smooth muscle cells requires signaling endosomes containing Nox1 and ClC-3.* Circ Res, 2007. **101**(7): p. 663-71.
44.Jones, S.A., et al., *Expression of phagocyte NADPH oxidase components in human endothelial cells.* Am J Physiol, 1996. **271**(4 Pt 2): p. H1626-34.
45.Bedard, K. and K.H. Krause, *The NOX family of ROS-generating NADPH oxidases: physiology and pathophysiology.* Physiol Rev, 2007. **87**(1): p. 245-313.
46.Touyz, R.M., et al., *Expression of a functionally active gp91phox-containing neutrophil-type NAD(P)H oxidase in smooth muscle cells from human resistance arteries: regulation by angiotensin II.* Circ Res, 2002. **90**(11): p. 1205-13.
47.Gorlach, A., et al., *A gp91phox containing NADPH oxidase selectively expressed in endothelial cells is a major source of oxygen radical generation in the arterial wall.* Circ Res, 2000. **87**(1): p. 26-32.
48.Petry, A., et al., *NOX2 and NOX4 mediate proliferative response in endothelial cells.* Antioxid Redox Signal, 2006. **8**(9-10): p. 1473-84.
49.Nakano, Y., et al., *Critical roles for p22phox in the structural maturation and subcellular targeting of Nox3.* Biochem J, 2007. **403**(1): p. 97-108.
50.Banfi, B., et al., *NOX3, a superoxide-generating NADPH oxidase of the inner ear.* J Biol Chem, 2004. **279**(44): p. 46065-72.
51.Hilenski, L.L., et al., *Distinct subcellular localizations of Nox1 and Nox4 in vascular smooth muscle cells.* Arterioscler Thromb Vasc Biol, 2004. **24**(4): p. 677-83.
52.Geiszt, M., et al., *Identification of renox, an NAD(P)H oxidase in kidney.* Proc Natl Acad Sci U S A, 2000. **97**(14): p. 8010-4.
53.Banfi, B., et al., *A Ca(2+)-activated NADPH oxidase in testis, spleen, and lymph nodes.* J Biol Chem, 2001. **276**(40): p. 37594-601.
54.Banfi, B., et al., *Mechanism of Ca2+ activation of the NADPH oxidase 5 (NOX5).* J Biol Chem, 2004. **279**(18): p. 18583-91.
55.De Deken, X., et al., *Characterization of ThOX proteins as components of the thyroid H(2)O(2)-generating system.* Exp Cell Res, 2002. **273**(2): p. 187-96.
56.De Deken, X., et al., *Cloning of two human thyroid cDNAs encoding new members of the NADPH oxidase family.* J Biol Chem, 2000. **275**(30): p. 23227-33.
57.Sedeek, M., et al., *Molecular mechanisms of hypertension: role of Nox family NADPH oxidases.* Curr Opin Nephrol Hypertens, 2009. **18**(2): p. 122-7.

58.Frazziano, G., H.C. Champion, and P.J. Pagano, *NADPH oxidase-derived ROS and the regulation of pulmonary vessel tone.* Am J Physiol Heart Circ Physiol, 2012. **302**(11): p. H2166-77.
59.Bishopric, N.H., *Evolution of the heart from bacteria to man.* Ann N Y Acad Sci, 2005. **1047**: p. 13-29.
60.Hall, J.E., *Guyton and Hall Textbook of Medical Physiology*. 12 ed2011, Philadelphia: Saunders Elsevier.
61.Mitchell, G.A., *The innervation of the heart.* Br Heart J, 1953. **15**(2): p. 159-71.
62.Roy, C.S. and J.G. Adami, *Contributions To The Physiology And Pathology Of The Mammalian Heart.* The British Medical Journal, 1892. **1**(1626): p. 428-430.
63.Kent, A.F.S., *Researches on the Structure and Function of the Mammalian Heart.* J Physiol, 1893. **14**(4-5): p. i2-254.
64.Pacher, P., et al., *Measurement of cardiac function using pressure-volume conductance catheter technique in mice and rats.* Nat Protoc, 2008. **3**(9): p. 1422-34.
65.Chesler, N.C., et al., *How to measure pulmonary vascular and right ventricular function.* Conf Proc IEEE Eng Med Biol Soc, 2009. **2009**: p. 177-80.
66.Mazzei, W.J., *Lecture Notes: Cardiac Physiology and Monitoring*, 1998, SciSense. p. 7.
67.Suga, H. and K. Sagawa, *Instantaneous pressure-volume relationships and their ratio in the excised, supported canine left ventricle.* Circ Res, 1974. **35**(1): p. 117-26.
68.Hayward, C.S., W.V. Kalnins, and R.P. Kelly, *Gender-related differences in left ventricular chamber function.* Cardiovasc Res, 2001. **49**(2): p. 340-50.
69.Nishio, R., S. Sasayama, and A. Matsumori, *Left ventricular pressure-volume relationship in a murine model of congestive heart failure due to acute viral myocarditis.* J Am Coll Cardiol, 2002. **40**(8): p. 1506-14.
70.Kass, D.A., et al., *Comparative influence of load versus inotropic states on indexes of ventricular contractility: experimental and theoretical analysis based on pressure-volume relationships.* Circulation, 1987. **76**(6): p. 1422-36.
71.Takimoto, E., et al., *Chronic inhibition of cyclic GMP phosphodiesterase 5A prevents and reverses cardiac hypertrophy.* Nat Med, 2005. **11**(2): p. 214-22.
72.Drummond, G.R., et al., *Combating oxidative stress in vascular disease: NADPH oxidases as therapeutic targets.* Nat Rev Drug Discov, 2011. **10**(6): p. 453-71.
73.Orekhov, A.N., Y.V. Bobryshev, and D.A. Chistiakov, *The complexity of cell composition of the intima of large arteries: focus on pericyte-like cells.* Cardiovasc Res, 2014.
74.Villanueva, A.G., et al., *Stimulation of fibroblast collagen and total protein formation by an endothelial cell-derived factor.* Circ Res, 1991. **69**(1): p. 134-41.
75.Pagano, P.J., et al., *Localization of a constitutively active, phagocyte-like NADPH oxidase in rabbit aortic adventitia: enhancement by angiotensin II.* Proc Natl Acad Sci U S A, 1997. **94**(26): p. 14483-8.
76.Pagano, P.J., et al., *An NADPH oxidase superoxide-generating system in the rabbit aorta.* Am J Physiol, 1995. **268**(6 Pt 2): p. H2274-80.
77.Bohr, D.F., *Vascular smooth muscle updated.* Circ Res, 1973. **32**(6): p. 665-72.
78.Ignarro, L.J., *Endothelium-derived nitric oxide: actions and properties.* FASEB J, 1989. **3**(1): p. 31-6.
79.Oltman, C.L., et al., *Reactive oxygen species mediate arachidonic acid-induced dilation in porcine coronary microvessels.* Am J Physiol Heart Circ Physiol, 2003. **285**(6): p. H2309-15.

80.Miura, H., et al., *Role for hydrogen peroxide in flow-induced dilation of human coronary arterioles.* Circ Res, 2003. **92**(2): p. e31-40.
81.Hein, T.W., L. Belardinelli, and L. Kuo, *Adenosine A(2A) receptors mediate coronary microvascular dilation to adenosine: role of nitric oxide and ATP-sensitive potassium channels.* J Pharmacol Exp Ther, 1999. **291**(2): p. 655-64.
82.Knighton, D.R., I.A. Silver, and T.K. Hunt, *Regulation of wound-healing angiogenesis-effect of oxygen gradients and inspired oxygen concentration.* Surgery, 1981. **90**(2): p. 262-70.
83.Arbiser, J.L., et al., *Reactive oxygen generated by Nox1 triggers the angiogenic switch.* Proc Natl Acad Sci U S A, 2002. **99**(2): p. 715-20.
84.Leung, D.W., et al., *Vascular endothelial growth factor is a secreted angiogenic mitogen.* Science, 1989. **246**(4935): p. 1306-9.
85.Arany, Z., et al., *An essential role for p300/CBP in the cellular response to hypoxia.* Proc Natl Acad Sci U S A, 1996. **93**(23): p. 12969-73.
86.Keck, P.J., et al., *Vascular permeability factor, an endothelial cell mitogen related to PDGF.* Science, 1989. **246**(4935): p. 1309-12.
87.Connolly, D.T., et al., *Tumor vascular permeability factor stimulates endothelial cell growth and angiogenesis.* J Clin Invest, 1989. **84**(5): p. 1470-8.
88.Kim, K.J., et al., *Inhibition of vascular endothelial growth factor-induced angiogenesis suppresses tumour growth in vivo.* Nature, 1993. **362**(6423): p. 841-4.
89.Senger, D.R., et al., *Tumor cells secrete a vascular permeability factor that promotes accumulation of ascites fluid.* Science, 1983. **219**(4587): p. 983-5.
90.Brekken, R.A., et al., *Selective inhibition of vascular endothelial growth factor (VEGF) receptor 2 (KDR/Flk-1) activity by a monoclonal anti-VEGF antibody blocks tumor growth in mice.* Cancer Res, 2000. **60**(18): p. 5117-24.
91.Tsuzuki, Y., et al., *Vascular endothelial growth factor (VEGF) modulation by targeting hypoxia-inducible factor-1alpha--> hypoxia response element--> VEGF cascade differentially regulates vascular response and growth rate in tumors.* Cancer Res, 2000. **60**(22): p. 6248-52.
92.Acker, T., J. Fandrey, and H. Acker, *The good, the bad and the ugly in oxygen-sensing: ROS, cytochromes and prolyl-hydroxylases.* Cardiovasc Res, 2006. **71**(2): p. 195-207.
93.Hill, P., et al., *Inhibition of hypoxia inducible factor hydroxylases protects against renal ischemia-reperfusion injury.* J Am Soc Nephrol, 2008. **19**(1): p. 39-46.
94.Yuan, G., et al., *Hypoxia-inducible factor 1 mediates increased expression of NADPH oxidase-2 in response to intermittent hypoxia.* J Cell Physiol, 2011. **226**(11): p. 2925-33.
95.Kar, S., et al., *Redox-control of matrix metalloproteinase-1: a critical link between free radicals, matrix remodeling and degenerative disease.* Respir Physiol Neurobiol, 2010. **174**(3): p. 299-306.
96.Martinez-Lemus, L.A., et al., *Inward remodeling of resistance arteries requires reactive oxygen species-dependent activation of matrix metalloproteinases.* Am J Physiol Heart Circ Physiol, 2011. **300**(6): p. H2005-15.
97.Ushio-Fukai, M., et al., *Novel role of gp91(phox)-containing NAD(P)H oxidase in vascular endothelial growth factor-induced signaling and angiogenesis.* Circ Res, 2002. **91**(12): p. 1160-7.
98.Garrido-Urbani, S., et al., *Targeting vascular NADPH oxidase 1 blocks tumor angiogenesis through a PPARalpha mediated mechanism.* PLoS One, 2011. **6**(2): p. e14665.

99.Zhang, M., et al., *NADPH oxidase-4 mediates protection against chronic load-induced stress in mouse hearts by enhancing angiogenesis.* Proc Natl Acad Sci U S A, 2010. **107**(42): p. 18121-6.
100.Suh, Y.A., et al., *Cell transformation by the superoxide-generating oxidase Mox1.* Nature, 1999. **401**(6748): p. 79-82.
101.Gray, S.P., et al., *NADPH oxidase 1 plays a key role in diabetes mellitus-accelerated atherosclerosis.* Circulation, 2013. **127**(18): p. 1888-902.
102.Morel, F. and P.V. Vignais, *Purification of cytochrome b558 from bovine polymorphonuclear neutrophils.* Biochem Biophys Res Commun, 1987. **149**(1): p. 46-55.
103.Bellavite, P., *The superoxide-forming enzymatic system of phagocytes.* Free Radic Biol Med, 1988. **4**(4): p. 225-61.
104.Corcionivoschi, N., et al., *Mucosal reactive oxygen species decrease virulence by disrupting Campylobacter jejuni phosphotyrosine signaling.* Cell Host Microbe, 2012. **12**(1): p. 47-59.
105.McPhail, L.C., L.R. DeChatelet, and P.S. Shirley, *Further characterization of NADPH oxidase activity of human polymorphonuclear leukocytes.* J Clin Invest, 1976. **58**(4): p. 774-80.
106.Babior, B.M., *The respiratory burst of phagocytes.* J Clin Invest, 1984. **73**(3): p. 599-601.
107.Wingler, K., et al., *Upregulation of the vascular NAD(P)H-oxidase isoforms Nox1 and Nox4 by the renin-angiotensin system in vitro and in vivo.* Free Radic Biol Med, 2001. **31**(11): p. 1456-64.
108.Cheng, G., et al., *Homologs of gp91phox: cloning and tissue expression of Nox3, Nox4, and Nox5.* Gene, 2001. **269**(1-2): p. 131-40.
109.Bedard, K., V. Jaquet, and K.H. Krause, *NOX5: from basic biology to signaling and disease.* Free Radic Biol Med, 2012. **52**(4): p. 725-34.
110.Sorescu, D., et al., *Superoxide production and expression of nox family proteins in human atherosclerosis.* Circulation, 2002. **105**(12): p. 1429-35.
111.Weisbrod, R.M., et al., *Reduced responsiveness of hypercholesterolemic rabbit aortic smooth muscle cells to nitric oxide.* Arterioscler Thromb Vasc Biol, 1997. **17**(2): p. 394-402.
112.Rey, F.E., et al., *Novel competitive inhibitor of NAD(P)H oxidase assembly attenuates vascular O(2)(-) and systolic blood pressure in mice.* Circ Res, 2001. **89**(5): p. 408-14.
113.Matsushima, S., et al., *Increased Oxidative Stress in the Nucleus Caused by Nox4 Mediates Oxidation of HDAC4 and Cardiac Hypertrophy.* Circulation Research, 2013. **112**(4): p. 651-663.
114.Rivera, J., et al., *Nox isoforms in vascular pathophysiology: insights from transgenic and knockout mouse models.* Redox Rep, 2010. **15**(2): p. 50-63.
115.Ambasta, R.K., et al., *Direct interaction of the novel Nox proteins with p22phox is required for the formation of a functionally active NADPH oxidase.* J Biol Chem, 2004. **279**(44): p. 45935-41.
116.Ambasta, R.K., et al., *Noxa1 is a central component of the smooth muscle NADPH oxidase in mice.* Free Radic Biol Med, 2006. **41**(2): p. 193-201.
117.Takeya, R., et al., *Novel human homologues of p47phox and p67phox participate in activation of superoxide-producing NADPH oxidases.* J Biol Chem, 2003. **278**(27): p. 25234-46.

118.Baumer, A.T., et al., *Phosphatidylinositol 3-kinase-dependent membrane recruitment of Rac-1 and p47phox is critical for alpha-platelet-derived growth factor receptor-induced production of reactive oxygen species.* J Biol Chem, 2008. **283**(12): p. 7864-76.
119.Gorzalczany, Y., et al., *A prenylated p67phox-Rac1 chimera elicits NADPH-dependent superoxide production by phagocyte membranes in the absence of an activator and of p47phox: conversion of a pagan NADPH oxidase to monotheism.* J Biol Chem, 2002. **277**(21): p. 18605-10.
120.Nobuhisa, I., et al., *Activation of the superoxide-producing phagocyte NADPH oxidase requires co-operation between the tandem SH3 domains of p47phox in recognition of a polyproline type II helix and an adjacent alpha-helix of p22phox.* Biochem J, 2006. **396**(1): p. 183-92.
121.DeLeo, F.R. and M.T. Quinn, *Assembly of the phagocyte NADPH oxidase: molecular interaction of oxidase proteins.* J Leukoc Biol, 1996. **60**(6): p. 677-91.
122.DeLeo, F.R., et al., *Mapping sites of interaction of p47-phox and flavocytochrome b with random-sequence peptide phage display libraries.* Proc Natl Acad Sci U S A, 1995. **92**(15): p. 7110-4.
123.Bromberg, Y. and E. Pick, *Activation of NADPH-dependent superoxide production in a cell-free system by sodium dodecyl sulfate.* J Biol Chem, 1985. **260**(25): p. 13539-45.
124.Roos, D., et al., *Hematologically important mutations: the autosomal recessive forms of chronic granulomatous disease (second update).* Blood Cells Mol Dis, 2010. **44**(4): p. 291-9.
125.Burnham, D.N., D.J. Uhlinger, and J.D. Lambeth, *Diradylglycerol synergizes with an anionic amphiphile to activate superoxide generation and phosphorylation of p47phox in a cell-free system from human neutrophils.* J Biol Chem, 1990. **265**(29): p. 17550-9.
126.Yuzawa, S., et al., *Solution structure of the tandem Src homology 3 domains of p47phox in an autoinhibited form.* J Biol Chem, 2004. **279**(28): p. 29752-60.
127.Han, C.H., et al., *Regulation of the neutrophil respiratory burst oxidase. Identification of an activation domain in p67(phox).* J Biol Chem, 1998. **273**(27): p. 16663-8.
128.Nisimoto, Y., et al., *The p67(phox) activation domain regulates electron flow from NADPH to flavin in flavocytochrome b(558).* J Biol Chem, 1999. **274**(33): p. 22999-3005.
129.Maehara, Y., et al., *A conserved region between the TPR and activation domains of p67phox participates in activation of the phagocyte NADPH oxidase.* J Biol Chem, 2010. **285**(41): p. 31435-45.
130.Csanyi, G., et al., *Nox2 B-loop peptide, Nox2ds, specifically inhibits the NADPH oxidase Nox2.* Free Radic Biol Med, 2011. **51**(6): p. 1116-25.
131.Shiose, A., et al., *A novel superoxide-producing NAD(P)H oxidase in kidney.* J Biol Chem, 2001. **276**(2): p. 1417-23.
132.Lyle, A.N., et al., *Poldip2, a novel regulator of Nox4 and cytoskeletal integrity in vascular smooth muscle cells.* Circ Res, 2009. **105**(3): p. 249-59.
133.Pollock, D.M., T.L. Keith, and R.F. Highsmith, *Endothelin receptors and calcium signaling.* FASEB J, 1995. **9**(12): p. 1196-204.
134.Liu, J., et al., *Gene transfer of NAD(P)H oxidase inhibitor to the vascular adventitia attenuates medial smooth muscle hypertrophy.* Circ Res, 2004. **95**(6): p. 587-94.
135.Csanyi, G., et al., *Thrombospondin-1 Regulates Blood Flow via CD47 Receptor-Mediated Activation of NADPH Oxidase 1.* Arterioscler Thromb Vasc Biol, 2012. **32**(12): p. 2966-73.

136.Dikalova, A., et al., *Nox1 overexpression potentiates angiotensin II-induced hypertension and vascular smooth muscle hypertrophy in transgenic mice.* Circulation, 2005. **112**(17): p. 2668-76.
137.Matsuno, K., et al., *Nox1 is involved in angiotensin II-mediated hypertension: a study in Nox1-deficient mice.* Circulation, 2005. **112**(17): p. 2677-85.
138.Lee, M.Y., et al., *Mechanisms of vascular smooth muscle NADPH oxidase 1 (Nox1) contribution to injury-induced neointimal formation.* Arterioscler Thromb Vasc Biol, 2009. **29**(4): p. 480-7.
139.Jacobson, G.M., et al., *Novel NAD(P)H oxidase inhibitor suppresses angioplasty-induced superoxide and neointimal hyperplasia of rat carotid artery.* Circ Res, 2003. **92**(6): p. 637-43.
140.Sullivan, J.M., R.L. Prewitt, and J.A. Josephs, *Attenuation of the microcirculation in young patients with high-output borderline hypertension.* Hypertension, 1983. **5**(6): p. 844-51.
141.Takeshita, A., et al., *Limited maximal vasodilator capacity of forearm resistance vessels in normotensive young men with a familial predisposition to hypertension.* Circ Res, 1982. **50**(5): p. 671-7.
142.Hahn, N.E., et al., *NOX5 expression is increased in intramyocardial blood vessels and cardiomyocytes after acute myocardial infarction in humans.* Am J Pathol, 2012. **180**(6): p. 2222-9.
143.Holterman, C.E., et al., *Nephropathy and elevated BP in mice with podocyte-specific NADPH oxidase 5 expression.* J Am Soc Nephrol, 2014. **25**(4): p. 784-97.
144.Musset, B., et al., *NOX5 in human spermatozoa: expression, function, and regulation.* J Biol Chem, 2012. **287**(12): p. 9376-88.
145.Wang, X., et al., *NADPH oxidase activation is required in reactive oxygen species generation and cell transformation induced by hexavalent chromium.* Toxicol Sci, 2011. **123**(2): p. 399-410.
146.Li, D. and W. Cao, *Role of intracellular calcium and NADPH oxidase NOX5-S in acid-induced DNA damage in Barrett's cells and Barrett's esophageal adenocarcinoma cells.* Am J Physiol Gastrointest Liver Physiol, 2014. **306**(10): p. G863-72.
147.Cucoranu, I., et al., *NAD(P)H oxidase 4 mediates transforming growth factor-beta1-induced differentiation of cardiac fibroblasts into myofibroblasts.* Circ Res, 2005. **97**(9): p. 900-7.
148.Zhao, Y., et al., *Nox2 NADPH oxidase promotes pathologic cardiac remodeling associated with Doxorubicin chemotherapy.* Cancer Res, 2010. **70**(22): p. 9287-97.
149.Nabeebaccus, A., M. Zhang, and A.M. Shah, *NADPH oxidases and cardiac remodelling.* Heart Fail Rev, 2011. **16**(1): p. 5-12.
150.Judkins, C.P., et al., *Direct evidence of a role for Nox2 in superoxide production, reduced nitric oxide bioavailability, and early atherosclerotic plaque formation in ApoE-/- mice.* Am J Physiol Heart Circ Physiol, 2010. **298**(1): p. H24-32.
151.Al-Shabrawey, M., et al., *Inhibition of NAD(P)H oxidase activity blocks vascular endothelial growth factor overexpression and neovascularization during ischemic retinopathy.* Am J Pathol, 2005. **167**(2): p. 599-607.
152.van Golen, R.F., T.M. van Gulik, and M. Heger, *Mechanistic overview of reactive species-induced degradation of the endothelial glycocalyx during hepatic ischemia/reperfusion injury.* Free Radic Biol Med, 2012.
153.Al Ghouleh, I., et al., *Aquaporin 1, Nox1, and Ask1 mediate oxidant-induced smooth muscle cell hypertrophy.* Cardiovasc Res, 2013. **97**(1): p. 134-42.

154.Oak, J.H. and H. Cai, *Attenuation of angiotensin II signaling recouples eNOS and inhibits nonendothelial NOX activity in diabetic mice.* Diabetes, 2007. **56**(1): p. 118-26.
155.Wind, S., et al., *Oxidative stress and endothelial dysfunction in aortas of aged spontaneously hypertensive rats by NOX1/2 is reversed by NADPH oxidase inhibition.* Hypertension, 2010. **56**(3): p. 490-7.
156.Xu, S., et al., *Increased expression of Nox1 in neointimal smooth muscle cells promotes activation of matrix metalloproteinase-9.* J Vasc Res, 2012. **49**(3): p. 242-8.
157.McGuire, J.J., D.J. Anderson, and B.M. Bennett, *Inhibition of the biotransformation and pharmacological actions of glyceryl trinitrate by the flavoprotein inhibitor, diphenyleneiodonium sulfate.* J Pharmacol Exp Ther, 1994. **271**(2): p. 708-14.
158.Hancock, J.T. and O.T. Jones, *The inhibition by diphenyleneiodonium and its analogues of superoxide generation by macrophages.* Biochem J, 1987. **242**(1): p. 103-7.
159.Gianni, D., et al., *A novel and specific NADPH oxidase-1 (Nox1) small-molecule inhibitor blocks the formation of functional invadopodia in human colon cancer cells.* ACS Chem Biol, 2010. **5**(10): p. 981-93.
160.Gaggini, F., et al., *Design, synthesis and biological activity of original pyrazolo-pyrido-diazepine, -pyrazine and -oxazine dione derivatives as novel dual Nox4/Nox1 inhibitors.* Bioorg Med Chem, 2011. **19**(23): p. 6989-99.
161.Thom, S.R., V.M. Bhopale, and M. Yang, *Neutrophils Generate Microparticles during Exposure to Inert Gases Due to Cytoskeletal Oxidative Stress.* J Biol Chem, 2014. **289**(27): p. 18831-45.
162.Straub, A.C., et al., *Arsenic-stimulated liver sinusoidal capillarization in mice requires NADPH oxidase-generated superoxide.* J Clin Invest, 2008. **118**(12): p. 3980-9.
163.Selemidis, S., et al., *NADPH oxidases in the vasculature: molecular features, roles in disease and pharmacological inhibition.* Pharmacol Ther, 2008. **120**(3): p. 254-91.
164.Aldieri, E., et al., *Classical inhibitors of NOX NAD(P)H oxidases are not specific.* Curr Drug Metab, 2008. **9**(8): p. 686-96.
165.Heumuller, S., et al., *Apocynin is not an inhibitor of vascular NADPH oxidases but an antioxidant.* Hypertension, 2008. **51**(2): p. 211-7.
166.*GKT137831*. June 11 2014 [cited 2014 July 7].
167.Girouard, H., et al., *Angiotensin II attenuates endothelium-dependent responses in the cerebral microcirculation through nox-2-derived radicals.* Arterioscler Thromb Vasc Biol, 2006. **26**(4): p. 826-32.
168.Sun, C., et al., *NAD(P)H oxidase inhibition attenuates neuronal chronotropic actions of angiotensin II.* Circ Res, 2005. **96**(6): p. 659-66.
169.Fawell, S., et al., *Tat-mediated delivery of heterologous proteins into cells.* Proceedings of the National Academy of Sciences, 1994. **91**(2): p. 664-668.
170.McLaughlin, V.V., et al., *ACCF/AHA 2009 expert consensus document on pulmonary hypertension a report of the American College of Cardiology Foundation Task Force on Expert Consensus Documents and the American Heart Association developed in collaboration with the American College of Chest Physicians; American Thoracic Society, Inc.; and the Pulmonary Hypertension Association.* J Am Coll Cardiol, 2009. **53**(17): p. 1573-619.
171.Penaloza, D. and J. Arias-Stella, *The heart and pulmonary circulation at high altitudes: healthy highlanders and chronic mountain sickness.* Circulation, 2007. **115**(9): p. 1132-46.

172.Tuder, R.M., et al., *Exuberant endothelial cell growth and elements of inflammation are present in plexiform lesions of pulmonary hypertension.* Am J Pathol, 1994. **144**(2): p. 275-85.
173.Lee, S.D., et al., *Monoclonal endothelial cell proliferation is present in primary but not secondary pulmonary hypertension.* J Clin Invest, 1998. **101**(5): p. 927-34.
174.Tuder, R.M., et al., *Expression of angiogenesis-related molecules in plexiform lesions in severe pulmonary hypertension: evidence for a process of disordered angiogenesis.* J Pathol, 2001. **195**(3): p. 367-74.
175.Jonigk, D., et al., *Plexiform lesions in pulmonary arterial hypertension composition, architecture, and microenvironment.* Am J Pathol, 2011. **179**(1): p. 167-79.
176.Schroder, K., et al., *NADPH oxidase Nox2 is required for hypoxia-induced mobilization of endothelial progenitor cells.* Circ Res, 2009. **105**(6): p. 537-44.
177.Quinlan, T.R., et al., *eNOS-deficient mice show reduced pulmonary vascular proliferation and remodeling to chronic hypoxia.* Am J Physiol Lung Cell Mol Physiol, 2000. **279**(4): p. L641-50.
178.Murata, T., et al., *Hypoxia impairs endothelium-dependent relaxation in organ cultured pulmonary artery.* Eur J Pharmacol, 2001. **421**(1): p. 45-53.
179.Mittal, M., et al., *Hypoxia-dependent regulation of nonphagocytic NADPH oxidase subunit NOX4 in the pulmonary vasculature.* Circ Res, 2007. **101**(3): p. 258-67.
180.Rafikova, O., et al., *Bosentan inhibits oxidative and nitrosative stress and rescues occlusive pulmonary hypertension.* Free Radic Biol Med, 2012.
181.Norton, C.E., et al., *Enhanced depolarization-induced pulmonary vasoconstriction following chronic hypoxia requires EGFR-dependent activation of NAD(P)H oxidase 2.* Antioxid Redox Signal, 2013. **18**(14): p. 1777-88.
182.Austin, E.D., et al., *Whole Exome Sequencing to Identify a Novel Gene (Caveolin-1) Associated with Human Pulmonary Arterial Hypertension.* Circ Cardiovasc Genet, 2012.
183.Mathew, R., *Cell-specific dual role of caveolin-1 in pulmonary hypertension.* Pulm Med, 2011. **2011**: p. 573432.
184.Drab, M., et al., *Loss of caveolae, vascular dysfunction, and pulmonary defects in caveolin-1 gene-disrupted mice.* Science, 2001. **293**(5539): p. 2449-52.
185.Garcia-Cardena, G., et al., *Endothelial nitric oxide synthase is regulated by tyrosine phosphorylation and interacts with caveolin-1.* J Biol Chem, 1996. **271**(44): p. 27237-40.
186.Landmesser, U., et al., *Oxidation of tetrahydrobiopterin leads to uncoupling of endothelial cell nitric oxide synthase in hypertension.* J Clin Invest, 2003. **111**(8): p. 1201-9.
187.Ozaki, M., et al., *Overexpression of endothelial nitric oxide synthase accelerates atherosclerotic lesion formation in apoE-deficient mice.* J Clin Invest, 2002. **110**(3): p. 331-40.
188.Babaei, S., et al., *Role of nitric oxide in the angiogenic response in vitro to basic fibroblast growth factor.* Circ Res, 1998. **82**(9): p. 1007-15.
189.Toby, I.T., et al., *Hypoxia-induced proliferation of human pulmonary microvascular endothelial cells depends on epidermal growth factor receptor tyrosine kinase activation.* Am J Physiol Lung Cell Mol Physiol, 2010. **298**(4): p. L600-6.
190.Nagendran, J., et al., *Endothelin axis is upregulated in human and rat right ventricular hypertrophy.* Circ Res, 2013. **112**(2): p. 347-54.
191.Spencer, J.A., et al., *Direct measurement of local oxygen concentration in the bone marrow of live animals.* Nature, 2014. **508**(7495): p. 269-73.

192.Sakadzic, S., et al., *Two-photon high-resolution measurement of partial pressure of oxygen in cerebral vasculature and tissue.* Nat Methods, 2010. **7**(9): p. 755-9.
193.Gammella, E., et al., *Evidence of synergistic/additive effects of sildenafil and erythropoietin in enhancing survival and migration of hypoxic endothelial cells.* Am J Physiol Lung Cell Mol Physiol, 2012.
194.de Jesus Perez, V.A., *Making sense of the estrogen paradox in pulmonary arterial hypertension.* Am J Respir Crit Care Med, 2011. **184**(6): p. 629-30.
195.Raat, N.J., et al., *Direct sGC activation bypasses NO scavenging reactions of intravascular free oxy-hemoglobin and limits vasoconstriction.* Antioxid Redox Signal, 2013. **19**(18): p. 2232-43.
196.Tofovic, S.P. and O. Rafikova, *Preventative and therapeutic effects of 2-methoxyestradiol, but not estradiol, in severe occlusive pulmonary arterial hypertension in female rats.* Am. J. Respir. Crit. Care Med., 2009. **179**.
197.Zeng, Q., et al., *Endothelin-1 regulates cardiac L-type calcium channels via NAD(P)H oxidase-derived superoxide.* J Pharmacol Exp Ther, 2008. **326**(3): p. 732-8.
198.Dahal, B.K., et al., *Role of epidermal growth factor inhibition in experimental pulmonary hypertension.* Am J Respir Crit Care Med, 2010. **181**(2): p. 158-67.
199.Tavolari, S., et al., *Selected polychlorobiphenyls congeners bind to estrogen receptor alpha in human umbilical vascular endothelial (HUVE) cells modulating angiogenesis.* Toxicology, 2006. **218**(1): p. 67-74.
200.Han, Y., et al., *Inhibition of ARNT severely compromises endothelial cell viability and function in response to moderate hypoxia.* Angiogenesis, 2012.
201.Johnson, J.A., et al., *ACE2 improves right ventricular function in a pressure overload model.* PLoS One, 2011. **6**(6): p. e20828.
202.Sharma, S., et al., *ApoA-I Mimetic Peptide 4F Rescues Pulmonary Hypertension by Inducing MicroRNA-193-3p.* Circulation, 2014.
203.Wilson, D.W., et al., *Mechanisms and pathology of monocrotaline pulmonary toxicity.* Crit Rev Toxicol, 1992. **22**(5-6): p. 307-25.
204.Huang, J., et al., *Pyrrolidine dithiocarbamate restores endothelial cell membrane integrity and attenuates monocrotaline-induced pulmonary artery hypertension.* Am J Physiol Lung Cell Mol Physiol, 2008. **294**(6): p. L1250-9.
205.Molteni, A., et al., *Monocrotaline-induced pulmonary fibrosis in rats: amelioration by captopril and penicillamine.* Proc Soc Exp Biol Med, 1985. **180**(1): p. 112-20.
206.Abe, K., et al., *Formation of plexiform lesions in experimental severe pulmonary arterial hypertension.* Circulation, 2010. **121**(25): p. 2747-54.
207.Rubin, L.J., et al., *Prostacyclin-induced acute pulmonary vasodilation in primary pulmonary hypertension.* Circulation, 1982. **66**(2): p. 334-8.
208.Hunter, C.J., et al., *Inhaled nebulized nitrite is a hypoxia-sensitive NO-dependent selective pulmonary vasodilator.* Nat Med, 2004. **10**(10): p. 1122-7.
209.Wessel, D.L., et al., *Use of inhaled nitric oxide and acetylcholine in the evaluation of pulmonary hypertension and endothelial function after cardiopulmonary bypass.* Circulation, 1993. **88**(5 Pt 1): p. 2128-38.
210.Zuckerbraun, B.S., P. George, and M.T. Gladwin, *Nitrite in pulmonary arterial hypertension: therapeutic avenues in the setting of dysregulated arginine/nitric oxide synthase signalling.* Cardiovasc Res, 2011. **89**(3): p. 542-52.

211.Humbert, M., et al., *Pulmonary edema complicating continuous intravenous prostacyclin in pulmonary capillary hemangiomatosis.* Am J Respir Crit Care Med, 1998. **157**(5 Pt 1): p. 1681-5.
212.Bellamy, T.C., et al., *Rapid desensitization of the nitric oxide receptor, soluble guanylyl cyclase, underlies diversity of cellular cGMP responses.* Proc Natl Acad Sci U S A, 2000. **97**(6): p. 2928-33.
213.Christou, D.D., et al., *Vascular Smooth Muscle Responsiveness to Nitric Oxide is Reduced in Healthy Adults with Increased Adiposity.* Am J Physiol Heart Circ Physiol, 2012.
214.Eriksson, C., et al., *Hepatotoxicity by bosentan in a patient with portopulmonary hypertension: a case-report and review of the literature.* J Gastrointestin Liver Dis, 2011. **20**(1): p. 77-80.
215.Ghofrani, H.A., et al., *Riociguat for the treatment of pulmonary arterial hypertension.* N Engl J Med, 2013. **369**(4): p. 330-40.
216.Ghofrani, H.A. and F. Grimminger, *Soluble guanylate cyclase stimulation: an emerging option in pulmonary hypertension therapy.* Eur Respir Rev, 2009. **18**(111): p. 35-41.
217.Cheng, G. and J.D. Lambeth, *NOXO1, regulation of lipid binding, localization, and activation of Nox1 by the Phox homology (PX) domain.* J Biol Chem, 2004. **279**(6): p. 4737-42.
218.Vilardaga, J.P., et al., *Conformational cross-talk between alpha2A-adrenergic and mu-opioid receptors controls cell signaling.* Nat Chem Biol, 2008. **4**(2): p. 126-31.
219.Molshanski-Mor, S., et al., *Cell-free assays: the reductionist approach to the study of NADPH oxidase assembly, or "all you wanted to know about cell-free assays but did not dare to ask".* Methods Mol Biol, 2007. **412**: p. 385-428.
220.Nisimoto, Y., et al., *Constitutive NADPH-dependent electron transferase activity of the Nox4 dehydrogenase domain.* Biochemistry. **49**(11): p. 2433-42.
221.Wheeler, D., et al., *NHERF-1 and the cytoskeleton regulate the traffic and membrane dynamics of G protein-coupled receptors.* J Biol Chem, 2007. **282**(34): p. 25076-87.
222.Chen, B.B. and R.K. Mallampalli, *Masking of a nuclear signal motif by monoubiquitination leads to mislocalization and degradation of the regulatory enzyme cytidylyltransferase.* Mol Cell Biol, 2009. **29**(11): p. 3062-75.
223.Liang, C.-C., A.Y. Park, and J.-L. Guan, *In vitro scratch assay: a convenient and inexpensive method for analysis of cell migration in vitro.* Nat. Protocols, 2007. **2**(2): p. 329-333.
224.Lassegue, B. and R.E. Clempus, *Vascular NAD(P)H oxidases: specific features, expression, and regulation.* Am J Physiol Regul Integr Comp Physiol, 2003. **285**(2): p. R277-97.
225.Leto, T.L., et al., *Characterization of neutrophil NADPH oxidase factors p47-phox and p67-phox from recombinant baculoviruses.* J Biol Chem, 1991. **266**(29): p. 19812-8.
226.Banfi, B., et al., *Two novel proteins activate superoxide generation by the NADPH oxidase NOX1.* J Biol Chem, 2003. **278**(6): p. 3510-3.
227.Kellogg, E.W., 3rd and I. Fridovich, *Superoxide, hydrogen peroxide, and singlet oxygen in lipid peroxidation by a xanthine oxidase system.* J Biol Chem, 1975. **250**(22): p. 8812-7.
228.Harrison, R., *Structure and function of xanthine oxidoreductase: where are we now?* Free Radic Biol Med, 2002. **33**(6): p. 774-97.
229.Gianni, D., et al., *The involvement of the tyrosine kinase c-Src in the regulation of reactive oxygen species generation mediated by NADPH oxidase-1.* Mol Biol Cell, 2008. **19**(7): p. 2984-94.

230.Ranayhossaini, D.J., et al., *Selective recapitulation of conserved and nonconserved regions of putative NOXA1 protein activation domain confers isoform-specific inhibition of Nox1 oxidase and attenuation of endothelial cell migration.* J Biol Chem, 2013. **288**(51): p. 36437-50.
231.Mishra, A., et al., *Translocation of HIV TAT peptide and analogues induced by multiplexed membrane and cytoskeletal interactions.* Proc Natl Acad Sci U S A, 2011. **108**(41): p. 16883-8.
232.Poillot, C., et al., *Small efficient cell-penetrating peptides derived from scorpion toxin maurocalcine.* J Biol Chem, 2012. **287**(21): p. 17331-42.
233.Kinoshita, M. and K. Hynynen, *Intracellular delivery of Bak BH3 peptide by microbubble-enhanced ultrasound.* Pharm Res, 2005. **22**(5): p. 716-20.
234.Meijering, B.D., et al., *Ultrasound and microbubble-targeted delivery of macromolecules is regulated by induction of endocytosis and pore formation.* Circ Res, 2009. **104**(5): p. 679-87.
235.Walensky, L.D., et al., *Activation of apoptosis in vivo by a hydrocarbon-stapled BH3 helix.* Science, 2004. **305**(5689): p. 1466-70.
236.Tugyi, R., et al., *Partial D-amino acid substitution: Improved enzymatic stability and preserved Ab recognition of a MUC2 epitope peptide.* Proc Natl Acad Sci U S A, 2005. **102**(2): p. 413-8.
237.Zhang, Q.G., et al., *Critical role of NADPH oxidase in neuronal oxidative damage and microglia activation following traumatic brain injury.* PLoS One, 2012. **7**(4): p. e34504.
238.Zhou, X., et al., *NAD(P)H oxidase-derived peroxide mediates elevated basal and impaired flow-induced NO production in SHR mesenteric arteries in vivo.* Am J Physiol Heart Circ Physiol, 2008. **295**(3): p. H1008-H1016.
239.Larsson, A., E. Skoldenberg, and H. Ericson, *Serum and plasma levels of FGF-2 and VEGF in healthy blood donors.* Angiogenesis, 2002. **5**(1-2): p. 107-10.
240.Ranayhossaini, D. and P.J. Pagano, *TrACEing angiotensin II type 1 to right ventricular hypertrophy: are the "sartans" a viable course to treating pulmonary arterial hypertension?* Am J Respir Crit Care Med, 2012. **186**(8): p. 705-7.
241.Veit, F., et al., *Function of NADPH oxidase 1 in pulmonary arterial smooth muscle cells after monocrotaline-induced pulmonary vascular remodeling.* Antioxid Redox Signal, 2013. **19**(18): p. 2213-31.
242.Freund-Michel, V., et al., *Reactive oxygen species as therapeutic targets in pulmonary hypertension.* Ther Adv Respir Dis, 2013. **7**(3): p. 175-200.
243.Hoeper, M.M., et al., *Definitions and diagnosis of pulmonary hypertension.* J Am Coll Cardiol, 2013. **62**(25 Suppl): p. D42-50.
244.Tofovic, S.P., *Estrogens and development of pulmonary hypertension: interaction of estradiol metabolism and pulmonary vascular disease.* J Cardiovasc Pharmacol, 2010. **56**(6): p. 696-708.
245.Zhao, Y.Y., et al., *Persistent eNOS activation secondary to caveolin-1 deficiency induces pulmonary hypertension in mice and humans through PKG nitration.* J Clin Invest, 2009. **119**(7): p. 2009-18.
246.Barman, S.A., et al., *NADPH Oxidase 4 Is Expressed in Pulmonary Artery Adventitia and Contributes to Hypertensive Vascular Remodeling.* Arterioscler Thromb Vasc Biol, 2014.
247.Parajuli, N., et al., *Loss of NOX 2 (gp91phox) prevents oxidative stress and progression to advanced heart failure.* Clin Sci (Lond), 2014.

248.Paulus, W.J. and C. Tschope, *A novel paradigm for heart failure with preserved ejection fraction: comorbidities drive myocardial dysfunction and remodeling through coronary microvascular endothelial inflammation.* J Am Coll Cardiol, 2013. **62**(4): p. 263-71.
249.Gu, J.W., et al., *Vascular endothelial growth factor receptor inhibitor enhances dietary salt-induced hypertension in Sprague-Dawley rats.* Am J Physiol Regul Integr Comp Physiol, 2009. **297**(1): p. R142-8.
250.Rouwet, E.V., et al., *Hypoxia induces aortic hypertrophic growth, left ventricular dysfunction, and sympathetic hyperinnervation of peripheral arteries in the chick embryo.* Circulation, 2002. **105**(23): p. 2791-6.
251.Larsen, K.O., et al., *Alveolar hypoxia induces left ventricular diastolic dysfunction and reduces phosphorylation of phospholamban in mice.* Am J Physiol Heart Circ Physiol, 2006. **291**(2): p. H507-16.
252.Chen, L., et al., *Left ventricular dysfunction and associated cellular injury in rats exposed to chronic intermittent hypoxia.* J Appl Physiol, 2008. **104**(1): p. 218-23.
253.Zangari, M., et al., *Phase II study of SU5416, a small molecule vascular endothelial growth factor tyrosine kinase receptor inhibitor, in patients with refractory multiple myeloma.* Clin Cancer Res, 2004. **10**(1 Pt 1): p. 88-95.
254.Lockhart, A.C., et al., *Phase I/pilot study of SU5416 (semaxinib) in combination with irinotecan/bolus 5-FU/LV (IFL) in patients with metastatic colorectal cancer.* Am J Clin Oncol, 2006. **29**(2): p. 109-15.
255.Chen, M.H., R. Kerkela, and T. Force, *Mechanisms of cardiac dysfunction associated with tyrosine kinase inhibitor cancer therapeutics.* Circulation, 2008. **118**(1): p. 84-95.
256.Szanto, I., et al., *Expression of NOX1, a superoxide-generating NADPH oxidase, in colon cancer and inflammatory bowel disease.* J Pathol, 2005. **207**(2): p. 164-76.